



Search for dark matter produced in association with a Higgs boson decaying to tau leptons at $\sqrt{s} = 13$ TeV with the ATLAS detector

The ATLAS Collaboration

A search for dark matter produced in association with a Higgs boson in final states with two hadronically decaying τ -leptons and missing transverse momentum is presented. The analysis uses 139 fb^{-1} of proton–proton collision data at $\sqrt{s} = 13$ TeV collected by the ATLAS experiment at the Large Hadron Collider between 2015 and 2018. No evidence of physics beyond the Standard Model is found. The results are interpreted in terms of a 2HDM+ a model featuring two scalar Higgs doublets and a pseudoscalar singlet field. Exclusion limits on the parameters of the model in selected benchmark scenarios are derived at 95% confidence level. Model-independent limits are also set on the visible cross-section for processes beyond the Standard Model producing missing transverse momentum in association with a Higgs boson decaying into τ -leptons.

Contents

1	Introduction	2
2	ATLAS detector	4
3	Data and simulated event samples	5
4	Event reconstruction	7
5	Event selection	9
6	Background estimation	13
7	Systematic uncertainties	18
8	Results	19
9	Conclusion	25

1 Introduction

The Standard Model (SM) of particle physics is a successful and experimentally validated theory describing elementary particles and their interactions, culminating with the discovery in 2012 [1, 2] of a particle consistent with the Higgs boson (h) predicted in the SM. However, in its current form, the SM does not contain any dark matter (DM) particle candidate, whose existence is supported by astrophysical observations [3–5]. This provides a strong motivation for searches for physics beyond the Standard Model (BSM physics), in particular DM candidates [6].

During the Run 2 data-taking period, the Large Hadron Collider (LHC) experiments collected a substantial dataset, which can be used to search for signs of DM. There is no evidence of non-gravitational interactions between the DM and SM particles; this makes direct observation with general-purpose detectors such as ATLAS [7] or CMS [8] unlikely. The majority of the candidate DM particles χ would not interact with the material of the detector, and would escape undetected. One alternative strategy is to focus on the case of DM particles produced in association with SM particles, focusing on topologies where a single SM particle X is produced [9]. Such events do not rely on any model-specific assumptions and are characterised by a transverse-momentum imbalance (E_T^{miss}) due to the DM particle escaping the detector, resulting in ‘ $X+E_T^{\text{miss}}$ ’ signatures, also referred to as ‘mono- X ’.

The visible SM particle X can be a jet, a photon, a W or Z boson, a top quark, or a Higgs boson [10]. Typically, the couplings of such particles to light quarks and gluons of the SM are much stronger than their coupling to DM particles. The one obvious exception is a Higgs boson h whose couplings to light quarks and gluons are suppressed. This means that the mono-Higgs topologies are only significantly sensitive to scenarios in which the Higgs boson couples directly to some BSM particle participating in DM production. In such cases the direct SM–BSM interactions are probed, making the mono-Higgs searches a window into the structure of BSM physics responsible for DM production. In many theories where the Higgs

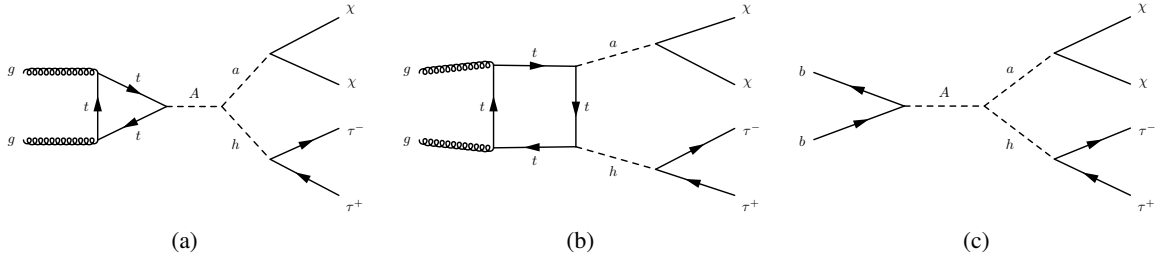


Figure 1: Feynman diagrams describing the 2HDM+ a scenarios leading to the production of the mono-Higgs signatures: (a) and (b) gluon–gluon fusion, (c) $b\bar{b}$ annihilation.

couplings to BSM particles are enhanced [11], such scenarios are possible, making mono-Higgs topologies an important tool in LHC DM searches.

The ATLAS and CMS collaborations have performed $h + E_{\text{T}}^{\text{miss}}$ searches where the Higgs boson decays into a pair of b -quarks [12, 13], τ -leptons¹ [14], or photons [15, 16], or into ZZ or W^+W^- [17]. This analysis presents a search for DM using the $h + E_{\text{T}}^{\text{miss}}$ topology with the Higgs boson decaying into two hadronically decaying τ -leptons, using the 139 fb^{-1} of proton–proton collision data collected by the ATLAS detector in 2015–2018 at $\sqrt{s} = 13 \text{ TeV}$. The presence of tau neutrinos can, in certain topologies, enhance the $E_{\text{T}}^{\text{miss}}$ signature of the signal and increase the sensitivity to the more challenging models [18].

One of the most straightforward and natural extensions of the SM is the two-Higgs-doublet model (2HDM) [19], extending the Higgs sector with a second scalar doublet. Such an extension of the Higgs sector is required in supersymmetric models, but is also of more general interest [20]. After electroweak symmetry breaking the model has five physical Higgs states: two neutral scalar states h and H , a pseudoscalar neutral state A , and two charged scalar states H^\pm . The 2HDM+ a model [21] extends the baseline 2HDM by adding a new pseudoscalar singlet a with Yukawa-like coupling to the DM candidate χ and the SM fermions. The singlet acts as a mediator between the SM particles and the DM sector. This is the simplest gauge-invariant and renormalisable extension of pseudoscalar mediator DM models [22]. The model leads to $h + E_{\text{T}}^{\text{miss}}$ final states through the gluon–gluon fusion and $b\bar{b}$ annihilation modes as depicted by the Feynman diagrams of Figure 1.

The present analysis considers the 2HDM+ a model as a benchmark and uses it to optimise the search and interpret the results. The model is described by 12 additional parameters not present in the SM. Following the LHC DM Working Group’s recommendations [22], two-dimensional parameter scans are performed with the following benchmark parameter choices:

- Masses of the CP-odd Higgs boson A , CP-even Higgs boson H , and charged Higgs bosons H^\pm are set to be equal to each other.
- The mass of the fermionic DM particle χ is set to 10 GeV.
- The DM Yukawa coupling y_χ to pseudoscalar a is set to 1.
- Mixing angles α and β are constrained to satisfy $\cos(\beta - \alpha) = 0$, where α is the mixing angle between CP-even Higgs bosons h and H , and $\tan \beta$ is the ratio of the vacuum expectation values (VEV) of the two Higgs doublets. In this so-called alignment limit the properties of the lightest Higgs boson h are very similar to those of the SM Higgs boson.

¹ Direct comparison with the presented search is not possible due to the difference between the models used for reinterpretation.

- Quartic couplings of the pseudoscalar potentials and Higgs potential λ_{1P} , λ_{2P} and λ_3 are all set to 3.
- The mass of the lightest Higgs boson h (similar to the SM Higgs boson) and the value of EW VEV v are fixed by observations to be $m_h \approx 125$ GeV [23] and $v \approx 246$ GeV [24].
- The mixing angle between the two pseudoscalars, Θ , is required to satisfy $\sin \Theta = 0.35$ or $\sin \Theta = 0.7$.

The analysis considers two two-dimensional scans in parameter values – the first in m_A and m_a , the second in m_A and $\tan \beta$. The kinematic dependence of the signal model on m_A in particular is non-trivial and the analysis is optimised for different ranges of m_A (‘low’ and ‘high’).

SM processes can also produce signatures with E_T^{miss} and two τ -leptons consistent with the decay products of a Higgs boson. The production of a Higgs boson in association with a Z boson decaying into neutrinos is of particular importance as, despite the relatively low cross-section, it can lead to final states indistinguishable from the signal. The production of a Z boson, a pair of vector bosons, $t\bar{t}$, or a Higgs boson in association with a W boson can also lead to final states with E_T^{miss} and two τ -leptons. Due to the larger cross-sections, finite detector resolution and acceptance, and the ambiguity introduced by the presence of two neutrinos, these processes can mimic the potential signal events.

The paper is structured as follows. Section 2 gives a short description of the ATLAS detector. Section 3 provides information about the dataset and Monte Carlo simulations used by the analysis. Section 4 describes the various physical objects used in the analysis. In Section 5, the selections applied to the dataset are summarised. Sections 6 and 7 describe the modelling and systematic uncertainties, respectively, of signal and SM backgrounds. The results of the analysis and the interpretations are discussed in Section 8, with a short summary given in Section 9.

2 ATLAS detector

The ATLAS experiment [7, 25, 26] is a multipurpose cylindrical particle detector at the LHC with nearly 4π coverage in solid angle.²

At the centre of the ATLAS detector is the inner tracking detector (ID). It is surrounded by a thin superconducting solenoid providing a 2 T axial magnetic field. The ID consists of silicon pixel, silicon microstrip, and transition radiation tracking detectors and covers the pseudorapidity range $|\eta| < 2.5$. The next layer of the ATLAS detector is made of lead/liquid-argon (LAr) sampling calorimeters that measure the energy and position of electromagnetic showers with high granularity. In the central region $|\eta| < 1.7$ the steel/scintillator-tile calorimeter is used to provide hadronic energy measurements. In the endcap and forward regions, LAr calorimeters with copper or tungsten absorbers are used for electromagnetic and hadronic shower measurements up to $|\eta| = 4.9$. The outermost layer of the ATLAS detector is the muon spectrometer. It consists of separate trigger and high-precision tracking chambers, operating in a magnetic field generated by three large air-core toroidal superconducting magnets with eight coils each.

To select and record interesting events, a two-level trigger system is used. The level-1 trigger is implemented in custom hardware. It uses information from the calorimeters and the muon spectrometer to reduce the

² ATLAS uses a right-handed coordinate system with its origin at the nominal interaction point (IP) in the centre of the detector and the z -axis along the beam pipe. The x -axis points from the IP to the centre of the LHC ring, and the y -axis points upwards. Cylindrical coordinates (r, ϕ) are used in the transverse plane, ϕ being the azimuthal angle around the z -axis. The pseudorapidity is defined in terms of the polar angle θ as $\eta = -\ln \tan(\theta/2)$. Angular distance is measured in units of $\Delta R \equiv \sqrt{(\Delta\eta)^2 + (\Delta\phi)^2}$.

event rate to below 100 kHz. This is followed by the high-level trigger (HLT), which is fully software-based. It is used to further reduce the event rate to 1 kHz on average.

An extensive software suite [27] is used in data simulation, in the reconstruction and analysis of real and simulated data, in detector operations, and in the trigger and data acquisition systems of the experiment.

3 Data and simulated event samples

The dataset used by the analysis was collected with the ATLAS detector during proton–proton collisions at a centre-of-mass energy $\sqrt{s} = 13$ TeV during Run 2 of the LHC (2015–2018). The recorded data correspond to an integrated luminosity of 139 fb^{-1} . A set of data-quality requirements are applied to the dataset to ensure that the LHC beam conditions were stable and the ATLAS detector was fully functional [28]. All data events considered by this analysis are required to pass a combined di- $\tau_{\text{had-vis}} + E_{\text{T}}^{\text{miss}}$ trigger [29, 30], where $\tau_{\text{had-vis}}$ is the visible part of a hadronically decaying τ -lepton.

The analysis uses Monte Carlo (MC) simulation to model 2HDM+ a signal events and the majority of SM the backgrounds. The ATLAS simulation framework [31] was used to produce all of the MC samples. A full detector-response simulation based on GEANT4 [32] is used. This section describes the technical details of the MC samples, which are also summarised in Table 1.

Table 1: Summary of the generators used to simulate the background processes considered in the analysis. The ‘dedicated’ tune refers to the set of tuned parton-shower parameters developed by the SHERPA authors. The symbol ‘V’ stands for a vector boson.

Physics process	Generator	Parton Shower	Accuracy	Tune	PDF (generator)	PDF (PS)
$Z(\rightarrow \ell\ell)$ +jets	SHERPA 2.2.1 [33]	SHERPA 2.2.1 [34]	NNLO [35]	Dedicated	NNPDF3.0NNLO [36]	NNPDF3.0NNLO [36]
$W(\rightarrow \ell\nu)$ +jets	SHERPA 2.2.1 [33]	SHERPA 2.2.1 [34]	NNLO [35]	Dedicated	NNPDF3.0NNLO [36]	NNPDF3.0NNLO [36]
Diboson	SHERPA 2.2.1, 2.2.2 [33]	SHERPA 2.2.1, 2.2.2 [34, 37]	NLO [38–41]	Dedicated	NNPDF3.0NNLO [36]	NNPDF3.0NNLO [36]
$t\bar{t}$	POWHEG Box v2 [42–45]	PYTHIA 8.230 [46]	NNLO+NNLL [47–53]	A14 [54]	NNPDF3.0NNLO [36]	NNPDF2.3LO [55]
Single-top:						
Wt	POWHEG Box v2 [43–45, 56]	PYTHIA 8.230 [46]	NLO+NNLL [57, 58]	A14 [54]	NNPDF3.0NNLO [36]	NNPDF2.3LO [55]
s - and t -channels	POWHEG Box v2 [43–45, 56]	PYTHIA 8.230 [46]	NLO [59, 60]	A14 [54]	NNPDF3.0NNLO [36]	NNPDF2.3LO [55]
$t\bar{t}+H$	POWHEG Box v2 [42–45, 61]	PYTHIA 8.230 [46]	NLO [62]	A14 [54]	NNPDF3.0NNLO [36]	NNPDF2.3LO [55]
$t\bar{t}+V$	MADGRAPH5_AMC@NLO 2.3.3 [62]	PYTHIA 8.210 [46]	NLO [63]	A14 [54]	NNPDF3.0NNLO [36]	NNPDF2.3LO [55]
$VH(\rightarrow \tau\tau)$	POWHEG Box v2 [43–45, 64–66]	PYTHIA 8.212 [46]	NNLO + NLO [67–73]	AZNLO [74]	NNPDF3.0NNLO [36]	PDF4LHC15NNLO [75]

For the simulated samples of Z and W bosons produced in association with jets (Z +jets and W +jets) the SHERPA 2.2.1 [33] generator was employed. Next-to-leading-order (NLO) matrix elements were used for up to two partons, while leading-order (LO) matrix elements were used for up to four partons. The Comix [37] and OPENLOOPS [76–78] libraries were utilised for their computation. SHERPA parton showers [34] were employed, with the MEPS@NLO prescription [38–41] used to match the parton showers to the matrix elements. The NNPDF3.0NNLO set of parton distribution functions (PDFs) [36] was utilised, and the samples were normalised to next-to-next-to-leading-order (NNLO) cross-section predictions [35].

Samples of diboson and triboson production were simulated with the SHERPA 2.2.1 or 2.2.2 [33] generator, depending on the process. The matrix elements were matched and merged with the SHERPA parton showers based on Catani–Seymour dipole factorisation [34, 37] using the MEPS@NLO prescription [38–41]. The OPENLOOPS library [76–78] was used to provide the virtual QCD corrections to the matrix elements where relevant. The samples were generated with the NNPDF3.0NNLO PDF set [36].

All SHERPA-produced samples used a dedicated set of tuned parton-shower parameters developed by the SHERPA authors [34, 37].

Higgs boson production and decay were simulated using the POWHEG BOX v2 [43–45, 64–66] generator interfaced with PYTHIA 8 [46] for parton showering and non-perturbative effects. The PDF4LHC15_{NLO} PDF set [75] and the AZNLO tune [74] of PYTHIA 8 were used. The gluon–gluon fusion prediction from POWHEG was normalised to the next-to-next-to-next-to-leading-order cross-section in QCD plus electroweak corrections at NLO [63, 79–88]. The vector-boson fusion prediction was normalised to an approximate-NNLO QCD cross-section with NLO electroweak corrections [89–91]. The Monte Carlo prediction of Higgs boson production in association with a vector boson was normalised to cross-sections calculated at NNLO in QCD with NLO electroweak corrections for $q\bar{q}/qg \rightarrow VH$ and at NLO and next-to-leading-logarithm accuracy in QCD for $gg \rightarrow ZH$ [67–73].

The production of top–antitop quark ($t\bar{t}$) events was simulated with the POWHEG BOX v2 [42–45] generator at the NLO accuracy. The NNPDF3.0_{NLO} [36] PDF set was used, m_{top} was set to 172.5 GeV, and the h_{damp} parameter was fixed at $1.5 m_{\text{top}}$ [92]. PYTHIA 8.230 [46] with the A14 tune [54] was used to model the parton shower, hadronisation, and underlying event. The NNPDF2.3_{LO} [55] PDF set was used.

Single-top-quark processes were similarly modelled with the POWHEG BOX v2 [43–45, 56] generator using the NNPDF3.0_{NLO} set of PDFs [36]. The associated production of a top quark with a W boson (Wt) and s -channel production utilised the five-flavour scheme, while the t -channel production used the four-flavour scheme. For Wt processes the diagram removal scheme [93] was used to remove interference with the $t\bar{t}$ samples. The events were then interfaced to PYTHIA 8.230 [46], which used the A14 tune [54] and the NNPDF2.3_{LO} set of PDFs [55]. The same configuration also applies to the production of $t\bar{t}H$ events.

The inclusive cross-sections for the previously described top-quark process samples were corrected to include higher-order effects. For $t\bar{t}$, the cross-section was calculated to NNLO in perturbative QCD with the resummation of next-to-next-to-leading logarithmic (NNLL) soft-gluon terms using the TOP++ program [47–53]. For Wt events, the corrections were to NLO+NNLL accuracy [57, 58], while s - and t -channel production was corrected to NLO accuracy [59, 60]. The $t\bar{t}H$ cross-section was corrected to NLO QCD+electroweak accuracy [63].

The $t\bar{t}V$ ($V = Z, W$) samples were produced with the MADGRAPH5_AMC@NLO 2.3.3 [62] generator at NLO accuracy using the NNPDF3.0_{NLO} [36] PDF set. The matrix elements were interfaced with PYTHIA 8.210 [46]. The A14 tune [54] and the NNPDF2.3_{LO} [36] PDF set were used.

Decays of bottom and charm hadrons for top-quark processes, including $t\bar{t}H$, were performed by EVTGEN 1.6.0 [94].

For the 2HDM+ a samples, the matrix elements were generated with MADGRAPH5_AMC@NLO 2.6.5 [62] at LO. PYTHIA 8.240 [46] with the A14 tune [54] was used to model the parton shower, hadronisation and underlying event. The CKKW-L merging procedure [95, 96] was employed to match the matrix element to the parton showers. Signal Monte Carlo samples were generated with the NNPDF3.0_{NLO} PDF set [55] and processed with a fast simulation that relies on a parameterisation of the calorimeter response [31]. Both the gluon–gluon fusion and $b\bar{b}$ annihilation signal production processes were considered.

The 2HDM+ a samples were generated with different choices of signal model parameters, varying two parameters at a time. In the first parameter scan, the pseudoscalar singlet mass m_a was varied in the range [100, 400] GeV while the mass of the pseudoscalar Higgs boson m_A was varied in the range [300, 1400] GeV. The requirements $\tan\beta = 1$ and $\sin\Theta = 0.35$ were applied. In the second parameter scan, m_A was varied in the range [500, 1300] GeV with $\tan\beta$ taking values from 0.3 to 20. In this scan, constant values of $m_a = 250$ GeV and $\sin\Theta = 0.7$ were used. The particular parameter choices are based on the recommendations from the LHC DM Working Group [22].

For all simulated samples, the effect of multiple interactions in the same and neighbouring bunch crossings (pile-up) was modelled by overlaying each simulated hard-scattering event with inelastic proton–proton events generated with PYTHIA 8.186 [97] using the NNPDF2.3LO set of PDFs [55] and the A3 tune [98].

To compensate for differences between data and simulation, dedicated per-object correction factors derived from data are applied to jets, b -jets, τ -leptons, electrons, and muons. Additional per-event correction factors are applied to account for differences in trigger efficiency between data and simulation.

4 Event reconstruction

An event is considered to have a primary vertex if at least two ID tracks with $p_T > 500$ MeV can be associated with it [99]. If there are several such vertices, the candidate with the highest sum of the squared transverse momenta of associated tracks, Σp_T^2 , is considered as the hard-scattering vertex.

Jet candidates are reconstructed from particle-flow objects [100] using the anti- k_t algorithm [101] with a distance parameter of $R = 0.4$. First, the calorimeter cells are grouped into topological clusters, with the energy measured at the electromagnetic scale to which all ATLAS calorimeters are calibrated. The energy deposited by the charged particles is then subtracted from the clusters and replaced by the momenta of matching tracks. The jet energy scale (JES) [102] calibration is applied to the jet candidates, restoring the energy to that measured at particle level. The jets are required to have a transverse momentum larger than 20 GeV and $|\eta| < 2.5$. In addition, jets with $p_T < 60$ GeV are required to pass the *tight* working point of the jet-vertex-tagger (JVT) algorithm [103] to suppress background from pile-up interactions.

The analysis aims for a selection orthogonal to that of the mono-Higgs search with b -jets [12], so robust b -tagging with the same selection efficiency is important. Jets containing b -hadrons are identified as b -jets using the classification algorithm DL1r [104] based on deep-learning techniques. The DL1r tagger uses secondary-vertex displacement information and kinematic properties of tracks to select b -jets and reject jets originating from charm or light quarks. The b -tagging working point used for the analysis has an efficiency of 77%, as measured in an inclusive $t\bar{t}$ sample, while providing rejection factors of 4.9, 14 and 130 against c -jets, τ -jets, and light-flavour jets, respectively [105].

Electrons are reconstructed from energy deposits in the electromagnetic calorimeter that are matched to an ID track. Electron candidates are required to satisfy the *loose* identification criteria [106, 107], and to have $p_T > 10$ GeV and $|\eta| < 2.47$, providing selection efficiency of 93%. Additionally, the longitudinal impact parameter z_0 has to satisfy $|z_0 \sin \theta| < 0.5$ mm to discard electron candidates not associated with the primary vertex. The objects meeting these selection criteria are called baseline electrons and participate in the computation of the missing transverse momentum and in the overlap-removal procedure, as described later. Baseline electrons that also satisfy $p_T > 25$ GeV, fulfil the *loose* isolation criteria and the *tight* identification criteria, and satisfy the condition $|d_0|/\sigma(d_0) < 5$ on the transverse impact parameter d_0 and its uncertainty $\sigma(d_0)$ are henceforth simply referred to as electrons.

Muons are reconstructed from tracks in the muon spectrometer that are matched to tracks in the ID. Muon candidates are required to satisfy the *medium* identification criteria [108, 109] and to have $p_T > 10$ GeV and $|\eta| < 2.7$. This working point has an efficiency of 97%. Additionally, the longitudinal impact parameter has to satisfy $|z_0 \sin \theta| < 0.5$ mm. The objects meeting these selection criteria are called baseline muons and participate in the computation of the missing transverse momentum and in the overlap-removal procedure. Baseline muons that also satisfy $p_T > 25$ GeV, fulfil the *loose* isolation criteria, and satisfy the condition $|d_0|/\sigma(d_0) < 3$ are henceforth simply referred to as muons.

Reconstruction of the visible part of a hadronically decaying τ -lepton [110] is seeded by anti- k_r jets with a distance parameter $R = 0.4$. The seed jet is built from topological clusters, calibrated with a hadronic weighting scheme [111], and is required to have $p_T > 10$ GeV and $|\eta| < 2.5$. The $\tau_{\text{had-vis}}$ candidate is then built from tracks and clusters within $\Delta R = 0.2$ of the seed jet's axis. Only candidates with one or three charged tracks with a sum of ± 1 are considered. $\tau_{\text{had-vis}}$ candidates are required to have $p_T > 20$ GeV and $|\eta| < 2.5$. Candidates in the transition region between the barrel and endcap calorimeters, $1.37 < |\eta| < 1.52$, are excluded. The $\tau_{\text{had-vis}}$ object's energy is calibrated with a boosted regression tree using information from the calorimeter and the particle-flow reconstruction, as well as the number of pile-up interactions [112], as input. To suppress electron background, a boosted decision tree is used to reject events with electrons misidentified as $\tau_{\text{had-vis}}$. It is trained using tracking detector and calorimeter information as well as variables related to the ratio of the energy deposited in the calorimeter and the visible momentum of the reconstructed tracks.

To further discriminate hadronically decaying τ -leptons from background jets, a recurrent neural network (RNN) algorithm is used [113]. The algorithm uses tracking and calorimeter measurement information, as well as individual track and cluster information, as input. The analysis makes use of three different ways to define τ -lepton objects using the RNN algorithm. The first type of object (baseline τ -lepton) is required to pass the *very loose* identification working point. These objects are used in the overlap-removal procedure. The baseline τ -leptons that also pass the *medium* identification working point are simply referred to as τ -leptons. The last type of object considered by the analysis consists of τ -lepton candidates that do not pass the *medium* identification working point. Such objects are referred to as anti-ID τ -leptons and are used by the analysis to estimate the contribution of fake τ -leptons.

The missing transverse momentum E_T^{miss} is a measure of the transverse-momentum imbalance in the detector and is computed as the magnitude of the missing transverse momentum vector \vec{p}_T^{miss} [114]. The latter is calculated as the negative vector sum of the transverse momenta of electrons, muons, τ -leptons and jets. Tracks that are associated with the primary vertex but not with any reconstructed object are also included in the calculation as the so-called 'soft term'.

The reconstructed objects are not exclusive, e.g. a single energy deposit in the calorimeter can be used in the reconstruction of several final-state objects. In order to resolve this ambiguity, an overlap-removal procedure is applied [115] so that at most one reconstructed object is associated with a detector signal:

- If two baseline electrons share a track, only the baseline electron with the higher transverse momentum is considered.
- A baseline τ -lepton is discarded if it is closer than $\Delta R = 0.2$ to a baseline electron or a muon.
- If a baseline muon and a baseline electron share an ID track the baseline electron is discarded. The only exception is when the baseline muon is calorimeter-tagged (i.e. a track in the ID matched to an energy deposit in the calorimeter compatible with a minimum-ionizing particle [108, 109]), then the baseline muon is discarded instead.
- If a jet is closer than $\Delta R = 0.2$ to a baseline electron or muon, it is discarded. The only exception is if the jet has three or more associated tracks, in which case it is kept instead of the baseline muon. This suppresses FSR and bremsstrahlung signatures that can be reconstructed as jets with low number of tracks.
- If any of the remaining baseline electrons or muons are closer than $\Delta R = 0.4$ to the remaining jets, they are discarded.

- If any of the remaining jets is closer than $\Delta R = 0.2$ to any of the remaining baseline τ -leptons, the jet is discarded.

For anti-ID τ -lepton candidates the overlap-removal procedure is performed in the same way, replacing the baseline τ -lepton identification criterion with that for anti-ID τ -leptons. However, two additional corrections are needed for the overlap-removal procedure compared to the one applied to baseline τ -leptons. First, the jets that do not pass the *tight* JVT working point selection requirements are given a priority over anti-ID τ -leptons not meeting the *very loose* identification criterion. This is done so that such jets are not masked by being treated as anti-ID τ -lepton candidates and can be vetoed successfully. The second correction is to give the same priority to b -jets. Otherwise, anti-ID τ -leptons can mask b -jets, whereas the analysis relies on an accurate counting of the number of b -jets.

5 Event selection

Data and simulated events are categorised in regions based on the properties of the reconstructed objects. The analysis uses three types of regions – control, validation, and signal regions. Signal regions (SRs) are regions where the sensitivity to the BSM signal model is maximised. Control regions (CRs) are regions enriched in particular background processes and are kinematically close to the SRs. A background-only fit of the simulated background processes to the data is performed in CRs using the HISTFITTER framework [116]. In this fit the normalisation of the dominant background processes is determined. The fitted normalisations are then propagated to the validation regions (VRs) and SRs. VRs are defined so that they lie between the SRs and CRs and serve to validate the extrapolation of background normalisation from the CRs to the SRs. The results of the background-only fit are discussed further in Section 8.

Events used by the analysis are required to have a primary vertex. The events are also required to pass a jet quality criterion to reject events containing jets not originating from proton–proton collisions [117], but from beam-induced backgrounds or cosmic-ray showers.

Events are required to have exactly two τ -lepton objects that geometrically match the objects activating the di- $\tau_{\text{had-vis}}$ part of the triggers. Both the $E_{\text{T}}^{\text{miss}}$ and the di- $\tau_{\text{had-vis}}$ parts of the trigger evolved during Run 2 to implement more efficient algorithms and adapt them to the data-taking conditions. While the HLT $E_{\text{T}}^{\text{miss}}$ trigger requirement was kept constant at 50 GeV, the level-1 threshold was increased from 35 to 40 GeV in 2018. The HLT threshold for the leading- $\tau_{\text{had-vis}}$ p_{T} was increased from 35 GeV to 60 GeV in 2018, while the sub-leading- $\tau_{\text{had-vis}}$ p_{T} threshold remained constant at 25 GeV. The HLT $\tau_{\text{had-vis}}$ identification algorithms were improved during Run 2, resulting in increased rejection power. The leading τ -lepton is required to have $p_{\text{T}} > 40(65)$ GeV when matched to the HLT $\tau_{\text{had-vis}}$ object passing the trigger’s 35(60) GeV threshold. The sub-leading τ -lepton is required to have $p_{\text{T}} > 30$ GeV. The events also have to satisfy the $E_{\text{T}}^{\text{miss}} > 150$ GeV requirement at which the trigger is operating at maximum efficiency.

Events containing an electron or a muon are vetoed. Events are required to have at most one b -jet. The common analysis preselection is summarised in Table 2, defining the analysis phase space. In the following, the analysis objects in an event are assumed to be ordered by decreasing transverse momentum with indices ‘1’ and ‘2’ referring to the leading and sub-leading objects respectively.

In order to improve the sensitivity to the 2HDM+ a signal models considered, two SRs are defined. This is done in two steps. First, a set of common SR preselection requirements is applied to suppress the dominant SM processes. After the common preselection, two non-orthogonal SRs are designed to target signal model parameter configurations with high and low masses of the heavy pseudoscalar Higgs boson A , as these

Table 2: Summary of the common analysis preselection. The upper part contains requirements related to optimising the trigger efficiency while the lower part contains analysis signature-related requirements.

Observable	Selection	
Year	2015–2017	2018
$p_T^{\tau_1}$	> 40 GeV	> 65 GeV
$p_T^{\tau_2}$	> 30 GeV	
E_T^{miss}	> 150 GeV	
N_τ	2	
N_e	0	
N_μ	0	
$N_{b\text{-jet}}$	≤ 1	

yield signal events with different kinematic properties. The combination of the results from the two SRs is described in Section 8.

The common SR preselection includes a veto on events with b -jets and a requirement that the two τ -leptons have opposite electric charges. The invariant mass of the two $\tau_{\text{had-vis}}$, or ‘visible invariant mass’ $m_{\text{vis}}(\tau_1, \tau_2)$, is constrained to be between 40 GeV and 125 GeV to ensure compatibility with a Higgs boson decay. The angular distance between the two τ -leptons is required to satisfy $\Delta R < 2$, suppressing background events in which the two τ -leptons do not originate from a resonant decay (such as $t\bar{t}$ and W +jets). Two kinematic variables combining E_T^{miss} and the τ -leptons’ p_T are used to suppress Z +jets events. The event-level m_T^{tot} is defined as

$$m_T^{\text{tot}} = \sqrt{(p_T^{\tau_1} + p_T^{\tau_2} + p_T^{\text{miss}})^2 - (p_x^{\tau_1} + p_x^{\tau_2} + p_x^{\text{miss}})^2 - (p_y^{\tau_1} + p_y^{\tau_2} + p_y^{\text{miss}})^2},$$

where p_x^{miss} and p_y^{miss} correspond to the x and y components of the missing transverse momentum vector. An event is required to have $m_T^{\text{tot}} > 50$ GeV to pass the common SR preselection, while $m_T^{\text{tot}} < 50$ GeV selection is used for trigger efficiency studies. The transverse mass of a τ -lepton is a per-object variable defined as

$$m_T^{\tau_i} = \sqrt{2p_T^{\tau_i} E_T^{\text{miss}} (1 - \cos \Delta\phi(\tau_i, p_T^{\text{miss}}))}.$$

The sum $m_T^{\tau_1} + m_T^{\tau_2}$ is required to be larger than 100 GeV to suppress events in which E_T^{miss} is collinear with the two- τ -lepton system, as this is typical for Z boson event topologies. A summary of the common SR preselection is presented in the upper part of Table 3.

A ‘Low $_{m_A}$ ’ SR is defined on top of the common SR preselection to target signal models with $m_A \leq 800$ GeV. The angular distance between the two τ -leptons is tightened to be $0.6 < \Delta R(\tau_1, \tau_2) < 1.9$ and the visible invariant mass of the two τ -leptons is required to be larger than 75 GeV. The transverse masses of the leading and sub-leading τ -leptons are required to be $m_T^{\tau_1} > 50$ GeV and $m_T^{\tau_2} > 25$ GeV. The SR is divided into four $m_T^{\tau_1} + m_T^{\tau_2}$ bins: < 250 GeV, $[250, 400]$ GeV, $[400, 550]$ GeV, and > 550 GeV.

A ‘High $_{m_A}$ ’ SR is constructed to improve the sensitivity to models with high m_A masses, leading to signal events with higher E_T^{miss} and boosted Higgs bosons. In addition to the common SR preselection, this SR requires $m_T^{\text{tot}} > 400$ GeV and $m_T^{\tau_1} + m_T^{\tau_2} > 400$ GeV. Similarly to the Low $_{m_A}$ SR, the events in the High $_{m_A}$ SR are separated in two $m_T^{\tau_1} + m_T^{\tau_2}$ bins, above and below 750 GeV.

Table 3: Summary of the selection requirements used to define the signal regions. The upper part of the table describes the common SR preselection while the lower part of the table describes specific selections to define the Low_{m_A} and High_{m_A} SRs. These are applied in addition to the common analysis preselection described in Table 2.

Common SR Preselection		
$\Delta R(\tau_1, \tau_2)$	< 2	
m_T^{tot}	$> 50 \text{ GeV}$	
$m_{\text{vis}}(\tau_1, \tau_2)$	$\in [40, 125] \text{ GeV}$	
$m_T^{\tau_1} + m_T^{\tau_2}$	$> 100 \text{ GeV}$	
Charge(τ_1, τ_2)	$q(\tau_1) \times q(\tau_2) = -1$	
$N_{b\text{-jet}}$	0	
	Low_{m_A} SR	High_{m_A} SR
$\Delta R(\tau_1, \tau_2)$	$\in [0.6, 1.9]$	< 2
m_T^{tot}	-	$> 400 \text{ GeV}$
$m_T^{\tau_1}$	$> 50 \text{ GeV}$	-
$m_T^{\tau_2}$	$> 25 \text{ GeV}$	-
$m_{\text{vis}}(\tau_1, \tau_2)$	$> 75 \text{ GeV}$	$\in [40, 125] \text{ GeV}$
$m_T^{\tau_1} + m_T^{\tau_2}$ binning	$[100, 250, 400, 550, \infty] \text{ GeV}$	$[400, 750, \infty] \text{ GeV}$

A summary of the High_{m_A} and Low_{m_A} SRs' requirements is presented in the lower part of Table 3. Examples of kinematic distributions of the important variables ($\Delta R(\tau_1, \tau_2)$, $m_{\text{vis}}(\tau_1, \tau_2)$, m_T^{tot} , $m_T^{\tau_1}$) after applying the common SR preselection are shown in Figure 2. The way the SM background estimations are performed is described in Section 6. Predictions from four benchmark parameter configurations of the 2HDM+ a model normalised to the theoretical cross-section and the integrated luminosity of the data are also shown in Figure 2.

The combined acceptance and efficiency of the Low_{m_A} SR bins varies from 0.0013 to $3 \cdot 10^{-6}$ over all of the parameter configurations of the 2HDM+ a model considered by the analysis for gluon–gluon fusion production. For the High_{m_A} SR bins the combined acceptance and efficiency varies from 0.0023 to 0 because the High_{m_A} SR is only designed to be sensitive to a subset of all the parameter configurations.

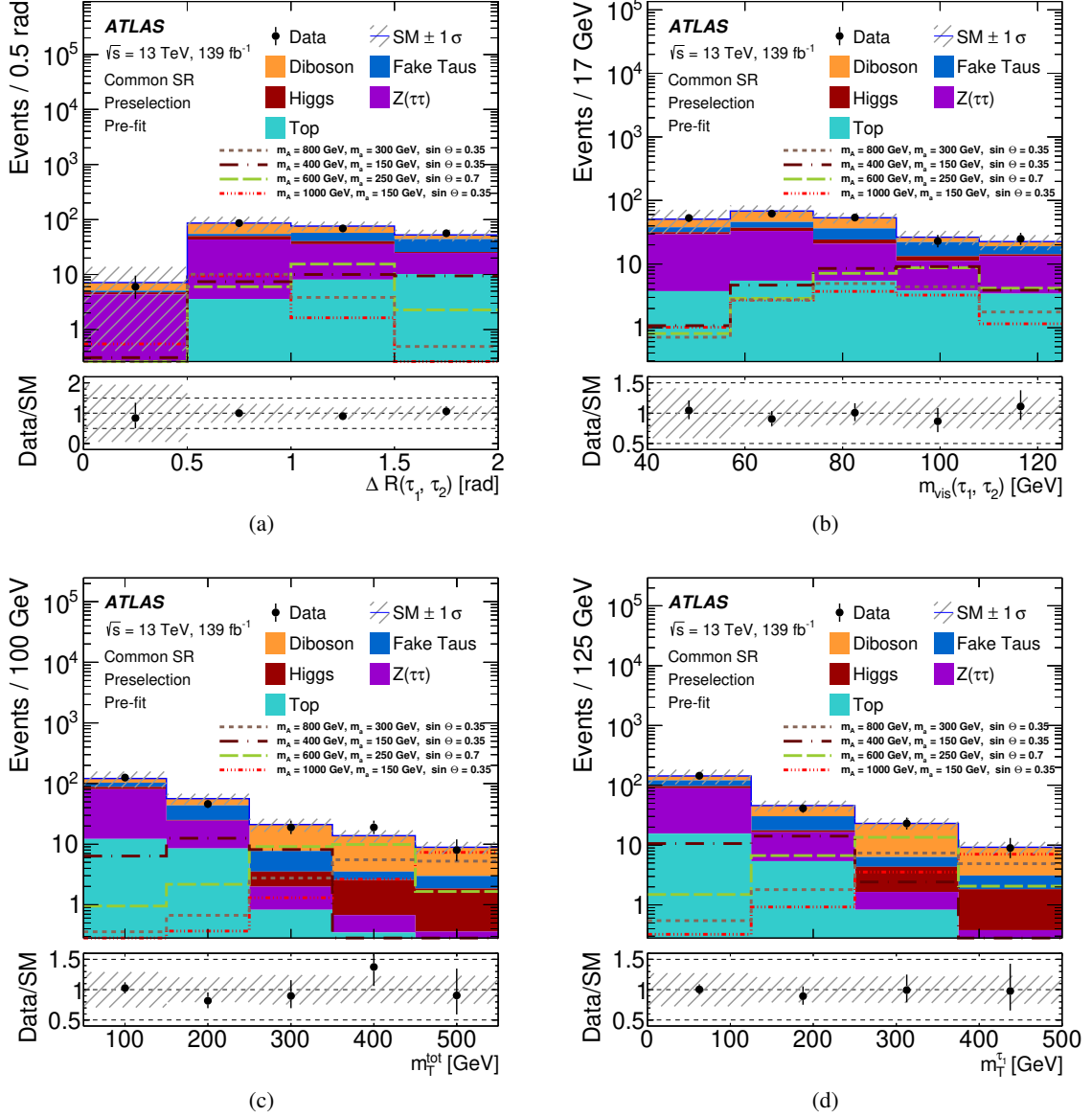


Figure 2: Kinematic distributions of some of the variables used to construct the SRs, shown in the common SR preselection region: (a) $\Delta R(\tau_1, \tau_2)$, (b) $m_{\text{vis}}(\tau_1, \tau_2)$, (c) m_T^{tot} , (d) $m_T^{\tau_1}$. Predictions for four benchmark parameter configurations of the 2HDM+a model are also shown for the parameter values given in the legend. The value $\tan(\beta) = 1$ is assumed for all parameter configurations. The total statistical and systematic uncertainty of the SM background is shown by the hatched band. The leftmost and rightmost bins include the underflow and overflow entries respectively. The ratio of the observed yield to the expected yield is shown in the lower panel.

6 Background estimation

Two sources of events are distinguished to perform the SM background estimation – those with both reconstructed $\tau_{\text{had-vis}}$ objects originating from the hadronic decays of prompt τ -leptons (true τ -leptons), and events with at least one of the reconstructed $\tau_{\text{had-vis}}$ objects being a non- τ -lepton object that satisfied the selection criteria, also referred to as a fake τ -lepton. Events from Z boson and multiboson production, and the majority of $t\bar{t}$ events, tend to have two true τ -leptons in the analysis phase space. Events from both W boson and multijet production, as well as approximately 25% of $t\bar{t}$ events, are expected to have at least one fake τ -lepton.

SM background processes are modelled using a combination of simulated events and data-driven methods. Events with only true τ -leptons are modelled using simulation normalised to the data in the dedicated CRs. In the following, when referring to the $t\bar{t}$ background modelling, for example, it is only the events with two true τ -leptons that are being addressed. Events with at least one fake τ -lepton are estimated in a data-driven way. Such events are referred to as fake τ -leptons or ‘Fake Taus’ background regardless of the underlying physical process.

The normalisation of Z boson production and various processes including top-quark production ($t\bar{t}$ production, single-top-quark production, $t\bar{t}$ production in association with Z/W) is fitted to the data in dedicated control regions. Other SM background contributions are normalised according to the theoretical predictions. For the derivation of the normalisation scale factors all top-quark-related processes are treated as one common ‘Top’ background.

The contribution of fake τ -lepton events (i.e. events with at least one fake τ -lepton) in the control, validation and signal regions is estimated with the fake factor method [118]. The assumption is that the probability that a non- τ -lepton object (such as a jet) meets the τ -lepton identification criteria depends purely on the object’s properties, such as its p_T , η , number of charged-particle tracks, and origin (i.e. quark/gluon), and not on event-level variables such as E_T^{miss} or number of τ -leptons. The ratio of the number of objects that pass the *medium* identification working point requirement to the number of objects that do not, but instead pass the much looser anti-ID τ -lepton selection, is called the fake factor. The fake factors were measured as a function of τ -lepton’s p_T , $|\eta|$, number of charged-particle tracks, and origin in regions enriched with fake τ -leptons and extrapolated to the analysis phase space. In the analysis regions with the τ -lepton selection requirement replaced by that for anti-ID τ -leptons, the fake factors are applied to the anti-ID τ -leptons to obtain a prediction of the fake τ -lepton background.

The Fake Tau VR is used to validate the modelling of fake τ -leptons. The events are required to have been recorded by the di- $\tau + E_T^{\text{miss}}$ trigger, to pass the common analysis preselection as described in Table 2, and to have no b -jets. To increase the fake τ -lepton purity of this VR, the two τ -leptons are required to have the same charge. The two τ -leptons are also required to have $\Delta R(\tau_1, \tau_2) < 2$ to remain kinematically close to the SRs. This selection ensures that the Fake Tau VR has a purity of over 85%.

Two CRs are defined by inverting or relaxing some of the common SR requirements (see Table 3) such that they are kinematically close to the SRs, suppress a potential signal contribution, and are enriched in Z boson and $t\bar{t}$ backgrounds respectively. Additionally, the analysis uses four VRs. Kinematically, the VRs are defined to be between the CRs and SRs and serve to validate the extrapolation of the modelling from the CRs to the SRs. The definitions of CRs and VRs are summarised in Table 4 and are further discussed in the following.

Table 4: Definitions of control and validation regions used by the analysis. The requirements are applied on top of the preselection described in Table 2. Entries in boldface indicate selections ensuring orthogonality to other regions. A dash is used when no requirements are placed on a variable. OS and SS stand for opposite-sign and same-sign τ -leptons respectively. ‘Comb VR’ refers to an inclusive validation region containing several important backgrounds.

Variable	Z CR	Z VR	Fake Tau VR	Top CR	Comb VR	Diboson VR
Charge(τ_1, τ_2)	OS	OS	SS	OS	OS	OS
$N_{b\text{-jet}}$	0	0	0	1	0	0
$\Delta R(\tau_1, \tau_2)$	< 2	< 2	> 2	> 1	> 2	< 2
$m_{\text{vis}}(\tau_1, \tau_2)$	< 40 GeV	[40, 75] GeV	-	-	> 125 GeV	[40, 75] GeV
$m_{\text{T}}^{\text{tot}}$	> 50 GeV	> 50 GeV	-	-	-	[50, 400] GeV
$m_{\text{T}}^{\tau_1}$	-	-	-	-	-	> 60 GeV
$m_{\text{T}}^{\tau_2}$	-	-	-	-	-	> 20 GeV
$m_{\text{T}}^{\tau_1} + m_{\text{T}}^{\tau_2}$	-	< 100 GeV	-	-	-	> 140 GeV
p_{T}	-	-	-	-	< 125 GeV	-

Figure 3 shows examples of kinematic distributions from the Top and Z CRs. The predicted background yields are shown without performing the fit and applying the resulting normalisation factors to the SM backgrounds (as described earlier in Section 5). Good agreement between the predicted and observed yields is seen in all plots.

In the analysis phase space, approximately 80% of background events with a top quark arise from $t\bar{t}$ processes; the remaining events come from single-top processes. Events in the Top CR are selected using the di- $\tau + E_{\text{T}}^{\text{miss}}$ triggers and are required to pass the common analysis preselection summarised in Table 2. To define a region enriched in $t\bar{t}$ while suppressing other common background processes such as Z+jets, the b -jet veto common to all other regions used in the analysis is relaxed and the events are required to have exactly one b -jet instead. The angular distance between the two τ -leptons is required to be $\Delta R(\tau_1, \tau_2) > 1$ to suppress Z boson background and to enhance the Top background purity of this CR. The two τ -leptons are also required to have opposite charges to suppress contributions from fake τ -leptons. The resulting Top CR has a top-quark background purity of over 90%, based on information from MC simulation, with over 70% of events containing two true τ -leptons. From simulation studies the majority of Top background events in the SRs (which all have a b -jet veto) are expected to have one jet that originated from a b -hadron but is not identified as such by the b -tagging algorithm. Similarly, the Top events in the Top CR are expected to have one or more jets originating from a b -hadron. Thus, the extrapolation from the Top CR to the SRs is physically meaningful because the same underlying processes are being considered.

Events from Z boson production constitute the largest background in the analysis phase space, and a high-purity region is straightforward to define. Events in the Z CR were recorded using the same trigger as in the SRs. The events are required to pass the common analysis preselection described in Table 2, and to have no b -jets. The two τ -leptons are required to have opposite charges and to satisfy $\Delta R(\tau_1, \tau_2) < 2$ and $m_{\text{vis}}(\tau_1, \tau_2) < 40$ GeV to improve the Z background purity. The events are also required to pass the $m_{\text{T}}^{\text{tot}} > 50$ GeV requirement. This results in the Z CR having 90% purity in Z boson background events.

While the SRs require $m_{\text{vis}}(\tau_1, \tau_2) > 40$ GeV, the Z CR demands $m_{\text{vis}}(\tau_1, \tau_2) < 40$ GeV. To validate the extrapolation to higher values of the di- τ visible invariant mass a Z VR is defined. The selection is similar to that of the Z CR, but the visible invariant mass must satisfy $40 \text{ GeV} < m_{\text{vis}}(\tau_1, \tau_2) < 75 \text{ GeV}$. To ensure orthogonality to the SRs, $m_{\text{T}}^{\tau_1} + m_{\text{T}}^{\tau_2}$ is required to be less than 100 GeV. The simulated events in the Z VR are affected by large theoretical systematic uncertainties. This is expected to be the case at large Z p_{T} ,

which is the regime where this analysis operates. Systematic uncertainties related to the estimation of Z events are discussed in Section 7.

The $\Delta R(\tau_1, \tau_2) > 2$ part of the analysis phase space has reasonably large expected Top and fake τ -lepton event yields. These two background processes are closely intertwined, considering that some of the fake τ -leptons originate from top-quark decays, and separating them is not practical. Instead, an inclusive validation region Comb VR is defined, containing Top, Fake Tau, Z boson, and diboson background processes. The Comb VR is defined by requiring that events are selected by the same trigger as used in the SRs, pass the common analysis preselection and have $\Delta R(\tau_1, \tau_2) > 2$. The charges of the two τ -leptons are required to be opposite and a b -jet veto is applied. The Comb VR also requires $m_{\text{vis}}(\tau_1, \tau_2) > 125$ GeV and $p_{\text{T}}^{\tau_1+\tau_2} < 125$ GeV in order to suppress potential signal contamination.

Diboson production is an important background process in the SRs. However, the overall event yields from diboson processes in the analysis phase space are too low to allow the construction of a statistically significant CR that wouldn't also be sensitive to potential signal contributions. Instead, a validation region is defined in order to validate the normalisation of the diboson backgrounds according to their cross-sections. The events in the Diboson VR are required to pass the common SR preselection described in the upper part of Table 3. The events are also required to have $m_{\text{T}}^{\tau_1} > 60$ GeV, $m_{\text{T}}^{\tau_2} > 20$ GeV, and $m_{\text{T}}^{\tau_1} + m_{\text{T}}^{\tau_2} > 140$ GeV to increase the diboson purity of this VR. To keep the Diboson VR orthogonal to the SRs, $m_{\text{vis}}(\tau_1, \tau_2) < 75$ GeV and $m_{\text{T}}^{\text{tot}} < 400$ GeV are required.

Figure 4 shows examples of kinematic distributions from the four VRs used by the analysis. The predicted background yields are shown without the derivation and extrapolation of normalisation factors in the CRs (as described in Section 5). The maximum contribution from potential signal models with the parameter choices considered by the analysis does not exceed 1% in the CRs and 10% in the VRs. The only exception is the Diboson VR, where the potential signal contribution can reach 35% of the total yield.

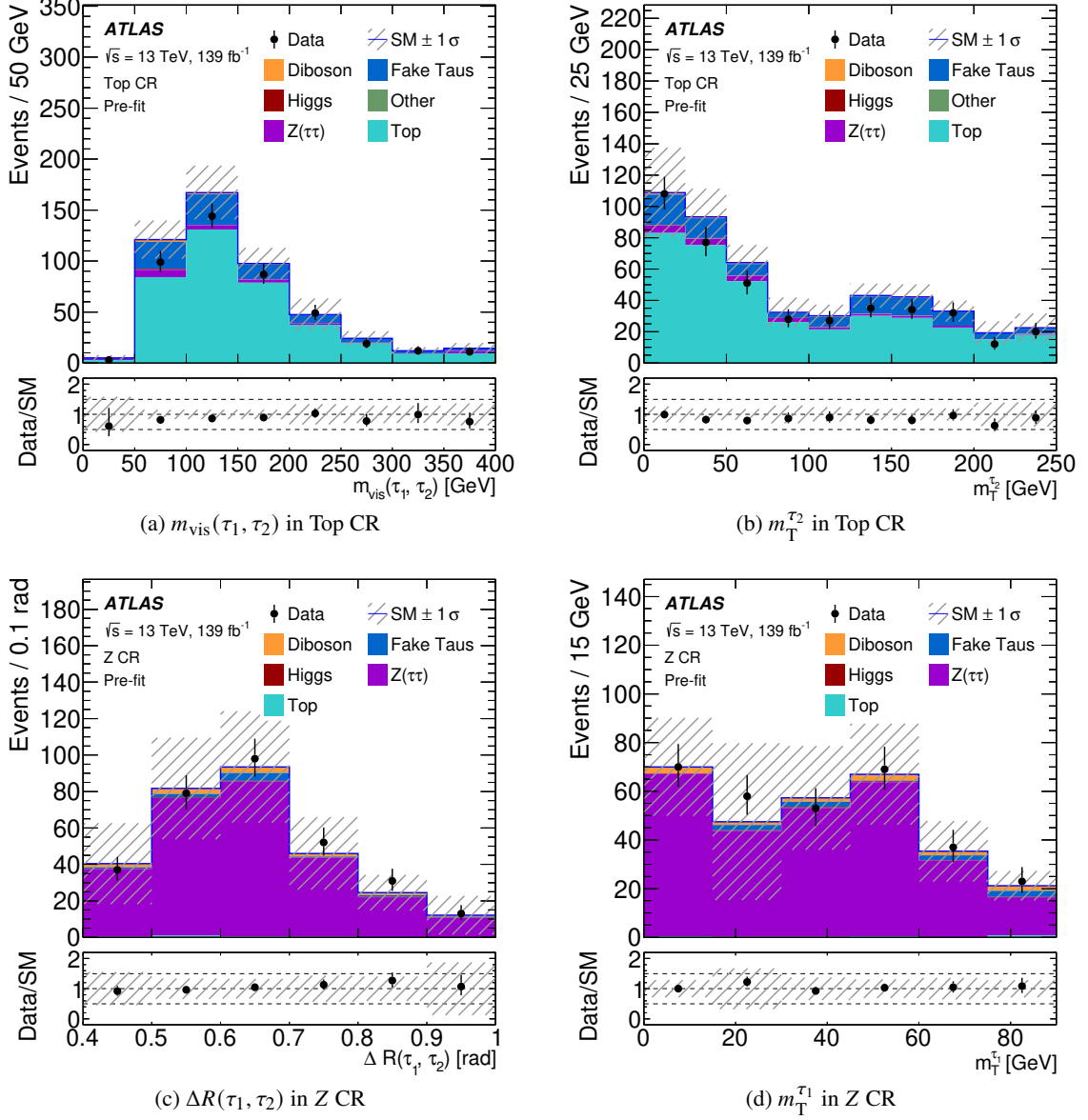


Figure 3: Kinematic distributions of some of the variables used to construct SRs are shown in the Top and Z CRs: (a) $m_{\text{vis}}(\tau_1, \tau_2)$ in Top CR, (b) $m_T^{\tau_2}$ in Top CR, (c) $\Delta R(\tau_1, \tau_2)$ in Z CR, (d) $m_T^{\tau_1}$ in Z CR. The total statistical and systematic uncertainty of the SM background is shown by the hatched band. The 'Other' contribution includes all the background processes not explicitly listed in the legend (V +jets except $Z(\tau\tau)$). The leftmost and rightmost bins include the underflow and overflow entries respectively. The ratio of the observed yield to the expected yield is shown in the lower panel.

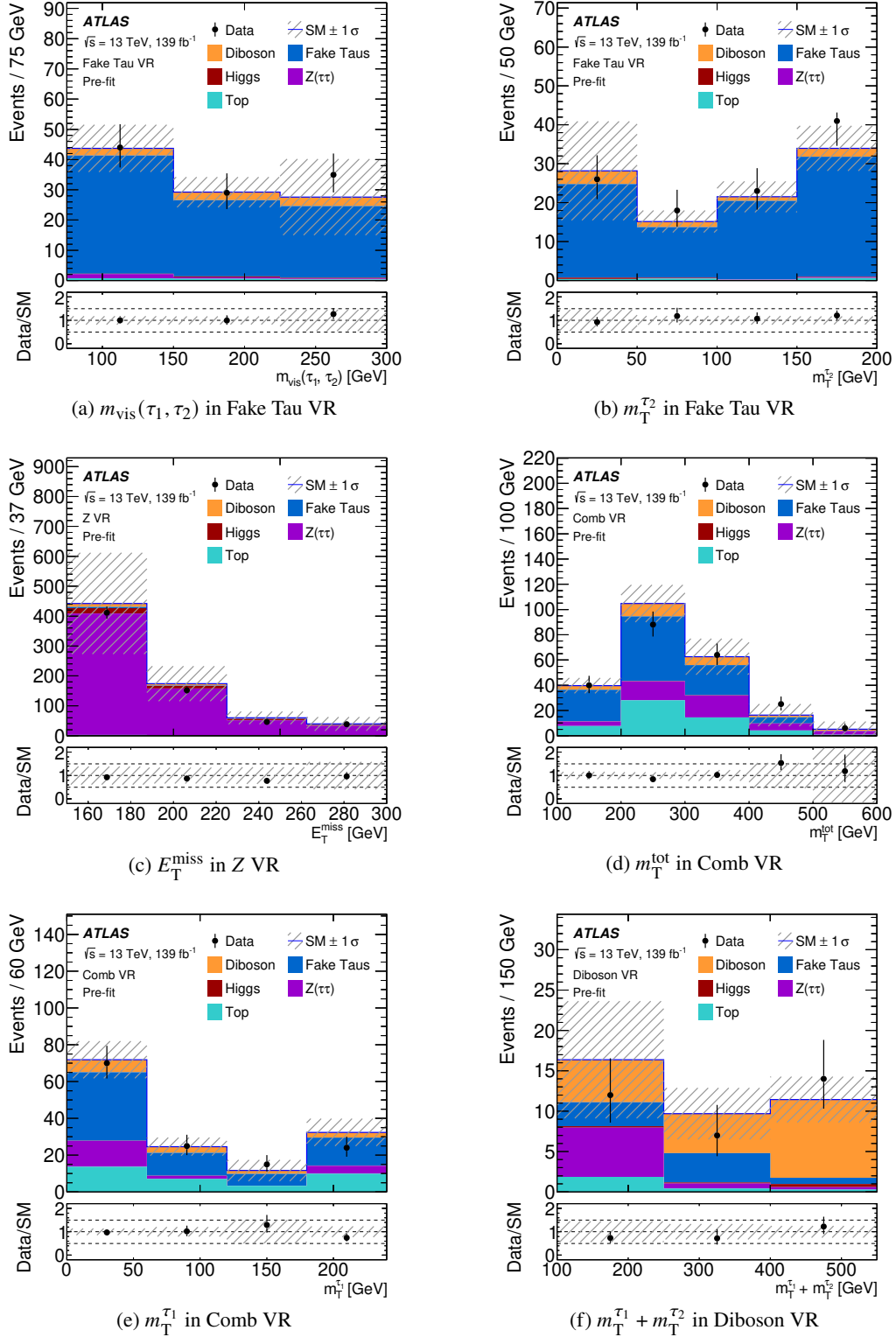


Figure 4: Kinematic distributions of some of the variables used to construct SRs are shown in the four VRs: (a) $m_{\text{vis}}(\tau_1, \tau_2)$ in Fake Tau VR, (b) $m_T^{\tau_2}$ in Fake Tau VR, (c) E_T^{miss} in Z VR, (d) m_T^{tot} in Comb VR, (e) $m_T^{\tau_1}$ in Comb VR, (f) $m_T^{\tau_1} + m_T^{\tau_2}$ in Diboson VR. The total statistical and systematic uncertainty of the SM background is shown by the hatched band. The leftmost and rightmost bins include the underflow and overflow entries respectively. The ratio of the observed yield to the expected yield is shown in the lower panel.

7 Systematic uncertainties

The analysis considers theoretical, experimental and statistical uncertainties in signal and SM background modelling. The uncertainties are included in the likelihood fits as nuisance parameters with Gaussian probability densities. Theoretical uncertainties comprise generator-modelling-related uncertainties, cross-section uncertainties, and uncertainties related to the choice of PDF set. Such uncertainties are assumed to be uncorrelated between background processes. Systematic uncertainties in the reconstruction, identification, corrections and calibrations of various analysis objects are referred to as experimental uncertainties. These uncertainties are assumed to be correlated across processes and analysis regions.

Jet-related experimental uncertainties include uncertainties in the energy scale [119] and resolution [102], as well as jet-vertex-tagging uncertainties [120] and flavour-tagging uncertainties [105, 121, 122]. The experimental uncertainties related to τ -leptons include uncertainties from the reconstruction and identification algorithms as well as energy scale and electron veto uncertainties [110, 112]. Uncertainties related to electrons [107] and muons [108] are negligible. Uncertainties in the E_T^{miss} are estimated by taking into account the uncertainties related to the energy or momentum of calibrated objects as well as the uncertainties affecting the soft-term contributions [114].

The uncertainty in the combined Run 2 integrated luminosity is 1.7% [123], obtained from luminosity measurements with the LUCID-2 detector [124]. The pile-up reweighting applied to simulated events to match the observed conditions in data is assigned systematic uncertainties, reaching at most 6.4%. Uncertainties related to the trigger efficiency correction factors are at most 4% depending on the E_T^{miss} of the event. All of the mentioned systematic uncertainties are applied to all simulated samples.

Systematic uncertainties related to the fake- τ modelling consist of uncertainties in the number of events in the regions used to measure the fake factors and in the regions where they are applied, the statistical and systematic uncertainties of the MC samples in the regions where fake factors are applied, and the uncertainties from the extrapolation and application of fake factors. Based on a comparison of different correlation schemes the correlation effects are found to be negligible and these uncertainties are considered to be uncorrelated across regions.

Theoretical uncertainties related to variations of the PDFs are computed for all background and signal samples. The effect of using the nominal PDF and 100 variations is represented by a set of generator weights. The standard deviation of all the variations is computed and used as the PDF uncertainty. The uncertainties related to the value of the strong coupling constant α_s are estimated by halving the difference of two PDF sets evaluated with $\alpha_s = 0.117$ and $\alpha_s = 0.119$. The PDF and α_s systematic uncertainties are then combined in quadrature, following the PDF4LHC recommendations [75]. To estimate the uncertainties due to missing higher-order corrections, the values of renormalisation and factorisation scales μ_r and μ_f [125] are varied independently by a factor of 2, requiring $0.5 \leq \mu_r/\mu_f \leq 2$. The envelope of the effects of these scale variations is used to estimate the effect of the scale uncertainty. The cross-section uncertainty is applied to all background processes that are not normalised to data in the likelihood fits.

For the simulated Z and W boson samples, additional uncertainties are estimated by varying the resummation and CKKW matching scales [40, 41]. For the $Z(\tau\tau)$ +jets and diboson backgrounds, comparisons of the nominal SHERPA-produced samples with MADGRAPH5_AMC@NLO+PYTHIA-produced samples are used to estimate the uncertainties. For the $t\bar{t}$ and single-top-quark production processes, comparisons of the nominal POWHEG+PYTHIA samples with MADGRAPH5_AMC@NLO+PYTHIA samples are used to estimate uncertainties related to hard scattering. Similarly, parton showering uncertainties are evaluated by comparing the POWHEG+PYTHIA samples with POWHEG+HERWIG 7 samples. Uncertainties related to

Table 5: Systematic uncertainties in the post-fit SM background prediction in the six SR bins. The normalisation uncertainty includes the effect of keeping the normalisation factors as free-floating parameters in the fit. ‘Other’ includes the uncertainties arising from trigger efficiency corrections, electrons, muons, modelling of pile-up, and the E_T^{miss} computation. The individual uncertainties can be correlated and do not necessarily add in quadrature to equal the total uncertainty.

Region $m_T^{\tau_1} + m_T^{\tau_2}$ [GeV]	Low $_{m_A}$ $\in [100, 250]$	Low $_{m_A}$ $\in [250, 400]$	Low $_{m_A}$ $\in [400, 550]$	Low $_{m_A}$ > 550	High $_{m_A}$ $\in [400, 750]$	High $_{m_A}$ > 750
Theoretical	15.9%	20.9%	15.4%	13.3%	14.2%	21.7%
Fake τ -leptons	6.2%	19.1%	6.0%	3.0%	4.0%	13.2%
Jets	6.2%	7.9%	5.2%	11.0%	3.4%	7.9%
True τ -leptons	1.6%	3.1%	7.0%	10.6%	4.8%	5.0%
Normalisation	4.5%	4.0%	4.8%	8.1%	4.8%	6.1%
MC statistical	7.6%	13.2%	9.3%	15.6%	9.2%	22.2%
Cross-section	2.7%	4.7%	10.0%	9.8%	11.3%	8.5%
Other	4.1%	2.7%	5.3%	6.3%	4.9%	4.5%
Total	20.8%	32.8%	23.8%	28.3%	22.2%	36.3%

initial-state and final-state radiation are also considered for $t\bar{t}$ and single-top-quark production. Finally, for single-top-quark production samples, the effect of the diagram removal scheme [93] is compared with the effect of the diagram subtraction scheme [92, 93] to parameterise the uncertainty in the treatment of the $Wt/t\bar{t}$ interference.

For the 2HDM+ a model signal samples the theoretical uncertainties related to the PDFs and renormalisation and factorisation scales are considered. Additional experimental uncertainties account for the use of the simplified parameterised calorimeter response instead of the full GEANT4-based detector simulation.

A breakdown of the different sources of uncertainty in the SRs is presented in Table 5. The largest contribution comes from a combination of various theoretical uncertainties – comparisons with alternative generators for diboson, Z boson, and $t\bar{t}$ production processes, as well as PDF and scale variations. Other significant sources of uncertainty are the limited number of MC events and uncertainties in the modelling of fake τ -leptons.

8 Results

Figure 5 summarises the observed and expected yields in all CRs and VRs used by the analysis. The normalisation factors determined by the background-only fit to the data in the CRs and propagated to the VRs and SRs to apply corrections to the SM backgrounds are $\omega_{\text{top}} = 0.82 \pm 0.15$ and $\omega_Z = 1.04 \pm 0.22$. All four validation regions show agreement within one standard deviation between the SM prediction and the data, signifying good modelling of the SM backgrounds.

The yields in each bin of the Low $_{m_A}$ SR are summarised in Table 6. Comparisons of observed and predicted yields and the corresponding statistical significances [126] are shown in Figure 6 together with the benchmark parameter configurations of the signal model predictions. These signal benchmarks represent different kinematic regimes that the Low $_{m_A}$ SR is sensitive to. The yields in the High $_{m_A}$ SR bins are summarised in Table 7 and Figure 7 together with the corresponding statistical significances and

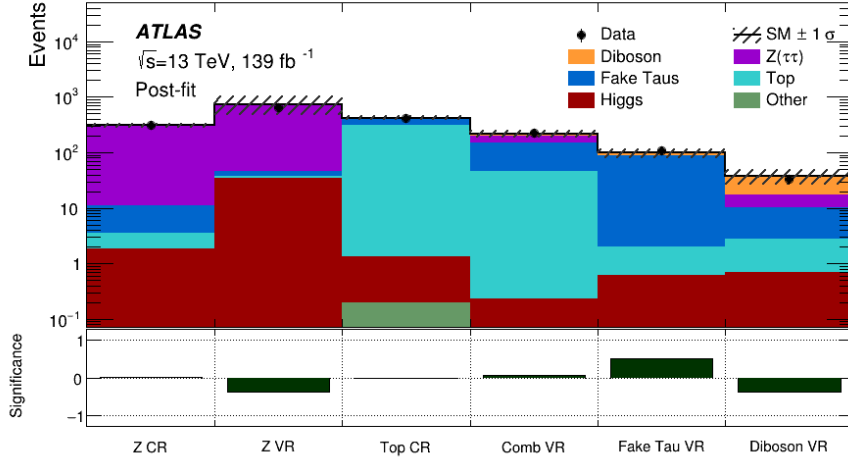


Figure 5: A comparison of the observed and expected yields in each of the two control regions and four validation regions used by the analysis is shown in the upper panel. The lower panel shows the statistical significance of the observation given the number of predicted events. The ‘Other’ contribution includes all the background processes not explicitly listed in the legend (V +jets except $Z(\tau\tau)$). The top-quark and $Z(\tau\tau)$ background predictions are normalised according to the background-only fit. The total statistical and systematic uncertainty of the SM background is shown by the hatched band.

benchmark parameter configurations of the signal model. No significant excess of data over the predicted SM backgrounds is observed in any of the bins.

For every signal model parameter configuration considered by the analysis a signal-plus-background fit is performed. The fit includes the CRs, and the Low_{m_A} or High_{m_A} SR. The contribution from the signal model is included as a free-floating parameter. The fit is performed simultaneously over all the CRs and SR bins. The probability that the observed yields in the Low_{m_A} SR or High_{m_A} SR are compatible with the signal-plus-background hypotheses are computed. A one-sided profile-likelihood-ratio test statistic as implemented in the `HISTFITTER` framework is used. The results are obtained using the CL_s prescription [127] and presented as exclusion contours at 95% confidence level (CL) in the two-dimensional parameter spaces.

The first parameter space is defined by setting $\tan\beta = 1$ and $\sin\Theta = 0.35$, while varying the values of $m_a \in [100, 400]$ GeV and $m_A \in [300, 1200]$ GeV. The Low_{m_A} SR is sensitive to models with $m_A \leq 800$ GeV, while the High_{m_A} SR is more sensitive to the $m_A \geq 1000$ GeV part of the parameter space. For the Low_{m_A} SR, computations of CL_s rely on the asymptotic properties of the profile-likelihood ratio [128]. For the High_{m_A} SR however, the asymptotic approximation is not valid because of the low yields in one of the regions, so Monte Carlo pseudo-experiments are used instead. The exclusion contours are derived for the Low_{m_A} SR and High_{m_A} SR separately and then combined using a method based on expected CL_s values, as the two SRs are not statistically independent. The observed data yields are higher than the predicted SM backgrounds in the $m_T^{T1} + m_T^{T2} \in [250, 550]$ GeV bins of the Low_{m_A} SR, resulting in the observed limits being weaker than the expected limits. Pseudoscalar singlets a with masses up to 300 GeV are excluded for $m_A = 800$ GeV. The combined exclusion contour is shown in Figure 8(a).

The second two-dimensional parameter space considered by the analysis spans $m_A \in [500, 1300]$ GeV and

Table 6: Observed and expected yields in the Low m_A SR bins after the background-only fit. The upper part of the table describes the breakdown of predicted SM backgrounds. The lower part of the table shows predicted yields of three signal model benchmark parameter configurations.

$m_T^{\tau_1} + m_T^{\tau_2}$	$\in [100, 250]$ GeV	$\in [250, 400]$ GeV	$\in [400, 550]$ GeV	> 550 GeV
Observed events	20	9	13	4
Fitted background events	28.3 ± 5.9	6.3 ± 2.1	10.1 ± 2.4	4.8 ± 1.3
Diboson	5.7 ± 2.4	2.0 ± 0.7	6.5 ± 2.1	2.8 ± 1.1
$Z(\tau\tau)$	12.3 ± 3.8	$0.8^{+1.0}_{-0.8}$	$0.1^{+0.2}_{-0.1}$	$0.1^{+0.2}_{-0.1}$
$t\bar{t}$	4.4 ± 2.7	$0.3^{+0.8}_{-0.3}$	0.0 ± 0.0	0.0 ± 0.0
Single-top	$0.2^{+0.4}_{-0.2}$	$0.2^{+0.3}_{-0.2}$	0.0 ± 0.0	0.0 ± 0.0
$t\bar{t}V$	0.1 ± 0.0	0.1 ± 0.1	0.1 ± 0.0	0.1 ± 0.0
Higgs	0.4 ± 0.1	0.4 ± 0.1	2.0 ± 0.4	1.5 ± 0.4
Fake tau	5.3 ± 1.8	2.6 ± 1.3	1.4 ± 0.6	0.3 ± 0.2
$m_a = 150$ GeV, $\sin \Theta = 0.35$ $m_A = 400$ GeV, $\tan \beta = 1$	4.1 ± 0.6	9.6 ± 1.2	1.9 ± 0.4	0.1 ± 0.0
$m_a = 250$ GeV, $\sin \Theta = 0.7$ $m_A = 600$ GeV, $\tan \beta = 1$	0.4 ± 0.1	2.0 ± 0.3	12.3 ± 1.3	4.3 ± 0.6
$m_a = 300$ GeV, $\sin \Theta = 0.35$ $m_A = 800$ GeV, $\tan \beta = 1$	0.2 ± 0.0	0.5 ± 0.1	3.1 ± 0.4	6.8 ± 0.9

$\tan \beta \in [0.3, 20]$ with the parameters m_a and $\sin \Theta$ fixed to the values of 250 GeV and 0.7 respectively. Only the Low m_A SR has significant sensitivity to the signal model with these parameter value choices. Monte Carlo pseudo-experiments are used for the computation of the exclusion limits because the asymptotic approximation is not appropriate for all parameter configurations of the signal model. Since in the Low m_A SR the data yields are higher than expected in the $m_T^{\tau_1} + m_T^{\tau_2} \in [250, 550]$ GeV bins, the observed limits are less stringent than the expected ones for the parameter configurations of the signal model that these bins are sensitive to. This corresponds to models with lower values of m_A . Signal points in the parameter space with $\tan \beta \leq 1$ are excluded for $m_A < 900$ GeV. The exclusion contour is shown in Figure 8(b).

For each of the four bins in the Low m_A SR and two bins in the High m_A SR, model-independent upper limits are set on the cross-sections of potential BSM processes. A signal-plus-background fit over all the CRs and the selected SR bin is performed. A generic signal contribution with free-floating normalisation is assumed in the SR, but not in the CRs. The profile-likelihood-ratio test statistic is evaluated using the HISTFITTER framework. Upper limits of 0.4–0.8 fb are placed on the visible cross-section σ_{vis} at 95% CL. Upper limits on the number of signal events given the observed number of events and predicted number of background events, confidence levels for the background-only hypotheses, the discovery p -value, and the associated significances in all of the SR bins are summarised in Table 8.

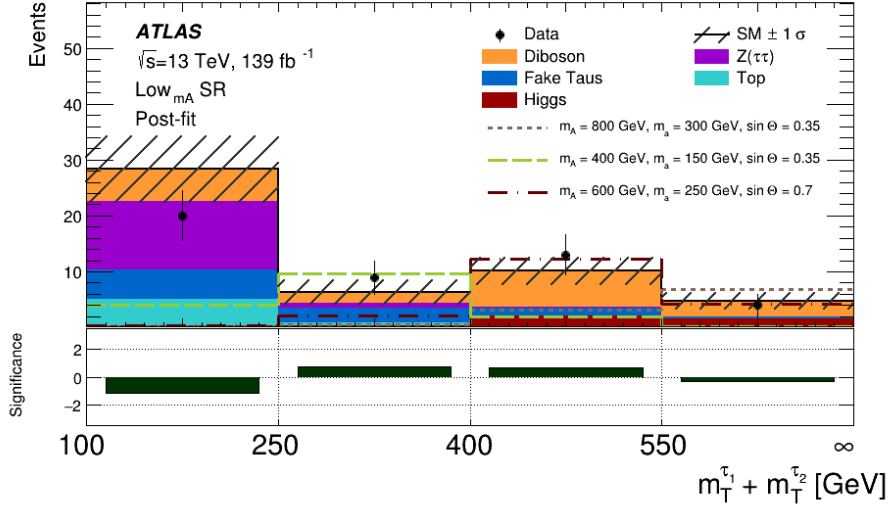


Figure 6: A comparison of the observed and expected yields in the four bins of the Low_{m_A} SR region used in the analysis is shown in the upper panel. The lower panel shows the statistical significance of the observation given the predicted number of events. The top-quark and $Z(\tau\tau)$ background predictions are normalised according to the background-only fit. The total statistical and systematic uncertainty of the SM background is shown by the hatched band.

Table 7: Observed and expected yields in the High_{m_A} SR bins after the background-only fit. The upper part of the table describes the breakdown of predicted SM backgrounds. The lower part of the table shows predicted yields of three signal model benchmark parameter configurations.

$m_T^{\tau_1} + m_T^{\tau_2}$	$\in [400, 750]$ GeV	> 750 GeV
Observed events	9	3
Fitted background events	11.8 ± 2.6	2.2 ± 0.8
Diboson	8.9 ± 2.4	1.1 ± 0.6
$Z(\tau\tau)$	$0.4^{+0.5}_{-0.4}$	$0.0^{+0.1}_{-0.0}$
$t\bar{t}V$	0.1 ± 0.0	0.1 ± 0.0
Higgs	1.5 ± 0.3	0.7 ± 0.2
Fake tau	0.9 ± 0.5	0.4 ± 0.3
$m_a = 150$ GeV, $\sin \Theta = 0.35$ $m_A = 1000$ GeV, $\tan \beta = 1$	4.0 ± 0.5	4.6 ± 0.6
$m_a = 250$ GeV, $\sin \Theta = 0.7$ $m_A = 600$ GeV, $\tan \beta = 1$	4.9 ± 0.7	0.2 ± 0.1
$m_a = 300$ GeV, $\sin \Theta = 0.35$ $m_A = 800$ GeV, $\tan \beta = 1$	6.4 ± 0.8	1.4 ± 0.3

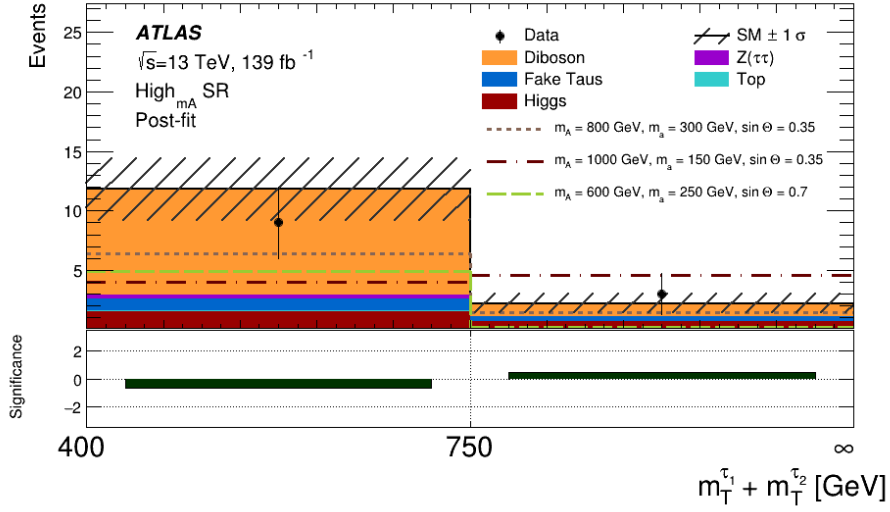


Figure 7: A comparison of the observed and expected yields in the two bins of the High_{*m_A*} SR region used in the analysis is shown in the upper panel. The lower panel shows the statistical significance of the observation given the predicted number of events. The top-quark and Z($\tau\tau$) background predictions are normalised according to the background-only fit. The total statistical and systematic uncertainty of the SM background is shown by the hatched band.

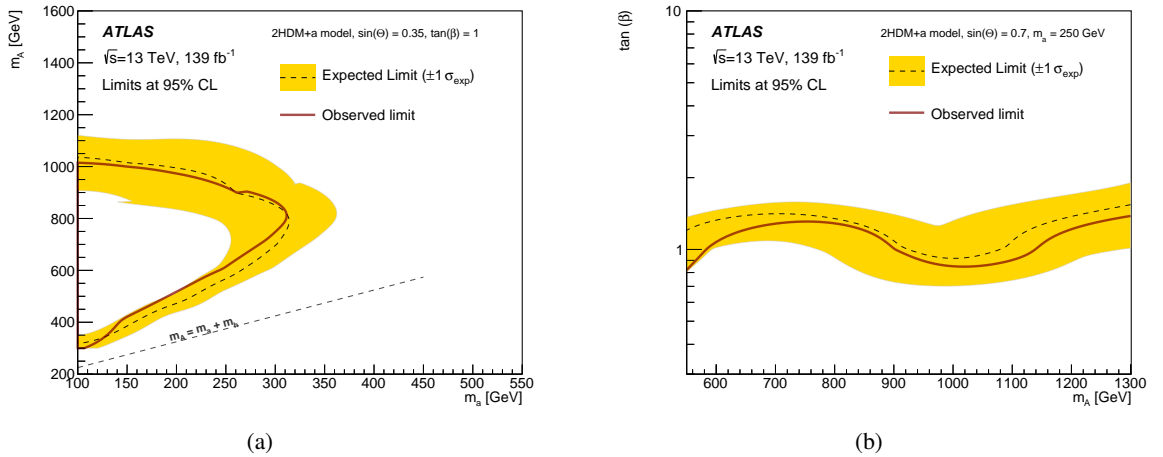


Figure 8: Observed and expected exclusion contours at 95% CL (a) as a function of m_a and m_A with $\tan\beta = 1$ and $\sin\Theta = 0.35$, and (b) as a function of m_A and $\tan\beta$ with $m_a = 250$ GeV and $\sin\Theta = 0.7$. The excluded area in (a) is to the left of the solid line, and in (b) below the solid line.

Table 8: Upper limits at 95% CL on the visible cross-section σ_{vis} , on the number of signal events (S_{obs}^{95}), and on the number of signal events given the expected number (and $\pm 1\sigma$ excursions of the expectation) of background events (S_{exp}^{95}). The last two columns indicate the CL_b value (i.e. the confidence level observed for the background-only hypothesis), the discovery p -value (p_0), and its associated significance Z .

Signal region	σ_{vis} [fb]	S_{obs}^{95}	S_{exp}^{95}	CL_b	p_0 (Z)
Low $_{m_A}$ SR					
$m_{\text{T}}^{\tau_1} + m_{\text{T}}^{\tau_2}$					
[100, 250] GeV	0.08	10.7	$12.5^{+5.2}_{-3.5}$	0.27	0.86 (-1.07)
[250, 400] GeV	0.07	9.1	$7.6^{+3.1}_{-1.6}$	0.72	0.30 (0.53)
[400, 550] GeV	0.08	10.8	$8.9^{+3.4}_{-2.3}$	0.75	0.26 (0.65)
> 550 GeV	0.04	5.8	$6.0^{+2.6}_{-1.6}$	0.42	0.61 (-0.29)
High $_{m_A}$ SR					
$m_{\text{T}}^{\tau_1} + m_{\text{T}}^{\tau_2}$					
[400, 750] GeV	0.05	7.6	$8.8^{+3.1}_{-2.4}$	0.34	0.85 (-1.03)
> 750 GeV	0.04	5.4	$4.6^{+1.8}_{-0.8}$	0.67	0.34 (0.42)

9 Conclusion

This paper presents a search for dark matter produced in association with a Higgs boson in final states with two hadronically decaying τ -leptons and large missing transverse momentum. The search is based on a 139 fb^{-1} dataset of $\sqrt{s} = 13 \text{ TeV}$ proton–proton collisions recorded by the ATLAS experiment at the LHC during 2015–2018. The analysis utilises two different signal regions which in turn are divided into four and two $m_{\text{T}}^{\tau_1} + m_{\text{T}}^{\tau_2}$ bins, respectively, to target different parts of the parameter space. No significant deviations from the Standard Model prediction is found.

The results are interpreted in the context of the 2HDM+ a model where parameters are varied to set 95% CL limits in the m_a – m_A and m_A – $\tan\beta$ planes. Model-independent upper limits are set on the visible cross-section σ_{vis} for eventual beyond the Standard Model physics processes producing a large missing transverse energy in association with a Higgs boson decaying to τ -leptons. These 95% CL limits vary between 0.04 and 0.08 fb depending on which of the signal region bins is considered.

The presented work is the first exploration of the mono-Higgs signature with the Higgs boson decaying into a pair of hadronically decaying τ -leptons with the ATLAS experiment. Compared to the $h + E_{\text{T}}^{\text{miss}}$ search with the Higgs boson decaying into a pair of b -quarks [12], this search offers sensitivity to the low $\tan\beta$ region of the m_A – $\tan\beta$ plane. In the m_a – m_A plane this search has comparable sensitivity in the low m_A region with an orthogonal selection, allowing for a combination of the two results.

Acknowledgements

We thank CERN for the very successful operation of the LHC, as well as the support staff from our institutions without whom ATLAS could not be operated efficiently.

We acknowledge the support of ANPCyT, Argentina; YerPhI, Armenia; ARC, Australia; BMWFW and FWF, Austria; ANAS, Azerbaijan; CNPq and FAPESP, Brazil; NSERC, NRC and CFI, Canada; CERN; ANID, Chile; CAS, MOST and NSFC, China; Minciencias, Colombia; MEYS CR, Czech Republic; DNRF and DNSRC, Denmark; IN2P3-CNRS and CEA-DRF/IRFU, France; SRNSFG, Georgia; BMBF, HGF and MPG, Germany; GSRI, Greece; RGC and Hong Kong SAR, China; ISF and Benoziyo Center, Israel; INFN, Italy; MEXT and JSPS, Japan; CNRST, Morocco; NWO, Netherlands; RCN, Norway; MEiN, Poland; FCT, Portugal; MNE/IFA, Romania; MESTD, Serbia; MSSR, Slovakia; ARRS and MIZŠ, Slovenia; DSI/NRF, South Africa; MICINN, Spain; SRC and Wallenberg Foundation, Sweden; SERI, SNSF and Cantons of Bern and Geneva, Switzerland; MOST, Taiwan; TENMAK, Türkiye; STFC, United Kingdom; DOE and NSF, United States of America. In addition, individual groups and members have received support from BCKDF, CANARIE, Compute Canada and CRC, Canada; PRIMUS 21/SCI/017 and UNCE SCI/013, Czech Republic; COST, ERC, ERDF, Horizon 2020 and Marie Skłodowska-Curie Actions, European Union; Investissements d’Avenir Labex, Investissements d’Avenir IDEX and ANR, France; DFG and AvH Foundation, Germany; Herakleitos, Thales and Aristeia programmes co-financed by EU-ESF and the Greek NSRF, Greece; BSF-NSF and MINERVA, Israel; Norwegian Financial Mechanism 2014–2021, Norway; NCN and NAWA, Poland; La Caixa Banking Foundation, CERCA Programme Generalitat de Catalunya and PROMETEO and GenT Programmes Generalitat Valenciana, Spain; Göran Gustafssons Stiftelse, Sweden; The Royal Society and Leverhulme Trust, United Kingdom.

The crucial computing support from all WLCG partners is acknowledged gratefully, in particular from CERN, the ATLAS Tier-1 facilities at TRIUMF (Canada), NDGF (Denmark, Norway, Sweden), CC-IN2P3

(France), KIT/GridKA (Germany), INFN-CNAF (Italy), NL-T1 (Netherlands), PIC (Spain), ASGC (Taiwan), RAL (UK) and BNL (USA), the Tier-2 facilities worldwide and large non-WLCG resource providers. Major contributors of computing resources are listed in Ref. [[129](#)].

References

- [1] ATLAS Collaboration, *Observation of a new particle in the search for the Standard Model Higgs boson with the ATLAS detector at the LHC*, *Phys. Lett. B* **716** (2012) 1, arXiv: [1207.7214 \[hep-ex\]](#).
- [2] CMS Collaboration, *Observation of a new boson at a mass of 125 GeV with the CMS experiment at the LHC*, *Phys. Lett. B* **716** (2012) 30, arXiv: [1207.7235 \[hep-ex\]](#).
- [3] D. Clowe, A. Gonzalez and M. Markevitch, *Weak-Lensing Mass Reconstruction of the Interacting Cluster 1E0657-558: Direct Evidence for the Existence of Dark Matter*, *Astrophys. J.* **604** (2004) 596, arXiv: [astro-ph/0312273](#).
- [4] G. Bertone, D. Hooper and J. Silk, *Particle dark matter: evidence, candidates and constraints*, *Phys. Rept.* **405** (2005) 279, arXiv: [hep-ph/0404175](#).
- [5] P. A. Zyla et al., *Review of Particle Physics*, *PTEP* **2020** (2020) 083C01.
- [6] F. Kahlhoefer, *Review of LHC dark matter searches*, *Int. J. Mod. Phys. A* **32** (2017) 1730006, arXiv: [1702.02430 \[hep-ph\]](#).
- [7] ATLAS Collaboration, *The ATLAS Experiment at the CERN Large Hadron Collider*, *JINST* **3** (2008) S08003.
- [8] CMS Collaboration, *The CMS Experiment at the CERN LHC*, *JINST* **3** (2008) S08004.
- [9] O. Nachtmann, A. Reiter and M. Wirbel, *Single jet and single photon production in proton - antiproton collisions and e^+e^- annihilation in a supersymmetric model*, *Z. Phys. C* **27** (1985) 577.
- [10] D. Abercrombie et al., *Dark Matter benchmark models for early LHC Run-2 Searches: Report of the ATLAS/CMS Dark Matter Forum*, *Phys. Dark Univ.* **27** (2020) 100371, ed. by A. Boveia, C. Doglioni, S. Lowette, S. Malik and S. Mrenna, arXiv: [1507.00966 \[hep-ex\]](#).
- [11] P. Athron et al., *Global analyses of Higgs portal singlet dark matter models using GAMBIT*, *Eur. Phys. J. C* **79** (2019) 38, arXiv: [1808.10465 \[hep-ph\]](#).
- [12] ATLAS Collaboration, *Search for dark matter produced in association with a Standard Model Higgs boson decaying into b -quarks using the full Run 2 dataset from the ATLAS detector*, *JHEP* **11** (2021) 209, arXiv: [2108.13391 \[hep-ex\]](#).
- [13] CMS Collaboration, *Search for dark matter produced in association with a Higgs boson decaying to a pair of bottom quarks in proton-proton collisions at $\sqrt{s} = 13$ TeV*, *Eur. Phys. J. C* **79** (2019) 280, arXiv: [1811.06562 \[hep-ex\]](#).
- [14] CMS Collaboration, *Search for dark matter produced in association with a Higgs boson decaying to $\gamma\gamma$ or $\tau^+\tau^-$ at $\sqrt{s} = 13$ TeV*, *JHEP* **09** (2018) 046, arXiv: [1806.04771 \[hep-ex\]](#).
- [15] ATLAS Collaboration, *Search for dark matter in events with missing transverse momentum and a Higgs boson decaying into two photons in pp collisions at $\sqrt{s} = 13$ TeV with the ATLAS detector*, *JHEP* **10** (2021) 013, arXiv: [2104.13240 \[hep-ex\]](#).
- [16] CMS Collaboration, *Search for associated production of dark matter with a Higgs boson decaying to $b\bar{b}$ or $\gamma\gamma$ at $\sqrt{s} = 13$ TeV*, *JHEP* **10** (2017) 180, arXiv: [1703.05236 \[hep-ex\]](#).
- [17] CMS Collaboration, *Search for dark matter particles produced in association with a Higgs boson in proton-proton collisions at $\sqrt{s} = 13$ TeV*, *JHEP* **03** (2020) 025, arXiv: [1908.01713 \[hep-ex\]](#).

- [18] ATLAS Collaboration, *Search for bottom-squark pair production with the ATLAS detector in final states containing Higgs bosons, b-jets and missing transverse momentum*, *JHEP* **12** (2019) 060, arXiv: 1908.03122 [hep-ex].
- [19] N. G. Deshpande and E. Ma, *Pattern of symmetry breaking with two Higgs doublets*, *Phys. Rev. D* **18** (7 1978) 2574, URL: <https://link.aps.org/doi/10.1103/PhysRevD.18.2574>.
- [20] G. C. Branco et al., *Theory and phenomenology of two-Higgs-doublet models*, *Phys. Rept.* **516** (2012) 1, arXiv: 1106.0034 [hep-ph].
- [21] M. Bauer, U. Haisch and F. Kahlhoefer, *Simplified dark matter models with two Higgs doublets: I. Pseudoscalar mediators*, *JHEP* **05** (2017) 138, arXiv: 1701.07427 [hep-ph].
- [22] T. Abe et al., *LHC Dark Matter Working Group: Next-generation spin-0 dark matter models*, *Phys. Dark Univ.* (2018) 100351. 67 p, This report was erroneously issued as CERN-LPCC-2018-001. Version two carries the correct reference, CERN-LPCC-2018-02., arXiv: 1810.09420, URL: <https://cds.cern.ch/record/2644694>.
- [23] ATLAS and CMS Collaborations, *Combined Measurement of the Higgs Boson Mass in pp Collisions at $\sqrt{s} = 7$ and 8 TeV with the ATLAS and CMS Experiments*, *Phys. Rev. Lett.* **114** (2015) 191803, arXiv: 1503.07589 [hep-ex].
- [24] M. Tanabashi et al., *Review of Particle Physics, 2018-2019*, *Phys. Rev. D* **98** (2018) 030001. 1898 p, URL: <https://cds.cern.ch/record/2636832>.
- [25] ATLAS Collaboration, *ATLAS Insertable B-Layer Technical Design Report*, ATLAS-TDR-19; CERN-LHCC-2010-013, 2010, URL: <https://cds.cern.ch/record/1291633>, Addendum: ATLAS-TDR-19-ADD-1; CERN-LHCC-2012-009, 2012, URL: <https://cds.cern.ch/record/1451888>.
- [26] B. Abbott et al., *Production and integration of the ATLAS Insertable B-Layer*, *JINST* **13** (2018) T05008, arXiv: 1803.00844 [physics.ins-det].
- [27] ATLAS Collaboration, *The ATLAS Collaboration Software and Firmware*, ATL-SOFT-PUB-2021-001, 2021, URL: <https://cds.cern.ch/record/2767187>.
- [28] ATLAS Collaboration, *ATLAS data quality operations and performance for 2015–2018 data-taking*, *JINST* **15** (2020) P04003, arXiv: 1911.04632 [physics.ins-det].
- [29] ATLAS Collaboration, *Performance of the ATLAS trigger system in 2015*, *Eur. Phys. J. C* **77** (2017) 317, arXiv: 1611.09661 [hep-ex].
- [30] ATLAS Collaboration, *The ATLAS Tau Trigger in Run 2*, ATLAS-CONF-2017-061, 2017, URL: <https://cds.cern.ch/record/2274201>.
- [31] ATLAS Collaboration, *The ATLAS Simulation Infrastructure*, *Eur. Phys. J. C* **70** (2010) 823, arXiv: 1005.4568 [physics.ins-det].
- [32] S. Agostinelli et al., *GEANT4 – a simulation toolkit*, *Nucl. Instrum. Meth. A* **506** (2003) 250.
- [33] E. Bothmann et al., *Event generation with Sherpa 2.2*, *SciPost Phys.* **7** (2019) 034, arXiv: 1905.09127 [hep-ph].

- [34] S. Schumann and F. Krauss, *A parton shower algorithm based on Catani–Seymour dipole factorisation*, *JHEP* **03** (2008) 038, arXiv: [0709.1027 \[hep-ph\]](#).
- [35] C. Anastasiou, L. Dixon, K. Melnikov and F. Petriello, *High-precision QCD at hadron colliders: Electroweak gauge boson rapidity distributions at next-to-next-to leading order*, *Phys. Rev. D* **69** (2004) 094008, arXiv: [hep-ph/0312266](#).
- [36] The NNPDF Collaboration, R. D. Ball et al., *Parton distributions for the LHC run II*, *JHEP* **04** (2015) 040, arXiv: [1410.8849 \[hep-ph\]](#).
- [37] T. Gleisberg and S. Höche, *Comix, a new matrix element generator*, *JHEP* **12** (2008) 039, arXiv: [0808.3674 \[hep-ph\]](#).
- [38] S. Höche, F. Krauss, M. Schönherr and F. Siegert, *A critical appraisal of NLO+PS matching methods*, *JHEP* **09** (2012) 049, arXiv: [1111.1220 \[hep-ph\]](#).
- [39] S. Höche, F. Krauss, M. Schönherr and F. Siegert, *QCD matrix elements + parton showers. The NLO case*, *JHEP* **04** (2013) 027, arXiv: [1207.5030 \[hep-ph\]](#).
- [40] S. Catani, F. Krauss, B. R. Webber and R. Kuhn, *QCD Matrix Elements + Parton Showers*, *JHEP* **11** (2001) 063, arXiv: [hep-ph/0109231](#).
- [41] S. Höche, F. Krauss, S. Schumann and F. Siegert, *QCD matrix elements and truncated showers*, *JHEP* **05** (2009) 053, arXiv: [0903.1219 \[hep-ph\]](#).
- [42] S. Frixione, G. Ridolfi and P. Nason, *A positive-weight next-to-leading-order Monte Carlo for heavy flavour hadroproduction*, *JHEP* **09** (2007) 126, arXiv: [0707.3088 \[hep-ph\]](#).
- [43] P. Nason, *A new method for combining NLO QCD with shower Monte Carlo algorithms*, *JHEP* **11** (2004) 040, arXiv: [hep-ph/0409146](#).
- [44] S. Frixione, P. Nason and C. Oleari, *Matching NLO QCD computations with parton shower simulations: the POWHEG method*, *JHEP* **11** (2007) 070, arXiv: [0709.2092 \[hep-ph\]](#).
- [45] S. Alioli, P. Nason, C. Oleari and E. Re, *A general framework for implementing NLO calculations in shower Monte Carlo programs: the POWHEG BOX*, *JHEP* **06** (2010) 043, arXiv: [1002.2581 \[hep-ph\]](#).
- [46] T. Sjöstrand et al., *An introduction to PYTHIA 8.2*, *Comput. Phys. Commun.* **191** (2015) 159, arXiv: [1410.3012 \[hep-ph\]](#).
- [47] M. Beneke, P. Falgari, S. Klein and C. Schwinn, *Hadronic top-quark pair production with NNLL threshold resummation*, *Nucl. Phys. B* **855** (2012) 695, arXiv: [1109.1536 \[hep-ph\]](#).
- [48] M. Cacciari, M. Czakon, M. Mangano, A. Mitov and P. Nason, *Top-pair production at hadron colliders with next-to-next-to-leading logarithmic soft-gluon resummation*, *Phys. Lett. B* **710** (2012) 612, arXiv: [1111.5869 \[hep-ph\]](#).
- [49] P. Bärnreuther, M. Czakon and A. Mitov, *Percent-Level-Precision Physics at the Tevatron: Next-to-Next-to-Leading Order QCD Corrections to $q\bar{q} \rightarrow t\bar{t} + X$* , *Phys. Rev. Lett.* **109** (2012) 132001, arXiv: [1204.5201 \[hep-ph\]](#).

- [50] M. Czakon and A. Mitov, *NNLO corrections to top-pair production at hadron colliders: the all-fermionic scattering channels*, *JHEP* **12** (2012) 054, arXiv: [1207.0236 \[hep-ph\]](#).
- [51] M. Czakon and A. Mitov, *NNLO corrections to top pair production at hadron colliders: the quark-gluon reaction*, *JHEP* **01** (2013) 080, arXiv: [1210.6832 \[hep-ph\]](#).
- [52] M. Czakon, P. Fiedler and A. Mitov, *Total Top-Quark Pair-Production Cross Section at Hadron Colliders Through $O(\alpha_S^4)$* , *Phys. Rev. Lett.* **110** (2013) 252004, arXiv: [1303.6254 \[hep-ph\]](#).
- [53] M. Czakon and A. Mitov, *Top++: A program for the calculation of the top-pair cross-section at hadron colliders*, *Comput. Phys. Commun.* **185** (2014) 2930, arXiv: [1112.5675 \[hep-ph\]](#).
- [54] ATLAS Collaboration, *ATLAS Pythia 8 tunes to 7 TeV data*, ATL-PHYS-PUB-2014-021, 2014, URL: <https://cds.cern.ch/record/1966419>.
- [55] NNPDF Collaboration, R. D. Ball et al., *Parton distributions with LHC data*, *Nucl. Phys. B* **867** (2013) 244, arXiv: [1207.1303 \[hep-ph\]](#).
- [56] E. Re, *Single-top Wt -channel production matched with parton showers using the POWHEG method*, *Eur. Phys. J. C* **71** (2011) 1547, arXiv: [1009.2450 \[hep-ph\]](#).
- [57] N. Kidonakis, *Two-loop soft anomalous dimensions for single top quark associated production with a W^- or H^-* , *Phys. Rev. D* **82** (2010) 054018, arXiv: [1005.4451 \[hep-ph\]](#).
- [58] N. Kidonakis, ‘Top Quark Production’, *Proceedings, Helmholtz International Summer School on Physics of Heavy Quarks and Hadrons (HQ 2013)* (JINR, Dubna, Russia, 15th–28th July 2013) 139, arXiv: [1311.0283 \[hep-ph\]](#).
- [59] M. Aliev et al., *HATHOR – HAdronic Top and Heavy quarks crOss section calculatoR*, *Comput. Phys. Commun.* **182** (2011) 1034, arXiv: [1007.1327 \[hep-ph\]](#).
- [60] P. Kant et al., *HatHor for single top-quark production: Updated predictions and uncertainty estimates for single top-quark production in hadronic collisions*, *Comput. Phys. Commun.* **191** (2015) 74, arXiv: [1406.4403 \[hep-ph\]](#).
- [61] H. B. Hartanto, B. Jäger, L. Reina and D. Wackerth, *Higgs boson production in association with top quarks in the POWHEG BOX*, *Phys. Rev. D* **91** (2015) 094003, arXiv: [1501.04498 \[hep-ph\]](#).
- [62] J. Alwall et al., *The automated computation of tree-level and next-to-leading order differential cross sections, and their matching to parton shower simulations*, *JHEP* **07** (2014) 079, arXiv: [1405.0301 \[hep-ph\]](#).
- [63] D. de Florian et al., *Handbook of LHC Higgs Cross Sections: 4. Deciphering the Nature of the Higgs Sector*, (2016), arXiv: [1610.07922 \[hep-ph\]](#).
- [64] P. Nason and C. Oleari, *NLO Higgs boson production via vector-boson fusion matched with shower in POWHEG*, *JHEP* **02** (2010) 037, arXiv: [0911.5299 \[hep-ph\]](#).

- [65] K. Hamilton, P. Nason, E. Re and G. Zanderighi, *NNLOPS simulation of Higgs boson production*, [JHEP **10** \(2013\) 222](#), arXiv: [1309.0017 \[hep-ph\]](#).
- [66] K. Hamilton, P. Nason and G. Zanderighi, *Finite quark-mass effects in the NNLOPS POWHEG+MiNLO Higgs generator*, [JHEP **05** \(2015\) 140](#), arXiv: [1501.04637 \[hep-ph\]](#).
- [67] M. L. Ciccolini, S. Dittmaier and M. Krämer, *Electroweak radiative corrections to associated WH and ZH production at hadron colliders*, [Phys. Rev. D **68** \(2003\) 073003](#), arXiv: [hep-ph/0306234 \[hep-ph\]](#).
- [68] O. Brein, A. Djouadi and R. Harlander, *NNLO QCD corrections to the Higgs-strahlung processes at hadron colliders*, [Phys. Lett. B **579** \(2004\) 149](#), arXiv: [hep-ph/0307206](#).
- [69] O. Brein, R. V. Harlander, M. Wiesemann and T. Zirke, *Top-quark mediated effects in hadronic Higgs-Strahlung*, [Eur. Phys. J. C **72** \(2012\) 1868](#), arXiv: [1111.0761 \[hep-ph\]](#).
- [70] L. Altenkamp, S. Dittmaier, R. V. Harlander, H. Rzehak and T. J. E. Zirke, *Gluon-induced Higgs-strahlung at next-to-leading order QCD*, [JHEP **02** \(2013\) 078](#), arXiv: [1211.5015 \[hep-ph\]](#).
- [71] A. Denner, S. Dittmaier, S. Kallweit and A. Mück, *HAWK 2.0: A Monte Carlo program for Higgs production in vector-boson fusion and Higgs strahlung at hadron colliders*, [Comput. Phys. Commun. **195** \(2015\) 161](#), arXiv: [1412.5390 \[hep-ph\]](#).
- [72] O. Brein, R. V. Harlander and T. J. E. Zirke, *vh@nnlo – Higgs Strahlung at hadron colliders*, [Comput. Phys. Commun. **184** \(2013\) 998](#), arXiv: [1210.5347 \[hep-ph\]](#).
- [73] R. V. Harlander, A. Kulesza, V. Theeuwes and T. Zirke, *Soft gluon resummation for gluon-induced Higgs Strahlung*, [JHEP **11** \(2014\) 082](#), arXiv: [1410.0217 \[hep-ph\]](#).
- [74] ATLAS Collaboration, *Measurement of the Z/ γ^* boson transverse momentum distribution in pp collisions at $\sqrt{s} = 7$ TeV with the ATLAS detector*, [JHEP **09** \(2014\) 145](#), arXiv: [1406.3660 \[hep-ex\]](#).
- [75] J. Butterworth et al., *PDF4LHC recommendations for LHC Run II*, [J. Phys. G **43** \(2016\) 023001](#), arXiv: [1510.03865 \[hep-ph\]](#).
- [76] F. Buccioni et al., *OpenLoops 2*, [Eur. Phys. J. C **79** \(2019\) 866](#), arXiv: [1907.13071 \[hep-ph\]](#).
- [77] F. Cascioli, P. Maierhöfer and S. Pozzorini, *Scattering Amplitudes with Open Loops*, [Phys. Rev. Lett. **108** \(2012\) 111601](#), arXiv: [1111.5206 \[hep-ph\]](#).
- [78] A. Denner, S. Dittmaier and L. Hofer, *COLLIER: A fortran-based complex one-loop library in extended regularizations*, [Comput. Phys. Commun. **212** \(2017\) 220](#), arXiv: [1604.06792 \[hep-ph\]](#).
- [79] C. Anastasiou et al., *High precision determination of the gluon fusion Higgs boson cross-section at the LHC*, [JHEP **05** \(2016\) 058](#), arXiv: [1602.00695 \[hep-ph\]](#).
- [80] C. Anastasiou, C. Duhr, F. Dulat, F. Herzog and B. Mistlberger, *Higgs Boson Gluon-Fusion Production in QCD at Three Loops*, [Phys. Rev. Lett. **114** \(2015\) 212001](#), arXiv: [1503.06056 \[hep-ph\]](#).

- [81] F. Dulat, A. Lazopoulos and B. Mistlberger, *iHixs 2 – Inclusive Higgs cross sections*, *Comput. Phys. Commun.* **233** (2018) 243, arXiv: [1802.00827 \[hep-ph\]](#).
- [82] R. V. Harlander and K. J. Ozeren, *Finite top mass effects for hadronic Higgs production at next-to-next-to-leading order*, *JHEP* **11** (2009) 088, arXiv: [0909.3420 \[hep-ph\]](#).
- [83] R. V. Harlander and K. J. Ozeren, *Top mass effects in Higgs production at next-to-next-to-leading order QCD: Virtual corrections*, *Phys. Lett. B* **679** (2009) 467, arXiv: [0907.2997 \[hep-ph\]](#).
- [84] R. V. Harlander, H. Mantler, S. Marzani and K. J. Ozeren, *Higgs production in gluon fusion at next-to-next-to-leading order QCD for finite top mass*, *Eur. Phys. J. C* **66** (2010) 359, arXiv: [0912.2104 \[hep-ph\]](#).
- [85] A. Pak, M. Rogal and M. Steinhauser, *Finite top quark mass effects in NNLO Higgs boson production at LHC*, *JHEP* **02** (2010) 025, arXiv: [0911.4662 \[hep-ph\]](#).
- [86] S. Actis, G. Passarino, C. Sturm and S. Uccirati, *NLO electroweak corrections to Higgs boson production at hadron colliders*, *Phys. Lett. B* **670** (2008) 12, arXiv: [0809.1301 \[hep-ph\]](#).
- [87] S. Actis, G. Passarino, C. Sturm and S. Uccirati, *NNLO computational techniques: The cases $H \rightarrow \gamma\gamma$ and $H \rightarrow gg$* , *Nucl. Phys. B* **811** (2009) 182, arXiv: [0809.3667 \[hep-ph\]](#).
- [88] M. Bonetti, K. Melnikov and L. Tancredi, *Higher order corrections to mixed QCD-EW contributions to Higgs boson production in gluon fusion*, *Phys. Rev. D* **97** (2018) 056017, arXiv: [1801.10403 \[hep-ph\]](#), Erratum: *Phys. Rev. D* **97** (2018) 099906(E).
- [89] M. Ciccolini, A. Denner and S. Dittmaier, *Strong and Electroweak Corrections to the Production of a Higgs Boson + 2 Jets via Weak Interactions at the Large Hadron Collider*, *Phys. Rev. Lett.* **99** (2007) 161803, arXiv: [0707.0381 \[hep-ph\]](#).
- [90] M. Ciccolini, A. Denner and S. Dittmaier, *Electroweak and QCD corrections to Higgs production via vector-boson fusion at the CERN LHC*, *Phys. Rev. D* **77** (2008) 013002, arXiv: [0710.4749 \[hep-ph\]](#).
- [91] P. Bolzoni, F. Maltoni, S.-O. Moch and M. Zaro, *Higgs Boson Production via Vector-Boson Fusion at Next-to-Next-to-Leading Order in QCD*, *Phys. Rev. Lett.* **105** (2010) 011801, arXiv: [1003.4451 \[hep-ph\]](#).
- [92] ATLAS Collaboration, *Studies on top-quark Monte Carlo modelling for Top2016*, ATL-PHYS-PUB-2016-020, 2016, URL: <https://cds.cern.ch/record/2216168>.
- [93] S. Frixione, E. Laenen, P. Motylinski, C. White and B. R. Webber, *Single-top hadroproduction in association with a W boson*, *JHEP* **07** (2008) 029, arXiv: [0805.3067 \[hep-ph\]](#).
- [94] D. J. Lange, *The EvtGen particle decay simulation package*, *Nucl. Instrum. Meth. A* **462** (2001) 152.
- [95] L. Lönnblad, *Correcting the Colour-Dipole Cascade Model with Fixed Order Matrix Elements*, *JHEP* **05** (2002) 046, arXiv: [hep-ph/0112284](#).

- [96] L. Lönnblad and S. Prestel, *Matching tree-level matrix elements with interleaved showers*, *JHEP* **03** (2012) 019, arXiv: [1109.4829 \[hep-ph\]](#).
- [97] T. Sjöstrand, S. Mrenna and P. Skands, *A brief introduction to PYTHIA 8.1*, *Comput. Phys. Commun.* **178** (2008) 852, arXiv: [0710.3820 \[hep-ph\]](#).
- [98] ATLAS Collaboration, *The Pythia 8 A3 tune description of ATLAS minimum bias and inelastic measurements incorporating the Donnachie–Landshoff diffractive model*, ATL-PHYS-PUB-2016-017, 2016, URL: <https://cds.cern.ch/record/2206965>.
- [99] ATLAS Collaboration, *Vertex Reconstruction Performance of the ATLAS Detector at $\sqrt{s} = 13$ TeV*, ATL-PHYS-PUB-2015-026, 2015, URL: <https://cds.cern.ch/record/2037717>.
- [100] ATLAS Collaboration, *Jet reconstruction and performance using particle flow with the ATLAS Detector*, *Eur. Phys. J. C* **77** (2017) 466, arXiv: [1703.10485 \[hep-ex\]](#).
- [101] M. Cacciari, G. P. Salam and G. Soyez, *The anti- k_t jet clustering algorithm*, *JHEP* **04** (2008) 063, arXiv: [0802.1189 \[hep-ph\]](#).
- [102] ATLAS Collaboration, *Jet energy scale and resolution measured in proton–proton collisions at $\sqrt{s} = 13$ TeV with the ATLAS detector*, *Eur. Phys. J. C* **81** (2020) 689, arXiv: [2007.02645 \[hep-ex\]](#).
- [103] ATLAS Collaboration, *Performance of pile-up mitigation techniques for jets in pp collisions at $\sqrt{s} = 8$ TeV using the ATLAS detector*, *Eur. Phys. J. C* **76** (2016) 581, arXiv: [1510.03823 \[hep-ex\]](#).
- [104] ATLAS Collaboration, *Optimisation and performance studies of the ATLAS b -tagging algorithms for the 2017-18 LHC run*, ATL-PHYS-PUB-2017-013, 2017, URL: <https://cds.cern.ch/record/2273281>.
- [105] ATLAS Collaboration, *ATLAS b -jet identification performance and efficiency measurement with $t\bar{t}$ events in pp collisions at $\sqrt{s} = 13$ TeV*, *Eur. Phys. J. C* **79** (2019) 970, arXiv: [1907.05120 \[hep-ex\]](#).
- [106] ATLAS Collaboration, *Electron reconstruction and identification in the ATLAS experiment using the 2015 and 2016 LHC proton–proton collision data at $\sqrt{s} = 13$ TeV*, *Eur. Phys. J. C* **79** (2019) 639, arXiv: [1902.04655 \[hep-ex\]](#).
- [107] ATLAS Collaboration, *Electron and photon performance measurements with the ATLAS detector using the 2015–2017 LHC proton–proton collision data*, *JINST* **14** (2019) P12006, arXiv: [1908.00005 \[hep-ex\]](#).
- [108] ATLAS Collaboration, *Muon reconstruction performance of the ATLAS detector in proton–proton collision data at $\sqrt{s} = 13$ TeV*, *Eur. Phys. J. C* **76** (2016) 292, arXiv: [1603.05598 \[hep-ex\]](#).
- [109] ATLAS Collaboration, *Muon reconstruction and identification efficiency in ATLAS using the full Run 2 pp collision data set at $\sqrt{s} = 13$ TeV*, *Eur. Phys. J. C* **81** (2021) 578, arXiv: [2012.00578 \[hep-ex\]](#).
- [110] ATLAS Collaboration, *Reconstruction, Energy Calibration, and Identification of Hadronically Decaying Tau Leptons in the ATLAS Experiment for Run-2 of the LHC*, ATL-PHYS-PUB-2015-045, 2015, URL: <https://cds.cern.ch/record/2064383>.
- [111] T. Barillari et al., *Local Hadronic Calibration*, ATL-LARG-PUB-2009-001-2, 2008, URL: <https://cds.cern.ch/record/1112035>.

- [112] ATLAS Collaboration, *Measurement of the tau lepton reconstruction and identification performance in the ATLAS experiment using pp collisions at $\sqrt{s} = 13$ TeV*, ATLAS-CONF-2017-029, 2017, URL: <https://cds.cern.ch/record/2261772>.
- [113] ATLAS Collaboration, *Identification of hadronic tau lepton decays using neural networks in the ATLAS experiment*, ATL-PHYS-PUB-2019-033, 2019, URL: <https://cds.cern.ch/record/2688062>.
- [114] ATLAS Collaboration, *E_T^{miss} performance in the ATLAS detector using 2015–2016 LHC pp collisions*, ATLAS-CONF-2018-023, 2018, URL: <https://cds.cern.ch/record/2625233>.
- [115] ATLAS Collaboration, *Measurements of Higgs boson production cross-sections in the $H \rightarrow \tau^+\tau^-$ decay channel in pp collisions at $\sqrt{s} = 13$ TeV with the ATLAS detector*, *JHEP* **08** (2022) 175, arXiv: [2201.08269](https://arxiv.org/abs/2201.08269) [[hep-ex](#)].
- [116] M. Baak et al., *HistFitter software framework for statistical data analysis*, *Eur. Phys. J. C* **75** (2015) 153, arXiv: [1410.1280](https://arxiv.org/abs/1410.1280) [[hep-ex](#)].
- [117] ATLAS Collaboration, *Selection of jets produced in 13 TeV proton–proton collisions with the ATLAS detector*, ATLAS-CONF-2015-029, 2015, URL: <https://cds.cern.ch/record/2037702>.
- [118] ATLAS Collaboration, *Cross-section measurements of the Higgs boson decaying into a pair of τ -leptons in proton–proton collisions at $\sqrt{s} = 13$ TeV with the ATLAS detector*, *Phys. Rev. D* **99** (2019) 072001, arXiv: [1811.08856](https://arxiv.org/abs/1811.08856) [[hep-ex](#)].
- [119] ATLAS Collaboration, *Jet energy scale measurements and their systematic uncertainties in proton–proton collisions at $\sqrt{s} = 13$ TeV with the ATLAS detector*, *Phys. Rev. D* **96** (2017) 072002, arXiv: [1703.09665](https://arxiv.org/abs/1703.09665) [[hep-ex](#)].
- [120] ATLAS Collaboration, *Tagging and suppression of pileup jets with the ATLAS detector*, ATLAS-CONF-2014-018, 2014, URL: <https://cds.cern.ch/record/1700870>.
- [121] ATLAS Collaboration, *Measurement of b-tagging efficiency of c-jets in $t\bar{t}$ events using a likelihood approach with the ATLAS detector*, ATLAS-CONF-2018-001, 2018, URL: <https://cds.cern.ch/record/2306649>.
- [122] ATLAS Collaboration, *Calibration of light-flavour b-jet mistagging rates using ATLAS proton–proton collision data at $\sqrt{s} = 13$ TeV*, ATLAS-CONF-2018-006, 2018, URL: <https://cds.cern.ch/record/2314418>.
- [123] ATLAS Collaboration, *Luminosity determination in pp collisions at $\sqrt{s} = 13$ TeV using the ATLAS detector at the LHC*, ATLAS-CONF-2019-021, 2019, URL: <https://cds.cern.ch/record/2677054>.
- [124] G. Avoni et al., *The new LUCID-2 detector for luminosity measurement and monitoring in ATLAS*, *JINST* **13** (2018) P07017.
- [125] ATLAS Collaboration, *Improvements in $t\bar{t}$ modelling using NLO+PS Monte Carlo generators for Run 2*, ATL-PHYS-PUB-2018-009, 2018, URL: <https://cds.cern.ch/record/2630327>.
- [126] ATLAS Collaboration, *Formulae for Estimating Significance*, ATL-PHYS-PUB-2020-025, 2020, URL: <https://cds.cern.ch/record/2736148>.
- [127] A. L. Read, *Presentation of search results: the CL_S technique*, *J. Phys. G* **28** (2002) 2693.

- [128] G. Cowan, K. Cranmer, E. Gross and O. Vitells,
Asymptotic formulae for likelihood-based tests of new physics, *Eur. Phys. J. C* **71** (2011) 1554,
arXiv: [1007.1727](https://arxiv.org/abs/1007.1727) [[physics.data-an](#)], Erratum: *Eur. Phys. J. C* **73** (2013) 2501.
- [129] ATLAS Collaboration, *ATLAS Computing Acknowledgements*, ATL-SOFT-PUB-2021-003, 2021,
URL: <https://cds.cern.ch/record/2776662>.

The ATLAS Collaboration

G. Aad ¹⁰², E. Aakvaag ¹⁶, B. Abbott ¹²⁰, K. Abeling ⁵⁵, S.H. Abidi ²⁹, A. Abouhorma ^{35e}, H. Abramowicz ¹⁵¹, H. Abreu ¹⁵⁰, Y. Abulaiti ¹¹⁷, A.C. Abusleme Hoffman ^{137a}, B.S. Acharya ^{69a,69b,p}, C. Adam Bourdarios ⁴, L. Adamczyk ^{85a}, L. Adamek ¹⁵⁵, S.V. Addepalli ²⁶, J. Adelman ¹¹⁵, A. Adiguzel ^{21c}, S. Adorni ⁵⁶, T. Adye ¹³⁴, A.A. Affolder ¹³⁶, Y. Afik ³⁶, M.N. Agaras ¹³, J. Agarwala ^{73a,73b}, A. Aggarwal ¹⁰⁰, C. Agheorghiesei ^{27c}, J.A. Aguilar-Saavedra ^{130f}, A. Ahmad ³⁶, F. Ahmadov ^{38,ab}, W.S. Ahmed ¹⁰⁴, S. Ahuja ⁹⁵, X. Ai ⁴⁸, G. Aielli ^{76a,76b}, M. Ait Tamlihat ^{35e}, B. Aitbenkikh ^{35a}, I. Aizenberg ¹⁶⁹, M. Akbiyik ¹⁰⁰, T.P.A. Åkesson ⁹⁸, A.V. Akimov ³⁷, N.N. Akolkar ²⁴, K. Al Khoury ⁴¹, G.L. Alberghi ^{23b}, J. Albert ¹⁶⁵, P. Albicocco ⁵³, S. Alderweireldt ⁵², M. Aleksa ³⁶, I.N. Aleksandrov ³⁸, C. Alexa ^{27b}, T. Alexopoulos ¹⁰, A. Alfonsi ¹¹⁴, F. Alfonsi ^{23b}, M. Alhroob ¹²⁰, B. Ali ¹³², S. Ali ¹⁴⁸, M. Aliev ³⁷, G. Alimonti ^{71a}, W. Alkakhri ⁵⁵, C. Allaire ⁶⁶, B.M.M. Allbrooke ¹⁴⁶, C.A. Allendes Flores ^{137f}, P.P. Allport ²⁰, A. Aloisio ^{72a,72b}, F. Alonso ⁹⁰, C. Alpigiani ¹³⁸, M. Alvarez Estevez ⁹⁹, A. Alvarez Fernandez ¹⁰⁰, M.G. Alvigi ^{72a,72b}, M. Aly ¹⁰¹, Y. Amaral Coutinho ^{82b}, A. Ambler ¹⁰⁴, C. Amelung ³⁶, M. Amerl ¹⁰¹, C.G. Ames ¹⁰⁹, D. Amidei ¹⁰⁶, S.P. Amor Dos Santos ^{130a}, K.R. Amos ¹⁶³, V. Ananiev ¹²⁵, C. Anastopoulos ¹³⁹, T. Andeen ¹¹, J.K. Anders ³⁶, S.Y. Andrean ^{47a,47b}, A. Andreazza ^{71a,71b}, S. Angelidakis ⁹, A. Angerami ^{41,ae}, A.V. Anisenkov ³⁷, A. Annovi ^{74a}, C. Antel ⁵⁶, M.T. Anthony ¹³⁹, E. Antipov ¹⁴⁵, M. Antonelli ⁵³, D.J.A. Antrim ^{17a}, F. Anulli ^{75a}, M. Aoki ⁸³, T. Aoki ¹⁵³, J.A. Aparisi Pozo ¹⁶³, M.A. Aparo ¹⁴⁶, L. Aperio Bella ⁴⁸, C. Appelt ¹⁸, N. Aranzabal ³⁶, V. Araujo Ferraz ^{82a}, C. Arcangeletti ⁵³, A.T.H. Arce ⁵¹, E. Arena ⁹², J-F. Arguin ¹⁰⁸, S. Argyropoulos ⁵⁴, J.-H. Arling ⁴⁸, A.J. Armbruster ³⁶, O. Arnaez ⁴, H. Arnold ¹¹⁴, Z.P. Arrubarrena Tame ¹⁰⁹, G. Artoni ^{75a,75b}, H. Asada ¹¹¹, K. Asai ¹¹⁸, S. Asai ¹⁵³, N.A. Asbah ⁶¹, J. Assahsah ^{35d}, K. Assamagan ²⁹, R. Astalos ^{28a}, R.J. Atkin ^{33a}, M. Atkinson ¹⁶², N.B. Atlay ¹⁸, H. Atmani ^{62b}, P.A. Atmasiddha ¹⁰⁶, K. Augsten ¹³², S. Auricchio ^{72a,72b}, A.D. Auriol ²⁰, V.A. Austrup ¹⁷¹, G. Avner ¹⁵⁰, G. Avolio ³⁶, K. Axiotis ⁵⁶, G. Azuelos ^{108,ai}, D. Babal ^{28b}, H. Bachacou ¹³⁵, K. Bachas ^{152,s}, A. Bachiu ³⁴, F. Backman ^{47a,47b}, A. Badea ⁶¹, P. Bagnaia ^{75a,75b}, M. Bahmani ¹⁸, A.J. Bailey ¹⁶³, V.R. Bailey ¹⁶², J.T. Baines ¹³⁴, C. Bakalis ¹⁰, O.K. Baker ¹⁷², E. Bakos ¹⁵, D. Bakshi Gupta ⁸, R. Balasubramanian ¹¹⁴, E.M. Baldin ³⁷, P. Balek ¹³³, E. Ballabene ^{71a,71b}, F. Balli ¹³⁵, L.M. Baltes ^{63a}, W.K. Balunas ³², J. Balz ¹⁰⁰, E. Banas ⁸⁶, M. Bandieramonte ¹²⁹, A. Bandyopadhyay ²⁴, S. Bansal ²⁴, L. Barak ¹⁵¹, E.L. Barberio ¹⁰⁵, D. Barberis ^{57b,57a}, M. Barbero ¹⁰², G. Barbour ⁹⁶, K.N. Barends ^{33a}, T. Barillari ¹¹⁰, M-S. Barisits ³⁶, T. Barklow ¹⁴³, P. Baron ¹²², D.A. Baron Moreno ¹⁰¹, A. Baroncelli ^{62a}, G. Barone ²⁹, A.J. Barr ¹²⁶, L. Barranco Navarro ^{47a,47b}, F. Barreiro ⁹⁹, J. Barreiro Guimarães da Costa ^{14a}, U. Barron ¹⁵¹, M.G. Barros Teixeira ^{130a}, S. Barsov ³⁷, F. Bartels ^{63a}, R. Bartoldus ¹⁴³, A.E. Barton ⁹¹, P. Bartos ^{28a}, A. Basan ¹⁰⁰, M. Baselga ⁴⁹, I. Bashta ^{77a,77b}, A. Bassalat ^{66,b}, M.J. Basso ¹⁵⁵, C.R. Basson ¹⁰¹, R.L. Bates ⁵⁹, S. Batlamous ^{35e}, J.R. Batley ³², B. Batool ¹⁴¹, M. Battaglia ¹³⁶, D. Battulga ¹⁸, M. Bauce ^{75a,75b}, M. Bauer ³⁶, P. Bauer ²⁴, J.B. Beacham ⁵¹, T. Beau ¹²⁷, P.H. Beauchemin ¹⁵⁸, F. Becherer ⁵⁴, P. Bechtel ²⁴, H.P. Beck ^{19,r}, K. Becker ¹⁶⁷, A.J. Beddall ^{21d}, V.A. Bednyakov ³⁸, C.P. Bee ¹⁴⁵, L.J. Beemster ¹⁵, T.A. Beermann ³⁶, M. Begalli ^{82d}, M. Begel ²⁹, A. Behera ¹⁴⁵, J.K. Behr ⁴⁸, C. Beirao Da Cruz E Silva ³⁶, J.F. Beirer ^{55,36}, F. Beisiegel ²⁴, M. Belfkir ¹⁵⁹, G. Bella ¹⁵¹, L. Bellagamba ^{23b}, A. Bellerive ³⁴, P. Bellos ²⁰, K. Beloborodov ³⁷, N.L. Belyaev ³⁷, D. Benchebroun ^{35a}, F. Bendebba ^{35a}, Y. Benhammou ¹⁵¹, M. Benoit ²⁹, J.R. Bensinger ²⁶, S. Bentvelsen ¹¹⁴, L. Beresford ⁴⁸,

M. Beretta ⁵³, E. Bergeaas Kuutmann ¹⁶¹, N. Berger ⁴, B. Bergmann ¹³², J. Beringer ^{17a},
S. Berlendis ⁷, G. Bernardi ⁵, C. Bernius ¹⁴³, F.U. Bernlochner ²⁴, T. Berry ⁹⁵, P. Berta ¹³³,
A. Berthold ⁵⁰, I.A. Bertram ⁹¹, S. Bethke ¹¹⁰, A. Betti ^{75a,75b}, A.J. Bevan ⁹⁴, M. Bhamjee ^{33c},
S. Bhatta ¹⁴⁵, D.S. Bhattacharya ¹⁶⁶, P. Bhattarai ²⁶, V.S. Bhopatkar ¹²¹, R. Bi ^{29,ak},
R.M. Bianchi ¹²⁹, O. Biebel ¹⁰⁹, R. Bielski ¹²³, M. Biglietti ^{77a}, T.R.V. Billoud ¹³², M. Bindi ⁵⁵,
A. Bingul ^{21b}, C. Bini ^{75a,75b}, A. Biondini ⁹², C.J. Birch-sykes ¹⁰¹, G.A. Bird ^{20,134},
M. Birman ¹⁶⁹, M. Biroš ¹³³, T. Bisanz ³⁶, E. Bisceglie ^{43b,43a}, D. Biswas ¹⁷⁰, A. Bitadze ¹⁰¹,
K. Bjørke ¹²⁵, I. Bloch ⁴⁸, C. Blocker ²⁶, A. Blue ⁵⁹, U. Blumenschein ⁹⁴, J. Blumenthal ¹⁰⁰,
G.J. Bobbink ¹¹⁴, V.S. Bobrovnikov ³⁷, M. Boehler ⁵⁴, D. Bogavac ³⁶, A.G. Bogdanchikov ³⁷,
C. Bohm ^{47a}, V. Boisvert ⁹⁵, P. Bokan ⁴⁸, T. Bold ^{85a}, M. Bomben ⁵, M. Bona ⁹⁴,
M. Boonekamp ¹³⁵, C.D. Booth ⁹⁵, A.G. Borbély ⁵⁹, H.M. Borecka-Bielska ¹⁰⁸, L.S. Borgna ⁹⁶,
G. Borissov ⁹¹, D. Bortoletto ¹²⁶, D. Boscherini ^{23b}, M. Bosman ¹³, J.D. Bossio Sola ³⁶,
K. Bouaouda ^{35a}, N. Bouchhar ¹⁶³, J. Boudreau ¹²⁹, E.V. Bouhova-Thacker ⁹¹, D. Boumediene ⁴⁰,
R. Bouquet ⁵, A. Boveia ¹¹⁹, J. Boyd ³⁶, D. Boye ²⁹, I.R. Boyko ³⁸, J. Bracinik ²⁰,
N. Brahimí ^{62d}, G. Brandt ¹⁷¹, O. Brandt ³², F. Braren ⁴⁸, B. Brau ¹⁰³, J.E. Brau ¹²³,
K. Brendlinger ⁴⁸, R. Brenner ¹⁶⁹, L. Brenner ¹¹⁴, R. Brenner ¹⁶¹, S. Bressler ¹⁶⁹, D. Britton ⁵⁹,
D. Britzger ¹¹⁰, I. Brock ²⁴, G. Brooijmans ⁴¹, W.K. Brooks ^{137f}, E. Brost ²⁹, L.M. Brown ¹⁶⁵,
T.L. Bruckler ¹²⁶, P.A. Bruckman de Renstrom ⁸⁶, B. Brüers ⁴⁸, D. Bruncko ^{28b,*}, A. Bruni ^{23b},
G. Bruni ^{23b}, M. Bruschi ^{23b}, N. Brusino ^{75a,75b}, T. Buanes ¹⁶, Q. Buat ¹³⁸, A.G. Buckley ⁵⁹,
I.A. Budagov ^{38,*}, M.K. Bugge ¹²⁵, O. Bulekov ³⁷, B.A. Bullard ¹⁴³, S. Burdin ⁹²,
C.D. Burgard ⁴⁹, A.M. Burger ⁴⁰, B. Burghgrave ⁸, O. Burlayenko ⁵⁴, J.T.P. Burr ³²,
C.D. Burton ¹¹, J.C. Burzynski ¹⁴², E.L. Busch ⁴¹, V. Büscher ¹⁰⁰, P.J. Bussey ⁵⁹,
J.M. Butler ²⁵, C.M. Buttar ⁵⁹, J.M. Butterworth ⁹⁶, W. Buttinger ¹³⁴, C.J. Buxo Vazquez ¹⁰⁷,
A.R. Buzykaev ³⁷, G. Cabras ^{23b}, S. Cabrera Urbán ¹⁶³, D. Caforio ⁵⁸, H. Cai ¹²⁹, Y. Cai ^{14a,14e},
V.M.M. Cairo ³⁶, O. Cakir ^{3a}, N. Calace ³⁶, P. Calafiura ^{17a}, G. Calderini ¹²⁷, P. Calfayan ⁶⁸,
G. Callea ⁵⁹, L.P. Caloba ^{82b}, D. Calvet ⁴⁰, S. Calvet ⁴⁰, T.P. Calvet ¹⁰², M. Calvetti ^{74a,74b},
R. Camacho Toro ¹²⁷, S. Camarda ³⁶, D. Camarero Munoz ²⁶, P. Camarri ^{76a,76b},
M.T. Camerlingo ^{72a,72b}, D. Cameron ¹²⁵, C. Camincher ¹⁶⁵, M. Campanelli ⁹⁶, A. Camplani ⁴²,
V. Canale ^{72a,72b}, A. Canesse ¹⁰⁴, M. Cano Bret ⁸⁰, J. Cantero ¹⁶³, Y. Cao ¹⁶², F. Capocasa ²⁶,
M. Capua ^{43b,43a}, A. Carbone ^{71a,71b}, R. Cardarelli ^{76a}, J.C.J. Cardenas ⁸, F. Cardillo ¹⁶³,
T. Carli ³⁶, G. Carlino ^{72a}, J.I. Carlotto ¹³, B.T. Carlson ^{129,t}, E.M. Carlson ^{165,156a},
L. Carminati ^{71a,71b}, M. Carnesale ^{75a,75b}, S. Caron ¹¹³, E. Carquin ^{137f}, S. Carrá ^{71a,71b},
G. Carratta ^{23b,23a}, F. Carrio Argos ^{33g}, J.W.S. Carter ¹⁵⁵, T.M. Carter ⁵², M.P. Casado ^{13,j},
A.F. Casha ¹⁵⁵, M. Caspar ⁴⁸, E.G. Castiglia ¹⁷², F.L. Castillo ^{63a}, L. Castillo Garcia ¹³,
V. Castillo Gimenez ¹⁶³, N.F. Castro ^{130a,130e}, A. Catinaccio ³⁶, J.R. Catmore ¹²⁵, V. Cavaliere ²⁹,
N. Cavalli ^{23b,23a}, V. Cavalinni ^{74a,74b}, E. Celebi ^{21a}, F. Celli ¹²⁶, M.S. Centonze ^{70a,70b},
K. Cerny ¹²², A.S. Cerqueira ^{82a}, A. Cerri ¹⁴⁶, L. Cerrito ^{76a,76b}, F. Cerutti ^{17a}, A. Cervelli ^{23b},
G. Cesarini ⁵³, S.A. Cetin ^{21d}, Z. Chadi ^{35a}, D. Chakraborty ¹¹⁵, M. Chala ^{130f}, J. Chan ¹⁷⁰,
W.Y. Chan ¹⁵³, J.D. Chapman ³², B. Chargeishvili ^{149b}, D.G. Charlton ²⁰, T.P. Charman ⁹⁴,
M. Chatterjee ¹⁹, C. Chauhan ¹³³, S. Chekanov ⁶, S.V. Chekulaev ^{156a}, G.A. Chelkov ^{38,a},
A. Chen ¹⁰⁶, B. Chen ¹⁵¹, B. Chen ¹⁶⁵, H. Chen ^{14c}, H. Chen ²⁹, J. Chen ^{62c}, J. Chen ¹⁴²,
S. Chen ¹⁵³, S.J. Chen ^{14c}, X. Chen ^{62c}, X. Chen ^{14b,ah}, Y. Chen ^{62a}, C.L. Cheng ¹⁷⁰,
H.C. Cheng ^{64a}, S. Cheong ¹⁴³, A. Cheplakov ³⁸, E. Cheremushkina ⁴⁸, E. Cherepanova ¹¹⁴,
R. Cherkaoui El Moursli ^{35e}, E. Cheu ⁷, K. Cheung ⁶⁵, L. Chevalier ¹³⁵, V. Chiarella ⁵³,
G. Chiarelli ^{74a}, N. Chiedde ¹⁰², G. Chiodini ^{70a}, A.S. Chisholm ²⁰, A. Chitan ^{27b},
M. Chitishvili ¹⁶³, M.V. Chizhov ³⁸, K. Choi ¹¹, A.R. Chomont ^{75a,75b}, Y. Chou ¹⁰³,
E.Y.S. Chow ¹¹⁴, T. Chowdhury ^{33g}, L.D. Christopher ^{33g}, K.L. Chu ^{64a}, M.C. Chu ^{64a},

X. Chu [ID14a,14e](#), J. Chudoba [ID131](#), J.J. Chwastowski [ID86](#), D. Cieri [ID110](#), K.M. Ciesla [ID85a](#), V. Cindro [ID93](#),
 A. Ciocio [ID17a](#), F. Cirotto [ID72a,72b](#), Z.H. Citron [ID169,m](#), M. Citterio [ID71a](#), D.A. Ciubotaru [ID27b](#),
 B.M. Ciungu [ID155](#), A. Clark [ID56](#), P.J. Clark [ID52](#), J.M. Clavijo Columbie [ID48](#), S.E. Clawson [ID101](#),
 C. Clement [ID47a,47b](#), J. Clercx [ID48](#), L. Clissa [ID23b,23a](#), Y. Coadou [ID102](#), M. Cobal [ID69a,69c](#),
 A. Cocco [ID57b](#), R.F. Coelho Barrue [ID130a](#), R. Coelho Lopes De Sa [ID103](#), S. Coelli [ID71a](#), H. Cohen [ID151](#),
 A.E.C. Coimbra [ID71a,71b](#), B. Cole [ID41](#), J. Collot [ID60](#), P. Conde Muiño [ID130a,130g](#), M.P. Connell [ID33c](#),
 S.H. Connell [ID33c](#), I.A. Connelly [ID59](#), E.I. Conroy [ID126](#), F. Conventi [ID72a,aj](#), H.G. Cooke [ID20](#),
 A.M. Cooper-Sarkar [ID126](#), F. Cormier [ID164](#), L.D. Corpe [ID36](#), M. Corradi [ID75a,75b](#), F. Corriveau [ID104,z](#),
 A. Cortes-Gonzalez [ID18](#), M.J. Costa [ID163](#), F. Costanza [ID4](#), D. Costanzo [ID139](#), B.M. Cote [ID119](#),
 G. Cowan [ID95](#), K. Cranmer [ID117](#), S. Crépe-Renaudin [ID60](#), F. Crescioli [ID127](#), M. Cristinziani [ID141](#),
 M. Cristoforetti [ID78a,78b,d](#), V. Croft [ID114](#), G. Crosetti [ID43b,43a](#), A. Cueto [ID36](#),
 T. Cuhadar Donszelmann [ID160](#), H. Cui [ID14a,14e](#), Z. Cui [ID7](#), W.R. Cunningham [ID59](#), F. Curcio [ID43b,43a](#),
 P. Czodrowski [ID36](#), M.M. Czurylo [ID63b](#), M.J. Da Cunha Sargedas De Sousa [ID62a](#),
 J.V. Da Fonseca Pinto [ID82b](#), C. Da Via [ID101](#), W. Dabrowski [ID85a](#), T. Dado [ID49](#), S. Dahbi [ID33g](#), T. Dai [ID106](#),
 C. Dallapiccola [ID103](#), M. Dam [ID42](#), G. D'amen [ID29](#), V. D'Amico [ID109](#), J. Damp [ID100](#), J.R. Dandoy [ID128](#),
 M.F. Daneri [ID30](#), M. Danninger [ID142](#), V. Dao [ID36](#), G. Darbo [ID57b](#), S. Darmora [ID6](#), S.J. Das [ID29,ak](#),
 S. D'Auria [ID71a,71b](#), C. David [ID156b](#), T. Davidek [ID133](#), B. Davis-Purcell [ID34](#), I. Dawson [ID94](#), K. De [ID8](#),
 R. De Asmundis [ID72a](#), N. De Biase [ID48](#), S. De Castro [ID23b,23a](#), N. De Groot [ID113](#), P. de Jong [ID114](#),
 H. De la Torre [ID107](#), A. De Maria [ID14c](#), A. De Salvo [ID75a](#), U. De Sanctis [ID76a,76b](#), A. De Santo [ID146](#),
 J.B. De Vivie De Regie [ID60](#), D.V. Dedovich [ID38](#), J. Degens [ID114](#), A.M. Deiana [ID44](#), F. Del Corso [ID23b,23a](#),
 J. Del Peso [ID99](#), F. Del Rio [ID63a](#), F. Deliot [ID135](#), C.M. Delitzsch [ID49](#), M. Della Pietra [ID72a,72b](#),
 D. Della Volpe [ID56](#), A. Dell'Acqua [ID36](#), L. Dell'Asta [ID71a,71b](#), M. Delmastro [ID4](#), P.A. Delsart [ID60](#),
 S. Demers [ID172](#), M. Demichev [ID38](#), S.P. Denisov [ID37](#), L. D'Eramo [ID115](#), D. Derendarz [ID86](#),
 F. Derue [ID127](#), P. Dervan [ID92](#), K. Desch [ID24](#), K. Dette [ID155](#), C. Deutsch [ID24](#), F.A. Di Bello [ID57b,57a](#),
 A. Di Ciaccio [ID76a,76b](#), L. Di Ciaccio [ID4](#), A. Di Domenico [ID75a,75b](#), C. Di Donato [ID72a,72b](#),
 A. Di Girolamo [ID36](#), G. Di Gregorio [ID5](#), A. Di Luca [ID78a,78b](#), B. Di Micco [ID77a,77b](#), R. Di Nardo [ID77a,77b](#),
 C. Diaconu [ID102](#), F.A. Dias [ID114](#), T. Dias Do Vale [ID142](#), M.A. Diaz [ID137a,137b](#), F.G. Diaz Capriles [ID24](#),
 M. Didenko [ID163](#), E.B. Diehl [ID106](#), L. Diehl [ID54](#), S. Díez Cornell [ID48](#), C. Diez Pardos [ID141](#),
 C. Dimitriadi [ID24,161](#), A. Dimitrievska [ID17a](#), J. Dingfelder [ID24](#), I-M. Dinu [ID27b](#), S.J. Dittmeier [ID63b](#),
 F. Dittus [ID36](#), F. Djama [ID102](#), T. Djobava [ID149b](#), J.I. Djuvsland [ID16](#), C. Doglioni [ID101,98](#), J. Dolejsi [ID133](#),
 Z. Dolezal [ID133](#), M. Donadelli [ID82c](#), B. Dong [ID107](#), J. Donini [ID40](#), A. D'Onofrio [ID77a,77b](#),
 M. D'Onofrio [ID92](#), J. Dopke [ID134](#), A. Doria [ID72a](#), M.T. Dova [ID90](#), A.T. Doyle [ID59](#), M.A. Draguet [ID126](#),
 E. Drechsler [ID142](#), E. Dreyer [ID169](#), I. Drivas-koulouris [ID10](#), A.S. Drobac [ID158](#), M. Drozdova [ID56](#),
 D. Du [ID62a](#), T.A. du Pree [ID114](#), F. Dubinin [ID37](#), M. Dubovsky [ID28a](#), E. Duchovni [ID169](#), G. Duckeck [ID109](#),
 O.A. Ducu [ID27b](#), D. Duda [ID110](#), A. Dudarev [ID36](#), E.R. Duden [ID26](#), M. D'uffizi [ID101](#), L. Dufflot [ID66](#),
 M. Dührssen [ID36](#), C. Dülsen [ID171](#), A.E. Dumitriu [ID27b](#), M. Dunford [ID63a](#), S. Dungs [ID49](#),
 K. Dunne [ID47a,47b](#), A. Duperrin [ID102](#), H. Duran Yildiz [ID3a](#), M. Düren [ID58](#), A. Durglishvili [ID149b](#),
 B.L. Dwyer [ID115](#), G.I. Dyckes [ID17a](#), M. Dyndal [ID85a](#), S. Dysch [ID101](#), B.S. Dziedzic [ID86](#),
 Z.O. Earnshaw [ID146](#), B. Eckerova [ID28a](#), S. Eggebrecht [ID55](#), M.G. Eggleston [ID51](#),
 E. Egidio Purcino De Souza [ID127](#), L.F. Ehrke [ID56](#), G. Eigen [ID16](#), K. Einsweiler [ID17a](#), T. Ekelof [ID161](#),
 P.A. Ekman [ID98](#), Y. El Ghazali [ID35b](#), H. El Jarrari [ID35e,148](#), A. El Moussaouy [ID35a](#), V. Ellajosyula [ID161](#),
 M. Ellert [ID161](#), F. Ellinghaus [ID171](#), A.A. Elliot [ID94](#), N. Ellis [ID36](#), J. Elmsheuser [ID29](#), M. Elsing [ID36](#),
 D. Emelianov [ID134](#), Y. Enari [ID153](#), I. Ene [ID17a](#), S. Epari [ID13](#), J. Erdmann [ID49](#), P.A. Erland [ID86](#),
 M. Errenst [ID171](#), M. Escalier [ID66](#), C. Escobar [ID163](#), E. Etzion [ID151](#), G. Evans [ID130a](#), H. Evans [ID68](#),
 M.O. Evans [ID146](#), A. Ezhilov [ID37](#), S. Ezzarqtouni [ID35a](#), F. Fabbri [ID59](#), L. Fabbri [ID23b,23a](#), G. Facini [ID96](#),
 V. Fadeyev [ID136](#), R.M. Fakhruddinov [ID37](#), S. Falciano [ID75a](#), L.F. Falda Ulhoa Coelho [ID36](#), P.J. Falke [ID24](#),
 S. Falke [ID36](#), J. Faltova [ID133](#), C. Fan [ID162](#), Y. Fan [ID14a](#), Y. Fang [ID14a,14e](#), M. Fanti [ID71a,71b](#),

M. Faraj [ID](#)^{69a,69b}, Z. Farazpay [ID](#)⁹⁷, A. Farbin [ID](#)⁸, A. Farilla [ID](#)^{77a}, T. Farooque [ID](#)¹⁰⁷, S.M. Farrington [ID](#)⁵²,
F. Fassi [ID](#)^{35e}, D. Fassouliotis [ID](#)⁹, M. Faucci Giannelli [ID](#)^{76a,76b}, W.J. Fawcett [ID](#)³², L. Fayard [ID](#)⁶⁶,
P. Federic [ID](#)¹³³, P. Federicova [ID](#)¹³¹, O.L. Fedin [ID](#)^{37,a}, G. Fedotov [ID](#)³⁷, M. Feickert [ID](#)¹⁷⁰,
L. Feligioni [ID](#)¹⁰², A. Fell [ID](#)¹³⁹, D.E. Fellers [ID](#)¹²³, C. Feng [ID](#)^{62b}, M. Feng [ID](#)^{14b}, Z. Feng [ID](#)¹¹⁴,
M.J. Fenton [ID](#)¹⁶⁰, A.B. Fenyuk [ID](#)³⁷, L. Ferencz [ID](#)⁴⁸, R.A.M. Ferguson [ID](#)⁹¹, S.I. Fernandez Luengo [ID](#)^{137f},
M.J.V. Fernoux [ID](#)¹⁰², J. Ferrando [ID](#)⁴⁸, A. Ferrari [ID](#)¹⁶¹, P. Ferrari [ID](#)^{114,113}, R. Ferrari [ID](#)^{73a}, D. Ferrere [ID](#)⁵⁶,
C. Ferretti [ID](#)¹⁰⁶, F. Fiedler [ID](#)¹⁰⁰, A. Filipčič [ID](#)⁹³, E.K. Filmer [ID](#)¹, F. Filthaut [ID](#)¹¹³,
M.C.N. Fiolhais [ID](#)^{130a,130c,c}, L. Fiorini [ID](#)¹⁶³, W.C. Fisher [ID](#)¹⁰⁷, T. Fitschen [ID](#)¹⁰¹, I. Fleck [ID](#)¹⁴¹,
P. Fleischmann [ID](#)¹⁰⁶, T. Flick [ID](#)¹⁷¹, L. Flores [ID](#)¹²⁸, M. Flores [ID](#)^{33d,af}, L.R. Flores Castillo [ID](#)^{64a},
F.M. Follega [ID](#)^{78a,78b}, N. Fomin [ID](#)¹⁶, J.H. Foo [ID](#)¹⁵⁵, B.C. Forland [ID](#)⁶⁸, A. Formica [ID](#)¹³⁵, A.C. Forti [ID](#)¹⁰¹,
E. Fortin [ID](#)³⁶, A.W. Fortman [ID](#)⁶¹, M.G. Foti [ID](#)^{17a}, L. Fountas [ID](#)^{9,k}, D. Fournier [ID](#)⁶⁶, H. Fox [ID](#)⁹¹,
P. Francavilla [ID](#)^{74a,74b}, S. Francescato [ID](#)⁶¹, S. Franchellucci [ID](#)⁵⁶, M. Franchini [ID](#)^{23b,23a},
S. Franchino [ID](#)^{63a}, D. Francis [ID](#)³⁶, L. Franco [ID](#)¹¹³, L. Franconi [ID](#)⁴⁸, M. Franklin [ID](#)⁶¹, G. Frattari [ID](#)²⁶,
A.C. Freegard [ID](#)⁹⁴, W.S. Freund [ID](#)^{82b}, Y.Y. Frid [ID](#)¹⁵¹, N. Fritzsche [ID](#)⁵⁰, A. Froch [ID](#)⁵⁴, D. Froidevaux [ID](#)³⁶,
J.A. Frost [ID](#)¹²⁶, Y. Fu [ID](#)^{62a}, M. Fujimoto [ID](#)¹¹⁸, E. Fullana Torregrosa [ID](#)^{163,*},
E. Furtado De Simas Filho [ID](#)^{82b}, J. Fuster [ID](#)¹⁶³, A. Gabrielli [ID](#)^{23b,23a}, A. Gabrielli [ID](#)¹⁵⁵, P. Gadow [ID](#)⁴⁸,
G. Gagliardi [ID](#)^{57b,57a}, L.G. Gagnon [ID](#)^{17a}, E.J. Gallas [ID](#)¹²⁶, B.J. Gallop [ID](#)¹³⁴, K.K. Gan [ID](#)¹¹⁹,
S. Ganguly [ID](#)¹⁵³, J. Gao [ID](#)^{62a}, Y. Gao [ID](#)⁵², F.M. Garay Walls [ID](#)^{137a,137b}, B. Garcia [ID](#)^{29,ak}, C. García [ID](#)¹⁶³,
J.E. García Navarro [ID](#)¹⁶³, M. Garcia-Sciveres [ID](#)^{17a}, R.W. Gardner [ID](#)³⁹, D. Garg [ID](#)⁸⁰, R.B. Garg [ID](#)^{143,q},
C.A. Garner [ID](#)¹⁵⁵, S.J. Gasiorowski [ID](#)¹³⁸, P. Gaspar [ID](#)^{82b}, G. Gaudio [ID](#)^{73a}, V. Gautam [ID](#)¹³, P. Gauzzi [ID](#)^{75a,75b},
I.L. Gavrilenko [ID](#)³⁷, A. Gavriyuk [ID](#)³⁷, C. Gay [ID](#)¹⁶⁴, G. Gaycken [ID](#)⁴⁸, E.N. Gazis [ID](#)¹⁰,
A.A. Geanta [ID](#)^{27b,27e}, C.M. Gee [ID](#)¹³⁶, C. Gemme [ID](#)^{57b}, M.H. Genest [ID](#)⁶⁰, S. Gentile [ID](#)^{75a,75b},
S. George [ID](#)⁹⁵, W.F. George [ID](#)²⁰, T. Gerialis [ID](#)⁴⁶, L.O. Gerlach [ID](#)⁵⁵, P. Gessinger-Befurt [ID](#)³⁶,
M.E. Geyik [ID](#)¹⁷¹, M. Ghneimat [ID](#)¹⁴¹, K. Ghorbanian [ID](#)⁹⁴, A. Ghosal [ID](#)¹⁴¹, A. Ghosh [ID](#)¹⁶⁰, A. Ghosh [ID](#)⁷,
B. Giacobbe [ID](#)^{23b}, S. Giagu [ID](#)^{75a,75b}, P. Giannetti [ID](#)^{74a}, A. Giannini [ID](#)^{62a}, S.M. Gibson [ID](#)⁹⁵,
M. Gignac [ID](#)¹³⁶, D.T. Gil [ID](#)^{85b}, A.K. Gilbert [ID](#)^{85a}, B.J. Gilbert [ID](#)⁴¹, D. Gillberg [ID](#)³⁴, G. Gilles [ID](#)¹¹⁴,
N.E.K. Gillwald [ID](#)⁴⁸, L. Ginabat [ID](#)¹²⁷, D.M. Gingrich [ID](#)^{2,ai}, M.P. Giordani [ID](#)^{69a,69c}, P.F. Giraud [ID](#)¹³⁵,
G. Giugliarelli [ID](#)^{69a,69c}, D. Giugni [ID](#)^{71a}, F. Giuli [ID](#)³⁶, I. Gkialas [ID](#)^{9,k}, L.K. Gladilin [ID](#)³⁷, C. Glasman [ID](#)⁹⁹,
G.R. Gledhill [ID](#)¹²³, M. Glisic [ID](#)¹²³, I. Gnesi [ID](#)^{43b,g}, Y. Go [ID](#)^{29,ak}, M. Goblirsch-Kolb [ID](#)³⁶, B. Gocke [ID](#)⁴⁹,
D. Godin [ID](#)¹⁰⁸, B. Gokturk [ID](#)^{21a}, S. Goldfarb [ID](#)¹⁰⁵, T. Golling [ID](#)⁵⁶, M.G.D. Gololo [ID](#)^{33g}, D. Golubkov [ID](#)³⁷,
J.P. Gombas [ID](#)¹⁰⁷, A. Gomes [ID](#)^{130a,130b}, G. Gomes Da Silva [ID](#)¹⁴¹, A.J. Gomez Delegido [ID](#)¹⁶³,
R. Gonçalves [ID](#)^{130a,130c}, G. Gonella [ID](#)¹²³, L. Gonella [ID](#)²⁰, A. Gongadze [ID](#)³⁸, F. Gonnella [ID](#)²⁰,
J.L. Gonski [ID](#)⁴¹, R.Y. González Andana [ID](#)⁵², S. González de la Hoz [ID](#)¹⁶³, S. Gonzalez Fernandez [ID](#)¹³,
R. Gonzalez Lopez [ID](#)⁹², C. Gonzalez Renteria [ID](#)^{17a}, R. Gonzalez Suarez [ID](#)¹⁶¹, S. Gonzalez-Sevilla [ID](#)⁵⁶,
G.R. Gonzalvo Rodriguez [ID](#)¹⁶³, L. Goossens [ID](#)³⁶, P.A. Gorbounov [ID](#)³⁷, B. Gorini [ID](#)³⁶, E. Gorini [ID](#)^{70a,70b},
A. Gorišek [ID](#)⁹³, T.C. Gosart [ID](#)¹²⁸, A.T. Goshaw [ID](#)⁵¹, M.I. Gostkin [ID](#)³⁸, S. Goswami [ID](#)¹²¹,
C.A. Gottardo [ID](#)³⁶, M. Goughri [ID](#)^{35b}, V. Goumarre [ID](#)⁴⁸, A.G. Goussiou [ID](#)¹³⁸, N. Govender [ID](#)^{33c},
I. Grabowska-Bold [ID](#)^{85a}, K. Graham [ID](#)³⁴, E. Gramstad [ID](#)¹²⁵, S. Grancagnolo [ID](#)^{70a,70b}, M. Grandi [ID](#)¹⁴⁶,
V. Gratchev [ID](#)^{37,*}, P.M. Gravila [ID](#)^{27f}, F.G. Gravili [ID](#)^{70a,70b}, H.M. Gray [ID](#)^{17a}, M. Greco [ID](#)^{70a,70b},
C. Grefe [ID](#)²⁴, I.M. Gregor [ID](#)⁴⁸, P. Grenier [ID](#)¹⁴³, C. Grieco [ID](#)¹³, A.A. Grillo [ID](#)¹³⁶, K. Grimm [ID](#)^{31,n},
S. Grinstein [ID](#)^{13,v}, J.-F. Grivaz [ID](#)⁶⁶, E. Gross [ID](#)¹⁶⁹, J. Grosse-Knetter [ID](#)⁵⁵, C. Grud [ID](#)¹⁰⁶, J.C. Grundy [ID](#)¹²⁶,
L. Guan [ID](#)¹⁰⁶, W. Guan [ID](#)²⁹, C. Gubbels [ID](#)¹⁶⁴, J.G.R. Guerrero Rojas [ID](#)¹⁶³, G. Guerrieri [ID](#)^{69a,69b},
F. Guescini [ID](#)¹¹⁰, R. Gugel [ID](#)¹⁰⁰, J.A.M. Guhit [ID](#)¹⁰⁶, A. Guida [ID](#)⁴⁸, T. Guillemin [ID](#)⁴,
E. Guilloton [ID](#)^{167,134}, S. Guindon [ID](#)³⁶, F. Guo [ID](#)^{14a,14e}, J. Guo [ID](#)^{62c}, L. Guo [ID](#)⁶⁶, Y. Guo [ID](#)¹⁰⁶,
R. Gupta [ID](#)⁴⁸, S. Gurbuz [ID](#)²⁴, S.S. Gurdasani [ID](#)⁵⁴, G. Gustavino [ID](#)³⁶, M. Guth [ID](#)⁵⁶, P. Gutierrez [ID](#)¹²⁰,
L.F. Gutierrez Zagazeta [ID](#)¹²⁸, C. Gutschow [ID](#)⁹⁶, C. Gwenlan [ID](#)¹²⁶, C.B. Gwilliam [ID](#)⁹², E.S. Haaland [ID](#)¹²⁵,
A. Haas [ID](#)¹¹⁷, M. Habedank [ID](#)⁴⁸, C. Haber [ID](#)^{17a}, H.K. Hadavand [ID](#)⁸, A. Hadeef [ID](#)¹⁰⁰, S. Hadzic [ID](#)¹¹⁰,

E.H. Haines ¹⁹⁶, M. Haleem ¹⁶⁶, J. Haley ¹²¹, J.J. Hall ¹³⁹, G.D. Hallewell ¹⁰², L. Halser ¹⁹,
 K. Hamano ¹⁶⁵, H. Hamdaoui ^{35e}, M. Hamer ²⁴, G.N. Hamity ⁵², E.J. Hampshire ⁹⁵, J. Han ^{62b},
 K. Han ^{62a}, L. Han ^{14c}, L. Han ^{62a}, S. Han ^{17a}, Y.F. Han ¹⁵⁵, K. Hanagaki ⁸³, M. Hance ¹³⁶,
 D.A. Hangal ^{41,ae}, H. Hanif ¹⁴², M.D. Hank ¹²⁸, R. Hankache ¹⁰¹, J.B. Hansen ⁴²,
 J.D. Hansen ⁴², P.H. Hansen ⁴², K. Hara ¹⁵⁷, D. Harada ⁵⁶, T. Harenberg ¹⁷¹, S. Harkusha ³⁷,
 Y.T. Harris ¹²⁶, N.M. Harrison ¹¹⁹, P.F. Harrison ¹⁶⁷, N.M. Hartman ¹⁴³, N.M. Hartmann ¹⁰⁹,
 Y. Hasegawa ¹⁴⁰, A. Hasib ⁵², S. Haug ¹⁹, R. Hauser ¹⁰⁷, M. Havranek ¹³², C.M. Hawkes ²⁰,
 R.J. Hawkings ³⁶, S. Hayashida ¹¹¹, D. Hayden ¹⁰⁷, C. Hayes ¹⁰⁶, R.L. Hayes ¹¹⁴, C.P. Hays ¹²⁶,
 J.M. Hays ⁹⁴, H.S. Hayward ⁹², F. He ^{62a}, Y. He ¹⁵⁴, Y. He ¹²⁷, N.B. Heatley ⁹⁴,
 V. Hedberg ⁹⁸, A.L. Heggelund ¹²⁵, N.D. Hehir ⁹⁴, C. Heidegger ⁵⁴, K.K. Heidegger ⁵⁴,
 W.D. Heidorn ⁸¹, J. Heilman ³⁴, S. Heim ⁴⁸, T. Heim ^{17a}, J.G. Heinlein ¹²⁸, J.J. Heinrich ¹²³,
 L. Heinrich ^{110,ag}, J. Hejbal ¹³¹, L. Helary ⁴⁸, A. Held ¹⁷⁰, S. Hellesund ¹⁶, C.M. Helling ¹⁶⁴,
 S. Hellman ^{47a,47b}, C. Helsens ³⁶, R.C.W. Henderson ⁹¹, L. Henkelmann ³²,
 A.M. Henriques Correia ³⁶, H. Herde ⁹⁸, Y. Hernández Jiménez ¹⁴⁵, L.M. Herrmann ²⁴,
 T. Herrmann ⁵⁰, G. Herten ⁵⁴, R. Hertenberger ¹⁰⁹, L. Hervas ³⁶, N.P. Hessey ^{156a}, H. Hibi ⁸⁴,
 S.J. Hillier ²⁰, F. Hinterkeuser ²⁴, M. Hirose ¹²⁴, S. Hirose ¹⁵⁷, D. Hirschbuehl ¹⁷¹,
 T.G. Hitchings ¹⁰¹, B. Hiti ⁹³, J. Hobbs ¹⁴⁵, R. Hobincu ^{27e}, N. Hod ¹⁶⁹, M.C. Hodgkinson ¹³⁹,
 B.H. Hodgkinson ³², A. Hoecker ³⁶, J. Hofer ⁴⁸, T. Holm ²⁴, M. Holzbock ¹¹⁰,
 L.B.A.H. Hommels ³², B.P. Honan ¹⁰¹, J. Hong ^{62c}, T.M. Hong ¹²⁹, J.C. Honig ⁵⁴,
 B.H. Hooberman ¹⁶², W.H. Hopkins ⁶, Y. Horii ¹¹¹, S. Hou ¹⁴⁸, A.S. Howard ⁹³, J. Howarth ⁵⁹,
 J. Hoya ⁶, M. Hrabovsky ¹²², A. Hrynevich ⁴⁸, T. Hryn'ova ⁴, P.J. Hsu ⁶⁵, S.-C. Hsu ¹³⁸,
 Q. Hu ⁴¹, Y.F. Hu ^{14a,14e}, D.P. Huang ⁹⁶, S. Huang ^{64b}, X. Huang ^{14c}, Y. Huang ^{62a},
 Y. Huang ^{14a}, Z. Huang ¹⁰¹, Z. Hubacek ¹³², M. Huebner ²⁴, F. Huegging ²⁴, T.B. Huffman ¹²⁶,
 M. Huhtinen ³⁶, S.K. Huiberts ¹⁶, R. Hulsken ¹⁰⁴, N. Huseynov ^{12,a}, J. Huston ¹⁰⁷, J. Huth ⁶¹,
 R. Hyneman ¹⁴³, G. Iacobucci ⁵⁶, G. Iakovidis ²⁹, I. Ibragimov ¹⁴¹, L. Iconomidou-Fayard ⁶⁶,
 P. Iengo ^{72a,72b}, R. Iguchi ¹⁵³, T. Iizawa ⁵⁶, Y. Ikegami ⁸³, A. Ilg ¹⁹, N. Ilic ¹⁵⁵, H. Imam ^{35a},
 T. Ingebretsen Carlson ^{47a,47b}, G. Introzzi ^{73a,73b}, M. Iodice ^{77a}, V. Ippolito ^{75a,75b}, M. Ishino ¹⁵³,
 W. Islam ¹⁷⁰, C. Issever ^{18,48}, S. Istin ^{21a,am}, H. Ito ¹⁶⁸, J.M. Iturbe Ponce ^{64a}, R. Iuppa ^{78a,78b},
 A. Ivina ¹⁶⁹, J.M. Izen ⁴⁵, V. Izzo ^{72a}, P. Jacka ^{131,132}, P. Jackson ¹, R.M. Jacobs ⁴⁸,
 B.P. Jaeger ¹⁴², C.S. Jagfeld ¹⁰⁹, P. Jain ⁵⁴, G. Jäkel ¹⁷¹, K. Jakobs ⁵⁴, T. Jakoubek ¹⁶⁹,
 J. Jamieson ⁵⁹, K.W. Janas ^{85a}, A.E. Jaspan ⁹², M. Javurkova ¹⁰³, F. Jeanneau ¹³⁵, L. Jeanty ¹²³,
 J. Jejelava ^{149a,ac}, P. Jenni ^{54,h}, C.E. Jessiman ³⁴, S. Jézéquel ⁴, C. Jia ^{62b}, J. Jia ¹⁴⁵, X. Jia ⁶¹,
 X. Jia ^{14a,14e}, Z. Jia ^{14c}, Y. Jiang ^{62a}, S. Jiggins ⁴⁸, J. Jimenez Pena ¹¹⁰, S. Jin ^{14c}, A. Jinaru ^{27b},
 O. Jinnouchi ¹⁵⁴, P. Johansson ¹³⁹, K.A. Johns ⁷, J.W. Johnson ¹³⁶, D.M. Jones ³², E. Jones ¹⁶⁷,
 P. Jones ³², R.W.L. Jones ⁹¹, T.J. Jones ⁹², R. Joshi ¹¹⁹, J. Jovicevic ¹⁵, X. Ju ^{17a},
 J.J. Junggeburth ³⁶, T. Junkermann ^{63a}, A. Juste Rozas ^{13,v}, S. Kabana ^{137e}, A. Kaczmariska ⁸⁶,
 M. Kado ¹¹⁰, H. Kagan ¹¹⁹, M. Kagan ¹⁴³, A. Kahn ⁴¹, A. Kahn ¹²⁸, C. Kahra ¹⁰⁰, T. Kaji ¹⁶⁸,
 E. Kajomovitz ¹⁵⁰, N. Kakati ¹⁶⁹, C.W. Kalderon ²⁹, A. Kamenshchikov ¹⁵⁵, S. Kanayama ¹⁵⁴,
 N.J. Kang ¹³⁶, D. Kar ^{33g}, K. Karava ¹²⁶, M.J. Kareem ^{156b}, E. Karentzos ⁵⁴, I. Karkanias ^{152,f},
 S.N. Karpov ³⁸, Z.M. Karpova ³⁸, V. Kartvelishvili ⁹¹, A.N. Karyukhin ³⁷, E. Kasimi ^{152,f},
 J. Katzy ⁴⁸, S. Kaur ³⁴, K. Kawade ¹⁴⁰, T. Kawamoto ¹³⁵, G. Kawamura ⁵⁵, E.F. Kay ¹⁶⁵,
 F.I. Kaya ¹⁵⁸, S. Kazakos ¹³, V.F. Kazanin ³⁷, Y. Ke ¹⁴⁵, J.M. Keaveney ^{33a}, R. Keeler ¹⁶⁵,
 G.V. Kehris ⁶¹, J.S. Keller ³⁴, A.S. Kelly ⁹⁶, D. Kelsey ¹⁴⁶, J.J. Kempster ¹⁴⁶, K.E. Kennedy ⁴¹,
 P.D. Kennedy ¹⁰⁰, O. Kepka ¹³¹, B.P. Kerridge ¹⁶⁷, S. Kersten ¹⁷¹, B.P. Kerševan ⁹³,
 S. Keshri ⁶⁶, L. Keszezhova ^{28a}, S. Ketabchi Haghghat ¹⁵⁵, M. Khandoga ¹²⁷, A. Khanov ¹²¹,
 A.G. Kharlamov ³⁷, T. Kharlamova ³⁷, E.E. Khoda ¹³⁸, T.J. Khoo ¹⁸, G. Khorauli ¹⁶⁶,
 J. Khubua ^{149b}, Y.A.R. Khwaira ⁶⁶, M. Kiehn ³⁶, A. Kilgallon ¹²³, D.W. Kim ^{47a,47b},

Y.K. Kim ³⁹, N. Kimura ⁹⁶, A. Kirchhoff ⁵⁵, C. Kirfel ²⁴, J. Kirk ¹³⁴, A.E. Kiryunin ¹¹⁰,
 T. Kishimoto ¹⁵³, D.P. Kisliuk ¹⁵⁵, C. Kitsaki ¹⁰, O. Kivernyk ²⁴, M. Klassen ^{63a}, C. Klein ³⁴,
 L. Klein ¹⁶⁶, M.H. Klein ¹⁰⁶, M. Klein ⁹², S.B. Klein ⁵⁶, U. Klein ⁹², P. Klimek ³⁶,
 A. Klimentov ²⁹, T. Klioutchnikova ³⁶, P. Kluit ¹¹⁴, S. Kluth ¹¹⁰, E. Kneringer ⁷⁹,
 T.M. Knight ¹⁵⁵, A. Knue ⁵⁴, R. Kobayashi ⁸⁷, M. Kocian ¹⁴³, P. Kodyš ¹³³, D.M. Koeck ¹²³,
 P.T. Koenig ²⁴, T. Koffas ³⁴, M. Kolb ¹³⁵, I. Koletsou ⁴, T. Komarek ¹²², K. Köneke ⁵⁴,
 A.X.Y. Kong ¹, T. Kono ¹¹⁸, N. Konstantinidis ⁹⁶, B. Konya ⁹⁸, R. Kopeliansky ⁶⁸,
 S. Koperny ^{85a}, K. Korcyl ⁸⁶, K. Kordas ^{152,f}, G. Koren ¹⁵¹, A. Korn ⁹⁶, S. Korn ⁵⁵,
 I. Korolkov ¹³, N. Korotkova ³⁷, B. Kortman ¹¹⁴, O. Kortner ¹¹⁰, S. Kortner ¹¹⁰,
 W.H. Kostecka ¹¹⁵, V.V. Kostyukhin ¹⁴¹, A. Kotsokechagia ¹³⁵, A. Kotwal ⁵¹, A. Koulouris ³⁶,
 A. Kourkoumeli-Charalampidi ^{73a,73b}, C. Kourkoumelis ⁹, E. Kourlitis ⁶, O. Kovanda ¹⁴⁶,
 R. Kowalewski ¹⁶⁵, W. Kozanecki ¹³⁵, A.S. Kozhin ³⁷, V.A. Kramarenko ³⁷, G. Kramberger ⁹³,
 P. Kramer ¹⁰⁰, M.W. Krasny ¹²⁷, A. Krasznahorkay ³⁶, J.A. Kremer ¹⁰⁰, T. Kresse ⁵⁰,
 J. Kretschmar ⁹², K. Kreul ¹⁸, P. Krieger ¹⁵⁵, S. Krishnamurthy ¹⁰³, M. Krivos ¹³³,
 K. Krizka ²⁰, K. Kroeninger ⁴⁹, H. Kroha ¹¹⁰, J. Kroll ¹³¹, J. Kroll ¹²⁸, K.S. Krowpman ¹⁰⁷,
 U. Kruchonak ³⁸, H. Krüger ²⁴, N. Krumnack ⁸¹, M.C. Kruse ⁵¹, J.A. Krzysiak ⁸⁶,
 O. Kuchinskaia ³⁷, S. Kuday ^{3a}, S. Kuehn ³⁶, R. Kuesters ⁵⁴, T. Kuhl ⁴⁸, V. Kukhtin ³⁸,
 Y. Kulchitsky ^{37,a}, S. Kuleshov ^{137d,137b}, M. Kumar ^{33g}, N. Kumari ¹⁰², A. Kupco ¹³¹,
 T. Kupfer ⁴⁹, A. Kupich ³⁷, O. Kuprash ⁵⁴, H. Kurashige ⁸⁴, L.L. Kurchaninov ^{156a}, O. Kurdysh ⁶⁶,
 Y.A. Kurochkin ³⁷, A. Kurova ³⁷, M. Kuze ¹⁵⁴, A.K. Kvam ¹⁰³, J. Kvita ¹²², T. Kwan ¹⁰⁴,
 N.G. Kyriacou ¹⁰⁶, L.A.O. Laatu ¹⁰², C. Lacasta ¹⁶³, F. Lacava ^{75a,75b}, H. Lacker ¹⁸,
 D. Lacour ¹²⁷, N.N. Lad ⁹⁶, E. Ladygin ³⁸, B. Laforge ¹²⁷, T. Lagouri ^{137e}, S. Lai ⁵⁵,
 I.K. Lakomic ^{85a}, N. Lalloue ⁶⁰, J.E. Lambert ¹²⁰, S. Lammers ⁶⁸, W. Lampl ⁷,
 C. Lampoudis ^{152,f}, A.N. Lancaster ¹¹⁵, E. Lançon ²⁹, U. Landgraf ⁵⁴, M.P.J. Landon ⁹⁴,
 V.S. Lang ⁵⁴, R.J. Langenberg ¹⁰³, A.J. Lankford ¹⁶⁰, F. Lanni ³⁶, K. Lantzsch ²⁴, A. Lanza ^{73a},
 A. Lapertosa ^{57b,57a}, J.F. Laporte ¹³⁵, T. Lari ^{71a}, F. Lasagni Manghi ^{23b}, M. Lassnig ³⁶,
 V. Latonova ¹³¹, A. Laudrain ¹⁰⁰, A. Laurier ¹⁵⁰, S.D. Lawlor ⁹⁵, Z. Lawrence ¹⁰¹,
 M. Lazzaroni ^{71a,71b}, B. Le ¹⁰¹, E.M. Le Boulicaut ⁵¹, B. Leban ⁹³, A. Lebedev ⁸¹, M. LeBlanc ³⁶,
 F. Ledroit-Guillon ⁶⁰, A.C.A. Lee ⁹⁶, G.R. Lee ¹⁶, S.C. Lee ¹⁴⁸, S. Lee ^{47a,47b}, T.F. Lee ⁹²,
 L.L. Leeuw ^{33c}, H.P. Lefebvre ⁹⁵, M. Lefebvre ¹⁶⁵, C. Leggett ^{17a}, K. Lehmann ¹⁴²,
 G. Lehmann Miotto ³⁶, M. Leigh ⁵⁶, W.A. Leight ¹⁰³, A. Leisos ^{152,u}, M.A.L. Leite ^{82c},
 C.E. Leitgeb ⁴⁸, R. Leitner ¹³³, K.J.C. Leney ⁴⁴, T. Lenz ²⁴, S. Leone ^{74a}, C. Leonidopoulos ⁵²,
 A. Leopold ¹⁴⁴, C. Leroy ¹⁰⁸, R. Les ¹⁰⁷, C.G. Lester ³², M. Levchenko ³⁷, J. Levêque ⁴,
 D. Levin ¹⁰⁶, L.J. Levinson ¹⁶⁹, M.P. Lewicki ⁸⁶, D.J. Lewis ⁴, A. Li ⁵, B. Li ^{62b}, C. Li ^{62a},
 C-Q. Li ^{62c}, H. Li ^{62a}, H. Li ^{62b}, H. Li ^{14c}, H. Li ^{62b}, J. Li ^{62c}, K. Li ¹³⁸, L. Li ^{62c},
 M. Li ^{14a,14e}, Q.Y. Li ^{62a}, S. Li ^{14a,14e}, S. Li ^{62d,62c,e}, T. Li ^{62b}, X. Li ¹⁰⁴, Z. Li ^{62b}, Z. Li ¹²⁶,
 Z. Li ¹⁰⁴, Z. Li ⁹², Z. Li ^{14a,14e}, Z. Liang ^{14a}, M. Liberatore ⁴⁸, B. Liberti ^{76a}, K. Lie ^{64c},
 J. Lieber Marin ^{82b}, H. Lien ⁶⁸, K. Lin ¹⁰⁷, R.A. Linck ⁶⁸, R.E. Lindley ⁷, J.H. Lindon ²,
 A. Linss ⁴⁸, E. Lipeles ¹²⁸, A. Lipniacka ¹⁶, A. Lister ¹⁶⁴, J.D. Little ⁴, B. Liu ^{14a},
 B.X. Liu ¹⁴², D. Liu ^{62d,62c}, J.B. Liu ^{62a}, J.K.K. Liu ³², K. Liu ^{62d,62c}, M. Liu ^{62a},
 M.Y. Liu ^{62a}, P. Liu ^{14a}, Q. Liu ^{62d,138,62c}, X. Liu ^{62a}, Y. Liu ^{14c,14e}, Y.L. Liu ¹⁰⁶, Y.W. Liu ^{62a},
 J. Llorente Merino ¹⁴², S.L. Lloyd ⁹⁴, E.M. Lobodzinska ⁴⁸, P. Loch ⁷, S. Loffredo ^{76a,76b},
 T. Lohse ¹⁸, K. Lohwasser ¹³⁹, E. Loiacono ⁴⁸, M. Lokajicek ^{131,*}, J.D. Lomas ²⁰,
 J.D. Long ¹⁶², I. Longarini ¹⁶⁰, L. Longo ^{70a,70b}, R. Longo ¹⁶², I. Lopez Paz ⁶⁷,
 A. Lopez Solis ⁴⁸, J. Lorenz ¹⁰⁹, N. Lorenzo Martinez ⁴, A.M. Lory ¹⁰⁹, X. Lou ^{47a,47b},
 X. Lou ^{14a,14e}, A. Lounis ⁶⁶, J. Love ⁶, P.A. Love ⁹¹, G. Lu ^{14a,14e}, M. Lu ⁸⁰, S. Lu ¹²⁸,
 Y.J. Lu ⁶⁵, H.J. Lubatti ¹³⁸, C. Luci ^{75a,75b}, F.L. Lucio Alves ^{14c}, A. Lucotte ⁶⁰, F. Luehring ⁶⁸,

I. Luise ¹⁴⁵, O. Lukianchuk ⁶⁶, O. Lundberg ¹⁴⁴, B. Lund-Jensen ¹⁴⁴, N.A. Luongo ¹²³,
 M.S. Lutz ¹⁵¹, D. Lynn ²⁹, H. Lyons ⁹², R. Lysak ¹³¹, E. Lytken ⁹⁸, V. Lyubushkin ³⁸,
 T. Lyubushkina ³⁸, M.M. Lyukova ¹⁴⁵, H. Ma ²⁹, L.L. Ma ^{62b}, Y. Ma ⁹⁶, D.M. Mac Donell ¹⁶⁵,
 G. Maccarrone ⁵³, J.C. MacDonald ¹³⁹, R. Madar ⁴⁰, W.F. Mader ⁵⁰, J. Maeda ⁸⁴, T. Maeno ²⁹,
 M. Maerker ⁵⁰, H. Maguire ¹³⁹, A. Maio ^{130a,130b,130d}, K. Maj ^{85a}, O. Majersky ⁴⁸,
 S. Majewski ¹²³, N. Makovec ⁶⁶, V. Maksimovic ¹⁵, B. Malaescu ¹²⁷, Pa. Malecki ⁸⁶,
 V.P. Maleev ³⁷, F. Malek ⁶⁰, D. Malito ^{43b,43a}, U. Mallik ⁸⁰, C. Malone ³², S. Maltezos ¹⁰,
 S. Malyukov ³⁸, J. Mamuzic ¹³, G. Mancini ⁵³, G. Manco ^{73a,73b}, J.P. Mandalia ⁹⁴, I. Mandić ⁹³,
 L. Manhaes de Andrade Filho ^{82a}, I.M. Maniatis ¹⁶⁹, J. Manjarres Ramos ^{102,ad}, D.C. Mankad ¹⁶⁹,
 A. Mann ¹⁰⁹, B. Mansoulie ¹³⁵, S. Manzoni ³⁶, A. Marantis ^{152,u}, G. Marchiori ⁵,
 M. Marcisovsky ¹³¹, C. Marcon ^{71a,71b}, M. Marinescu ²⁰, M. Marjanovic ¹²⁰, E.J. Marshall ⁹¹,
 Z. Marshall ^{17a}, S. Marti-Garcia ¹⁶³, T.A. Martin ¹⁶⁷, V.J. Martin ⁵², B. Martin dit Latour ¹⁶,
 L. Martinelli ^{75a,75b}, M. Martinez ^{13,v}, P. Martinez Agullo ¹⁶³, V.I. Martinez Outschoorn ¹⁰³,
 P. Martinez Suarez ¹³, S. Martin-Haugh ¹³⁴, V.S. Martoiu ^{27b}, A.C. Martyniuk ⁹⁶, A. Marzin ³⁶,
 S.R. Maschek ¹¹⁰, D. Mascione ^{78a,78b}, L. Masetti ¹⁰⁰, T. Mashimo ¹⁵³, J. Masik ¹⁰¹,
 A.L. Maslennikov ³⁷, L. Massa ^{23b}, P. Massarotti ^{72a,72b}, P. Mastrandrea ^{74a,74b},
 A. Mastroberardino ^{43b,43a}, T. Masubuchi ¹⁵³, T. Mathisen ¹⁶¹, N. Matsuzawa ¹⁵³, J. Maurer ^{27b},
 B. Maček ⁹³, D.A. Maximov ³⁷, R. Mazini ¹⁴⁸, I. Maznas ^{152,f}, M. Mazza ¹⁰⁷, S.M. Mazza ¹³⁶,
 C. Mc Ginn ²⁹, J.P. Mc Gowan ¹⁰⁴, S.P. Mc Kee ¹⁰⁶, E.F. McDonald ¹⁰⁵, A.E. McDougall ¹¹⁴,
 J.A. Mcfayden ¹⁴⁶, R.P. McGovern ¹²⁸, G. Mchedlidze ^{149b}, R.P. Mckenzie ^{33g},
 T.C. McLachlan ⁴⁸, D.J. McLaughlin ⁹⁶, K.D. McLean ¹⁶⁵, S.J. McMahon ¹³⁴, P.C. McNamara ¹⁰⁵,
 C.M. Mcpartland ⁹², R.A. McPherson ^{165,z}, T. Megy ⁴⁰, S. Mehlhase ¹⁰⁹, A. Mehta ⁹²,
 D. Melini ¹⁵⁰, B.R. Mellado Garcia ^{33g}, A.H. Melo ⁵⁵, F. Meloni ⁴⁸,
 A.M. Mendes Jacques Da Costa ¹⁰¹, H.Y. Meng ¹⁵⁵, L. Meng ⁹¹, S. Menke ¹¹⁰, M. Mentink ³⁶,
 E. Meoni ^{43b,43a}, C. Merlassino ¹²⁶, L. Merola ^{72a,72b}, C. Meroni ^{71a,71b}, G. Merz ¹⁰⁶,
 O. Meshkov ³⁷, J. Metcalfe ⁶, A.S. Mete ⁶, C. Meyer ⁶⁸, J-P. Meyer ¹³⁵, R.P. Middleton ¹³⁴,
 L. Mijović ⁵², G. Mikenberg ¹⁶⁹, M. Mikesikova ¹³¹, M. Mikuž ⁹³, H. Mildner ¹³⁹, A. Milic ³⁶,
 C.D. Milke ⁴⁴, D.W. Miller ³⁹, L.S. Miller ³⁴, A. Milov ¹⁶⁹, D.A. Milstead ^{47a,47b}, T. Min ^{14c},
 A.A. Minaenko ³⁷, I.A. Minashvili ^{149b}, L. Mince ⁵⁹, A.I. Mincer ¹¹⁷, B. Mindur ^{85a},
 M. Mineev ³⁸, Y. Mino ⁸⁷, L.M. Mir ¹³, M. Miralles Lopez ¹⁶³, M. Mironova ^{17a},
 M.C. Missio ¹¹³, T. Mitani ¹⁶⁸, A. Mitra ¹⁶⁷, V.A. Mitsou ¹⁶³, O. Miu ¹⁵⁵, P.S. Miyagawa ⁹⁴,
 Y. Miyazaki ⁸⁹, A. Mizukami ⁸³, T. Mkrtychyan ^{63a}, M. Mlinarevic ⁹⁶, T. Mlinarevic ⁹⁶,
 M. Mlynarikova ³⁶, S. Mobius ⁵⁵, K. Mochizuki ¹⁰⁸, P. Moder ⁴⁸, P. Mogg ¹⁰⁹,
 A.F. Mohammed ^{14a,14e}, S. Mohapatra ⁴¹, G. Mokgatitwane ^{33g}, B. Mondal ¹⁴¹, S. Mondal ¹³²,
 G. Monig ¹⁴⁶, K. Mönig ⁴⁸, E. Monnier ¹⁰², L. Monsonis Romero ¹⁶³, J. Montejo Berlingen ⁸³,
 M. Montella ¹¹⁹, F. Monticelli ⁹⁰, N. Morange ⁶⁶, A.L. Moreira De Carvalho ^{130a},
 M. Moreno Llácer ¹⁶³, C. Moreno Martinez ⁵⁶, P. Moretini ^{57b}, S. Morgenstern ³⁶, M. Morii ⁶¹,
 M. Morinaga ¹⁵³, A.K. Morley ³⁶, F. Morodei ^{75a,75b}, L. Morvaj ³⁶, P. Moschovakos ³⁶,
 B. Moser ³⁶, M. Mosidze ^{149b}, T. Moskalets ⁵⁴, P. Moskvitina ¹¹³, J. Moss ^{31,o}, E.J.W. Moyses ¹⁰³,
 O. Mtintsilana ^{33g}, S. Muanza ¹⁰², J. Mueller ¹²⁹, D. Muenstermann ⁹¹, R. Müller ¹⁹,
 G.A. Mullier ¹⁶¹, J.J. Mullin ¹²⁸, D.P. Mungo ¹⁵⁵, J.L. Munoz Martinez ¹³, D. Munoz Perez ¹⁶³,
 F.J. Munoz Sanchez ¹⁰¹, M. Murin ¹⁰¹, W.J. Murray ^{167,134}, A. Murrone ^{71a,71b}, J.M. Muse ¹²⁰,
 M. Muškinja ^{17a}, C. Mwewa ²⁹, A.G. Myagkov ^{37,a}, A.J. Myers ⁸, A.A. Myers ¹²⁹, G. Myers ⁶⁸,
 M. Myska ¹³², B.P. Nachman ^{17a}, O. Nackenhorst ⁴⁹, A. Nag ⁵⁰, K. Nagai ¹²⁶, K. Nagano ⁸³,
 J.L. Nagle ^{29,ak}, E. Nagy ¹⁰², A.M. Nairz ³⁶, Y. Nakahama ⁸³, K. Nakamura ⁸³, H. Nanjo ¹²⁴,
 R. Narayan ⁴⁴, E.A. Narayanan ¹¹², I. Naryshkin ³⁷, M. Naseri ³⁴, C. Nass ²⁴, G. Navarro ^{22a},
 J. Navarro-Gonzalez ¹⁶³, R. Nayak ¹⁵¹, A. Nayaz ¹⁸, P.Y. Nechaeva ³⁷, F. Nechansky ⁴⁸,

L. Nedic ¹²⁶, T.J. Neep ²⁰, A. Negri ^{73a,73b}, M. Negrini ^{23b}, C. Nellist ¹¹⁴, C. Nelson ¹⁰⁴,
 K. Nelson ¹⁰⁶, S. Nemecek ¹³¹, M. Nessi ^{36,i}, M.S. Neubauer ¹⁶², F. Neuhaus ¹⁰⁰,
 J. Neundorf ⁴⁸, R. Newhouse ¹⁶⁴, P.R. Newman ²⁰, C.W. Ng ¹²⁹, Y.W.Y. Ng ⁴⁸, B. Ngair ^{35e},
 H.D.N. Nguyen ¹⁰⁸, R.B. Nickerson ¹²⁶, R. Nicolaidou ¹³⁵, J. Nielsen ¹³⁶, M. Niemeyer ⁵⁵,
 N. Nikiforou ³⁶, V. Nikolaenko ^{37,a}, I. Nikolic-Audit ¹²⁷, K. Nikolopoulos ²⁰, P. Nilsson ²⁹,
 I. Ninca ⁴⁸, H.R. Nindhito ⁵⁶, G. Ninio ¹⁵¹, A. Nisati ^{75a}, N. Nishu ², R. Nisius ¹¹⁰,
 J-E. Nitschke ⁵⁰, E.K. Nkadimeng ^{33g}, S.J. Noacco Rosende ⁹⁰, T. Nobe ¹⁵³, D.L. Noel ³²,
 T. Nommensen ¹⁴⁷, M.A. Nomura ²⁹, M.B. Norfolk ¹³⁹, R.R.B. Norisam ⁹⁶, B.J. Norman ³⁴,
 J. Novak ⁹³, T. Novak ⁴⁸, L. Novotny ¹³², R. Novotny ¹¹², L. Nozka ¹²², K. Ntekas ¹⁶⁰,
 N.M.J. Nunes De Moura Junior ^{82b}, E. Nurse ⁹⁶, J. Ocariz ¹²⁷, A. Ochi ⁸⁴, I. Ochoa ^{130a},
 S. Oerdeek ¹⁶¹, J.T. Offermann ³⁹, A. Ogrodnik ^{85a}, A. Oh ¹⁰¹, C.C. Ohm ¹⁴⁴, H. Oide ⁸³,
 R. Oishi ¹⁵³, M.L. Ojeda ⁴⁸, Y. Okazaki ⁸⁷, M.W. O'Keefe ⁹², Y. Okumura ¹⁵³,
 L.F. Oleiro Seabra ^{130a}, S.A. Olivares Pino ^{137d}, D. Oliveira Damazio ²⁹, D. Oliveira Goncalves ^{82a},
 J.L. Oliver ¹⁶⁰, M.J.R. Olsson ¹⁶⁰, A. Olszewski ⁸⁶, J. Olszowska ^{86,*}, Ö.O. Öncel ⁵⁴,
 D.C. O'Neil ¹⁴², A.P. O'Neill ¹⁹, A. Onofre ^{130a,130e}, P.U.E. Onyisi ¹¹, M.J. Oreglia ³⁹,
 G.E. Orellana ⁹⁰, D. Orestano ^{77a,77b}, N. Orlando ¹³, R.S. Orr ¹⁵⁵, V. O'Shea ⁵⁹, R. Ospanov ^{62a},
 G. Otero y Garzon ³⁰, H. Otono ⁸⁹, P.S. Ott ^{63a}, G.J. Ottino ^{17a}, M. Ouchrif ^{35d}, J. Ouellette ²⁹,
 F. Ould-Saada ¹²⁵, M. Owen ⁵⁹, R.E. Owen ¹³⁴, K.Y. Oyulmaz ^{21a}, V.E. Ozcan ^{21a}, N. Ozturk ⁸,
 S. Ozturk ^{21d}, H.A. Pacey ³², A. Pacheco Pages ¹³, C. Padilla Aranda ¹³, G. Padovano ^{75a,75b},
 S. Pagan Griso ^{17a}, G. Palacino ⁶⁸, A. Palazzo ^{70a,70b}, S. Palestini ³⁶, J. Pan ¹⁷², T. Pan ^{64a},
 D.K. Panchal ¹¹, C.E. Pandini ¹¹⁴, J.G. Panduro Vazquez ⁹⁵, H. Pang ^{14b}, P. Pani ⁴⁸,
 G. Panizzo ^{69a,69c}, L. Paolozzi ⁵⁶, C. Papadatos ¹⁰⁸, S. Parajuli ⁴⁴, A. Paramonov ⁶,
 C. Paraskevopoulos ¹⁰, D. Paredes Hernandez ^{64b}, T.H. Park ¹⁵⁵, M.A. Parker ³², F. Parodi ^{57b,57a},
 E.W. Parrish ¹¹⁵, V.A. Parrish ⁵², J.A. Parsons ⁴¹, U. Parzefall ⁵⁴, B. Pascual Dias ¹⁰⁸,
 L. Pascual Dominguez ¹⁵¹, F. Pasquali ¹¹⁴, E. Pasqualucci ^{75a}, S. Passaggio ^{57b}, F. Pastore ⁹⁵,
 P. Pasuwan ^{47a,47b}, P. Patel ⁸⁶, U.M. Patel ⁵¹, J.R. Pater ¹⁰¹, T. Pauly ³⁶, J. Pearkes ¹⁴³,
 M. Pedersen ¹²⁵, R. Pedro ^{130a}, S.V. Peleganchuk ³⁷, O. Penc ³⁶, E.A. Pender ⁵², H. Peng ^{62a},
 K.E. Penski ¹⁰⁹, M. Penzin ³⁷, B.S. Peralva ^{82d}, A.P. Pereira Peixoto ⁶⁰, L. Pereira Sanchez ^{47a,47b},
 D.V. Perepelitsa ^{29,ak}, E. Perez Codina ^{156a}, M. Perganti ¹⁰, L. Perini ^{71a,71b,*}, H. Pernegger ³⁶,
 S. Perrella ³⁶, A. Perrevoort ¹¹³, O. Perrin ⁴⁰, K. Peters ⁴⁸, R.F.Y. Peters ¹⁰¹, B.A. Petersen ³⁶,
 T.C. Petersen ⁴², E. Petit ¹⁰², V. Petousis ¹³², C. Petridou ^{152,f}, A. Petrukhin ¹⁴¹, M. Pettee ^{17a},
 N.E. Pettersson ³⁶, A. Petukhov ³⁷, K. Petukhova ¹³³, A. Peyaud ¹³⁵, R. Pezoa ^{137f},
 L. Pezzotti ³⁶, G. Pezzullo ¹⁷², T.M. Pham ¹⁷⁰, T. Pham ¹⁰⁵, P.W. Phillips ¹³⁴, M.W. Phipps ¹⁶²,
 G. Piacquadio ¹⁴⁵, E. Pianori ^{17a}, F. Piazza ^{71a,71b}, R. Piegaia ³⁰, D. Pietreanu ^{27b},
 A.D. Pilkington ¹⁰¹, M. Pinamonti ^{69a,69c}, J.L. Pinfeld ², B.C. Pinheiro Pereira ^{130a},
 C. Pitman Donaldson ⁹⁶, D.A. Pizzi ³⁴, L. Pizzimento ^{76a,76b}, A. Pizzini ¹¹⁴, M.-A. Pleier ²⁹,
 V. Plesanovs ⁵⁴, V. Pleskot ¹³³, E. Plotnikova ³⁸, G. Poddar ⁴, R. Poettgen ⁹⁸, L. Poggioli ¹²⁷,
 D. Pohl ²⁴, I. Pokharel ⁵⁵, S. Polacek ¹³³, G. Polesello ^{73a}, A. Poley ^{142,156a}, R. Polifka ¹³²,
 A. Polini ^{23b}, C.S. Pollard ¹⁶⁷, Z.B. Pollock ¹¹⁹, V. Polychronakos ²⁹, E. Pompa Pacchi ^{75a,75b},
 D. Ponomarenko ¹¹³, L. Pontecorvo ³⁶, S. Popa ^{27a}, G.A. Popeneciu ^{27d},
 D.M. Portillo Quintero ^{156a}, S. Pospisil ¹³², P. Postolache ^{27c}, K. Potamianos ¹²⁶, P.A. Potepa ^{85a},
 I.N. Potrap ³⁸, C.J. Potter ³², H. Potti ¹, T. Poulsen ⁴⁸, J. Poveda ¹⁶³, M.E. Pozo Astigarraga ³⁶,
 A. Prades Ibanez ¹⁶³, M.M. Prapa ⁴⁶, J. Pretel ⁵⁴, D. Price ¹⁰¹, M. Primavera ^{70a},
 M.A. Principe Martin ⁹⁹, R. Privara ¹²², M.L. Proffitt ¹³⁸, N. Proklova ¹²⁸, K. Prokofiev ^{64c},
 G. Proto ^{76a,76b}, S. Protopopescu ²⁹, J. Proudfoot ⁶, M. Przybycien ^{85a}, W.W. Przygoda ^{85b},
 J.E. Puddefoot ¹³⁹, D. Pudzha ³⁷, D. Pyatiizbyantseva ³⁷, J. Qian ¹⁰⁶, D. Qichen ¹⁰¹, Y. Qin ¹⁰¹,
 T. Qiu ⁵², A. Quadt ⁵⁵, M. Queitsch-Maitland ¹⁰¹, G. Quetant ⁵⁶, G. Rabanal Bolanos ⁶¹,

D. Rafanoharana [ID⁵⁴](#), F. Ragusa [ID^{71a,71b}](#), J.L. Rainbolt [ID³⁹](#), J.A. Raine [ID⁵⁶](#), S. Rajagopalan [ID²⁹](#),
 E. Ramakoti [ID³⁷](#), K. Ran [ID^{48,14e}](#), N.P. Rapheeha [ID^{33g}](#), V. Raskina [ID¹²⁷](#), D.F. Rassloff [ID^{63a}](#), S. Rave [ID¹⁰⁰](#),
 B. Ravina [ID⁵⁵](#), I. Ravinovich [ID¹⁶⁹](#), M. Raymond [ID³⁶](#), A.L. Read [ID¹²⁵](#), N.P. Readioff [ID¹³⁹](#),
 D.M. Rebuzzi [ID^{73a,73b}](#), G. Redlinger [ID²⁹](#), K. Reeves [ID²⁶](#), J.A. Reidelsturz [ID¹⁷¹](#), D. Reikher [ID¹⁵¹](#),
 A. Rej [ID¹⁴¹](#), C. Rembser [ID³⁶](#), A. Renardi [ID⁴⁸](#), M. Renda [ID^{27b}](#), M.B. Rendel [ID¹¹⁰](#), F. Renner [ID⁴⁸](#),
 A.G. Rennie [ID⁵⁹](#), S. Resconi [ID^{71a}](#), M. Ressegotti [ID^{57b,57a}](#), E.D. Resseguie [ID^{17a}](#), S. Rettie [ID³⁶](#),
 J.G. Reyes Rivera [ID¹⁰⁷](#), B. Reynolds [ID¹¹⁹](#), E. Reynolds [ID^{17a}](#), M. Rezaei Estabragh [ID¹⁷¹](#), O.L. Rezanova [ID³⁷](#),
 P. Reznicek [ID¹³³](#), N. Ribaric [ID⁹¹](#), E. Ricci [ID^{78a,78b}](#), R. Richter [ID¹¹⁰](#), S. Richter [ID^{47a,47b}](#),
 E. Richter-Was [ID^{85b}](#), M. Ridel [ID¹²⁷](#), S. Ridouani [ID^{35d}](#), P. Rieck [ID¹¹⁷](#), P. Riedler [ID³⁶](#),
 M. Rijssenbeek [ID¹⁴⁵](#), A. Rimoldi [ID^{73a,73b}](#), M. Rimoldi [ID⁴⁸](#), L. Rinaldi [ID^{23b,23a}](#), T.T. Rinn [ID²⁹](#),
 M.P. Rinnagel [ID¹⁰⁹](#), G. Ripellino [ID¹⁶¹](#), I. Riu [ID¹³](#), P. Rivadeneira [ID⁴⁸](#), J.C. Rivera Vergara [ID¹⁶⁵](#),
 F. Rizatdinova [ID¹²¹](#), E. Rizvi [ID⁹⁴](#), C. Rizzi [ID⁵⁶](#), B.A. Roberts [ID¹⁶⁷](#), B.R. Roberts [ID^{17a}](#),
 S.H. Robertson [ID^{104,z}](#), M. Robin [ID⁴⁸](#), D. Robinson [ID³²](#), C.M. Robles Gajardo [ID^{137f}](#),
 M. Robles Manzano [ID¹⁰⁰](#), A. Robson [ID⁵⁹](#), A. Rocchi [ID^{76a,76b}](#), C. Roda [ID^{74a,74b}](#), S. Rodriguez Bosca [ID^{63a}](#),
 Y. Rodriguez Garcia [ID^{22a}](#), A. Rodriguez Rodriguez [ID⁵⁴](#), A.M. Rodríguez Vera [ID^{156b}](#), S. Roe [ID³⁶](#),
 J.T. Roemer [ID¹⁶⁰](#), A.R. Roepe-Gier [ID¹³⁶](#), J. Roggel [ID¹⁷¹](#), O. Røhne [ID¹²⁵](#), R.A. Rojas [ID¹⁰³](#),
 C.P.A. Roland [ID⁶⁸](#), J. Roloff [ID²⁹](#), A. Romaniouk [ID³⁷](#), E. Romano [ID^{73a,73b}](#), M. Romano [ID^{23b}](#),
 A.C. Romero Hernandez [ID¹⁶²](#), N. Rompotis [ID⁹²](#), L. Roos [ID¹²⁷](#), S. Rosati [ID^{75a}](#), B.J. Rosser [ID³⁹](#),
 E. Rossi [ID⁴](#), E. Rossi [ID^{72a,72b}](#), L.P. Rossi [ID^{57b}](#), L. Rossini [ID⁴⁸](#), R. Rosten [ID¹¹⁹](#), M. Rotaru [ID^{27b}](#),
 B. Rottler [ID⁵⁴](#), C. Rougier [ID^{102,ad}](#), D. Rousseau [ID⁶⁶](#), D. Rousso [ID³²](#), A. Roy [ID¹⁶²](#), S. Roy-Garand [ID¹⁵⁵](#),
 A. Rozanov [ID¹⁰²](#), Y. Rozen [ID¹⁵⁰](#), X. Ruan [ID^{33g}](#), A. Rubio Jimenez [ID¹⁶³](#), A.J. Ruby [ID⁹²](#),
 V.H. Ruelas Rivera [ID¹⁸](#), T.A. Ruggeri [ID¹](#), A. Ruiz-Martinez [ID¹⁶³](#), A. Rummler [ID³⁶](#), Z. Rurikova [ID⁵⁴](#),
 N.A. Rusakovich [ID³⁸](#), H.L. Russell [ID¹⁶⁵](#), J.P. Rutherford [ID⁷](#), K. Rybacki [ID⁹¹](#), M. Rybar [ID¹³³](#),
 E.B. Rye [ID¹²⁵](#), A. Ryzhov [ID³⁷](#), J.A. Sabater Iglesias [ID⁵⁶](#), P. Sabatini [ID¹⁶³](#), L. Sabetta [ID^{75a,75b}](#),
 H.F-W. Sadrozinski [ID¹³⁶](#), F. Safai Tehrani [ID^{75a}](#), B. Safarzadeh Samani [ID¹⁴⁶](#), M. Safdari [ID¹⁴³](#),
 S. Saha [ID¹⁰⁴](#), M. Sahinsoy [ID¹¹⁰](#), M. Saimpert [ID¹³⁵](#), M. Saito [ID¹⁵³](#), T. Saito [ID¹⁵³](#), D. Salamani [ID³⁶](#),
 A. Salnikov [ID¹⁴³](#), J. Salt [ID¹⁶³](#), A. Salvador Salas [ID¹³](#), D. Salvatore [ID^{43b,43a}](#), F. Salvatore [ID¹⁴⁶](#),
 A. Salzburger [ID³⁶](#), D. Sammel [ID⁵⁴](#), D. Sampsonidis [ID^{152,f}](#), D. Sampsonidou [ID^{123,62c}](#), J. Sánchez [ID¹⁶³](#),
 A. Sanchez Pineda [ID⁴](#), V. Sanchez Sebastian [ID¹⁶³](#), H. Sandaker [ID¹²⁵](#), C.O. Sander [ID⁴⁸](#),
 J.A. Sandesara [ID¹⁰³](#), M. Sandhoff [ID¹⁷¹](#), C. Sandoval [ID^{22b}](#), D.P.C. Sankey [ID¹³⁴](#), T. Sano [ID⁸⁷](#),
 A. Sansoni [ID⁵³](#), L. Santi [ID^{75a,75b}](#), C. Santoni [ID⁴⁰](#), H. Santos [ID^{130a,130b}](#), S.N. Santpur [ID^{17a}](#), A. Santra [ID¹⁶⁹](#),
 K.A. Saoucha [ID¹³⁹](#), J.G. Saraiva [ID^{130a,130d}](#), J. Sardain [ID⁷](#), O. Sasaki [ID⁸³](#), K. Sato [ID¹⁵⁷](#), C. Sauer [ID^{63b}](#),
 F. Sauerburger [ID⁵⁴](#), E. Sauvan [ID⁴](#), P. Savard [ID^{155,ai}](#), R. Sawada [ID¹⁵³](#), C. Sawyer [ID¹³⁴](#), L. Sawyer [ID⁹⁷](#),
 I. Sayago Galvan [ID¹⁶³](#), C. Sbarra [ID^{23b}](#), A. Sbrizzi [ID^{23b,23a}](#), T. Scanlon [ID⁹⁶](#), J. Schaarschmidt [ID¹³⁸](#),
 P. Schacht [ID¹¹⁰](#), D. Schaefer [ID³⁹](#), U. Schäfer [ID¹⁰⁰](#), A.C. Schaffer [ID^{66,44}](#), D. Schaile [ID¹⁰⁹](#),
 R.D. Schamberger [ID¹⁴⁵](#), E. Schanet [ID¹⁰⁹](#), C. Scharf [ID¹⁸](#), M.M. Schefer [ID¹⁹](#), V.A. Schegelsky [ID³⁷](#),
 D. Scheirich [ID¹³³](#), F. Schenck [ID¹⁸](#), M. Schernau [ID¹⁶⁰](#), C. Scheulen [ID⁵⁵](#), C. Schiavi [ID^{57b,57a}](#),
 E.J. Schioppa [ID^{70a,70b}](#), M. Schioppa [ID^{43b,43a}](#), B. Schlag [ID^{143,q}](#), K.E. Schleicher [ID⁵⁴](#), S. Schlenker [ID³⁶](#),
 J. Schmeing [ID¹⁷¹](#), M.A. Schmidt [ID¹⁷¹](#), K. Schmieden [ID¹⁰⁰](#), C. Schmitt [ID¹⁰⁰](#), S. Schmitt [ID⁴⁸](#),
 L. Schoeffel [ID¹³⁵](#), A. Schoening [ID^{63b}](#), P.G. Scholer [ID⁵⁴](#), E. Schopf [ID¹²⁶](#), M. Schott [ID¹⁰⁰](#),
 J. Schovancova [ID³⁶](#), S. Schramm [ID⁵⁶](#), F. Schroeder [ID¹⁷¹](#), H-C. Schultz-Coulon [ID^{63a}](#), M. Schumacher [ID⁵⁴](#),
 B.A. Schumm [ID¹³⁶](#), Ph. Schune [ID¹³⁵](#), H.R. Schwartz [ID¹³⁶](#), A. Schwartzman [ID¹⁴³](#), T.A. Schwarz [ID¹⁰⁶](#),
 Ph. Schwemling [ID¹³⁵](#), R. Schwienhorst [ID¹⁰⁷](#), A. Sciandra [ID¹³⁶](#), G. Sciolla [ID²⁶](#), F. Scuri [ID^{74a}](#), F. Scutti [ID¹⁰⁵](#),
 C.D. Sebastiani [ID⁹²](#), K. Sedlaczek [ID⁴⁹](#), P. Seema [ID¹⁸](#), S.C. Seidel [ID¹¹²](#), A. Seiden [ID¹³⁶](#),
 B.D. Seidlitz [ID⁴¹](#), C. Seitz [ID⁴⁸](#), J.M. Seixas [ID^{82b}](#), G. Sekhniaidze [ID^{72a}](#), S.J. Sekula [ID⁴⁴](#), L. Selam [ID⁴](#),
 N. Semprini-Cesari [ID^{23b,23a}](#), S. Sen [ID⁵¹](#), D. Sengupta [ID⁵⁶](#), V. Senthilkumar [ID¹⁶³](#), L. Serin [ID⁶⁶](#),
 L. Serkin [ID^{69a,69b}](#), M. Sessa [ID^{77a,77b}](#), H. Severini [ID¹²⁰](#), F. Sforza [ID^{57b,57a}](#), A. Sfyrla [ID⁵⁶](#),

E. Shabalina ⁵⁵, R. Shaheen ¹⁴⁴, J.D. Shahinian ¹²⁸, D. Shaked Renous ¹⁶⁹, L.Y. Shan ^{14a},
 M. Shapiro ^{17a}, A. Sharma ³⁶, A.S. Sharma ¹⁶⁴, P. Sharma ⁸⁰, S. Sharma ⁴⁸, P.B. Shatalov ³⁷,
 K. Shaw ¹⁴⁶, S.M. Shaw ¹⁰¹, Q. Shen ^{62c,5}, P. Sherwood ⁹⁶, L. Shi ⁹⁶, C.O. Shimmin ¹⁷²,
 Y. Shimogama ¹⁶⁸, J.D. Shinner ⁹⁵, I.P.J. Shipsey ¹²⁶, S. Shirabe ⁶⁰, M. Shiyakova ^{38,x},
 J. Shlomi ¹⁶⁹, M.J. Shochet ³⁹, J. Shojaii ¹⁰⁵, D.R. Shope ¹²⁵, S. Shrestha ^{119,al}, E.M. Shrif ^{33g},
 M.J. Shroff ¹⁶⁵, P. Sicho ¹³¹, A.M. Sickles ¹⁶², E. Sideras Haddad ^{33g}, A. Sidoti ^{23b},
 F. Siegert ⁵⁰, Dj. Sijacki ¹⁵, R. Sikora ^{85a}, F. Sili ⁹⁰, J.M. Silva ²⁰, M.V. Silva Oliveira ³⁶,
 S.B. Silverstein ^{47a}, S. Simion ⁶⁶, R. Simoniello ³⁶, E.L. Simpson ⁵⁹, H. Simpson ¹⁴⁶,
 L.R. Simpson ¹⁰⁶, N.D. Simpson ⁹⁸, S. Simsek ^{21d}, S. Sindhu ⁵⁵, P. Sinervo ¹⁵⁵, S. Singh ¹⁴²,
 S. Singh ¹⁵⁵, S. Sinha ⁴⁸, S. Sinha ^{33g}, M. Sioli ^{23b,23a}, I. Siral ³⁶, S.Yu. Sivoklov ^{37,*},
 J. Sjölin ^{47a,47b}, A. Skaf ⁵⁵, E. Skorda ⁹⁸, P. Skubic ¹²⁰, M. Slawinska ⁸⁶, V. Smakhtin ¹⁶⁹,
 B.H. Smart ¹³⁴, J. Smiesko ³⁶, S.Yu. Smirnov ³⁷, Y. Smirnov ³⁷, L.N. Smirnova ^{37,a},
 O. Smirnova ⁹⁸, A.C. Smith ⁴¹, E.A. Smith ³⁹, H.A. Smith ¹²⁶, J.L. Smith ⁹², R. Smith ¹⁴³,
 M. Smizanska ⁹¹, K. Smolek ¹³², A.A. Snesarev ³⁷, H.L. Snoek ¹¹⁴, S. Snyder ²⁹, R. Sobie ^{165,z},
 A. Soffer ¹⁵¹, C.A. Solans Sanchez ³⁶, E.Yu. Soldatov ³⁷, U. Soldevila ¹⁶³, A.A. Solodkov ³⁷,
 S. Solomon ⁵⁴, A. Soloshenko ³⁸, K. Solovieva ⁵⁴, O.V. Solovyanov ⁴⁰, V. Solovyev ³⁷,
 P. Sommer ³⁶, A. Sonay ¹³, W.Y. Song ^{156b}, J.M. Sonneveld ¹¹⁴, A. Sopczak ¹³², A.L. Sopio ⁹⁶,
 F. Sopkova ^{28b}, V. Sothilingam ^{63a}, S. Sottocornola ⁶⁸, R. Soualah ^{116b}, Z. Soumami ^{35e},
 D. South ⁴⁸, S. Spagnolo ^{70a,70b}, M. Spalla ¹¹⁰, D. Sperlich ⁵⁴, G. Spigo ³⁶, M. Spina ¹⁴⁶,
 S. Spinali ⁹¹, D.P. Spiteri ⁵⁹, M. Spousta ¹³³, E.J. Staats ³⁴, A. Stabile ^{71a,71b}, R. Stamen ^{63a},
 M. Stamenkovic ¹¹⁴, A. Stampekis ²⁰, M. Standke ²⁴, E. Stanecka ⁸⁶, M.V. Stange ⁵⁰,
 B. Stanislaus ^{17a}, M.M. Stanitzki ⁴⁸, M. Stankaityte ¹²⁶, B. Stapf ⁴⁸, E.A. Starchenko ³⁷,
 G.H. Stark ¹³⁶, J. Stark ^{102,ad}, D.M. Starko ^{156b}, P. Staroba ¹³¹, P. Starovoitov ^{63a}, S. Stärz ¹⁰⁴,
 R. Staszewski ⁸⁶, G. Stavropoulos ⁴⁶, J. Steentoft ¹⁶¹, P. Steinberg ²⁹, B. Stelzer ^{142,156a},
 H.J. Stelzer ¹²⁹, O. Stelzer-Chilton ^{156a}, H. Stenzel ⁵⁸, T.J. Stevenson ¹⁴⁶, G.A. Stewart ³⁶,
 J.R. Stewart ¹²¹, M.C. Stockton ³⁶, G. Stoicea ^{27b}, M. Stolarski ^{130a}, S. Stonjek ¹¹⁰,
 A. Straessner ⁵⁰, J. Strandberg ¹⁴⁴, S. Strandberg ^{47a,47b}, M. Strauss ¹²⁰, T. Strebler ¹⁰²,
 P. Strizenc ^{28b}, R. Ströhmer ¹⁶⁶, D.M. Strom ¹²³, L.R. Strom ⁴⁸, R. Stroynowski ⁴⁴,
 A. Strubig ^{47a,47b}, S.A. Stucci ²⁹, B. Stugu ¹⁶, J. Stupak ¹²⁰, N.A. Styles ⁴⁸, D. Su ¹⁴³,
 S. Su ^{62a}, W. Su ^{62d,138,62c}, X. Su ^{62a,66}, K. Sugizaki ¹⁵³, V.V. Sulin ³⁷, M.J. Sullivan ⁹²,
 D.M.S. Sultan ^{78a,78b}, L. Sultanaliyeva ³⁷, S. Sultansoy ^{3b}, T. Sumida ⁸⁷, S. Sun ¹⁰⁶, S. Sun ¹⁷⁰,
 O. Sunneborn Gudnadottir ¹⁶¹, M.R. Sutton ¹⁴⁶, M. Svatos ¹³¹, M. Swiatlowski ^{156a},
 T. Swirski ¹⁶⁶, I. Sykora ^{28a}, M. Sykora ¹³³, T. Sykora ¹³³, D. Ta ¹⁰⁰, K. Tackmann ^{48,w},
 A. Taffard ¹⁶⁰, R. Tafirout ^{156a}, J.S. Tafoya Vargas ⁶⁶, R.H.M. Taibah ¹²⁷, R. Takashima ⁸⁸,
 E.P. Takeva ⁵², Y. Takubo ⁸³, M. Talby ¹⁰², A.A. Talyshev ³⁷, K.C. Tam ^{64b}, N.M. Tamir ¹⁵¹,
 A. Tanaka ¹⁵³, J. Tanaka ¹⁵³, R. Tanaka ⁶⁶, M. Tanasini ^{57b,57a}, J. Tang ^{62c}, Z. Tao ¹⁶⁴,
 S. Tapia Araya ^{137f}, S. Tapprogge ¹⁰⁰, A. Tarek Abouelfadl Mohamed ¹⁰⁷, S. Tarem ¹⁵⁰,
 K. Tariq ^{62b}, G. Tarna ^{102,27b}, G.F. Tartarelli ^{71a}, P. Tas ¹³³, M. Tasevsky ¹³¹, E. Tassi ^{43b,43a},
 A.C. Tate ¹⁶², G. Tateno ¹⁵³, Y. Tayalati ^{35e,y}, G.N. Taylor ¹⁰⁵, W. Taylor ^{156b}, H. Teagle ⁹²,
 A.S. Tee ¹⁷⁰, R. Teixeira De Lima ¹⁴³, P. Teixeira-Dias ⁹⁵, J.J. Teoh ¹⁵⁵, K. Terashi ¹⁵³,
 J. Terron ⁹⁹, S. Terzo ¹³, M. Testa ⁵³, R.J. Teuscher ^{155,z}, A. Thaler ⁷⁹, O. Theiner ⁵⁶,
 N. Themistokleous ⁵², T. Thevenaux-Pelzer ¹⁰², O. Thielmann ¹⁷¹, D.W. Thomas ⁹⁵,
 J.P. Thomas ²⁰, E.A. Thompson ^{17a}, P.D. Thompson ²⁰, E. Thomson ¹²⁸, Y. Tian ⁵⁵,
 V. Tikhomirov ^{37,a}, Yu.A. Tikhonov ³⁷, S. Timoshenko ³⁷, E.X.L. Ting ¹, P. Tipton ¹⁷²,
 S.H. Tlou ^{33g}, A. Tnourji ⁴⁰, K. Todome ^{23b,23a}, S. Todorova-Nova ¹³³, S. Todt ⁵⁰, M. Togawa ⁸³,
 J. Tojo ⁸⁹, S. Tokár ^{28a}, K. Tokushuku ⁸³, O. Toldaiev ⁶⁸, R. Tombs ³², M. Tomoto ^{83,111},
 L. Tompkins ^{143,q}, K.W. Topolnicki ^{85b}, E. Torrence ¹²³, H. Torres ^{102,ad}, E. Torró Pastor ¹⁶³,

M. Toscani ³⁰, C. Tosciri ³⁹, M. Tost ¹¹, D.R. Tovey ¹³⁹, A. Traeet ¹⁶, I.S. Trandafir ^{27b},
T. Trefzger ¹⁶⁶, A. Tricoli ²⁹, I.M. Trigger ^{156a}, S. Trincaz-Duvoid ¹²⁷, D.A. Trischuk ²⁶,
B. Trocmé ⁶⁰, C. Troncon ^{71a}, L. Truong ^{33c}, M. Trzebinski ⁸⁶, A. Trzupke ⁸⁶, F. Tsai ¹⁴⁵,
M. Tsai ¹⁰⁶, A. Tsiamis ^{152,f}, P.V. Tsiareshka ³⁷, S. Tsigaridas ^{156a}, A. Tsirigotis ^{152,u},
V. Tsiskaridze ¹⁴⁵, E.G. Tskhadadze ^{149a}, M. Tsopoulou ^{152,f}, Y. Tsujikawa ⁸⁷, I.I. Tsukerman ³⁷,
V. Tsulaia ^{17a}, S. Tsuno ⁸³, O. Tsur ¹⁵⁰, D. Tsybychev ¹⁴⁵, Y. Tu ^{64b}, A. Tudorache ^{27b},
V. Tudorache ^{27b}, A.N. Tuna ³⁶, S. Turchikhin ³⁸, I. Turk Cakir ^{3a}, R. Turra ^{71a},
T. Turtuvshin ^{38,aa}, P.M. Tuts ⁴¹, S. Tzamarias ^{152,f}, P. Tzanis ¹⁰, E. Tzovara ¹⁰⁰, K. Uchida ¹⁵³,
F. Ukegawa ¹⁵⁷, P.A. Ulloa Poblete ^{137c}, E.N. Umaka ²⁹, G. Unal ³⁶, M. Unal ¹¹, A. Undrus ²⁹,
G. Unel ¹⁶⁰, J. Urban ^{28b}, P. Urquijo ¹⁰⁵, G. Usai ⁸, R. Ushioda ¹⁵⁴, M. Usman ¹⁰⁸,
Z. Uysal ^{21b}, L. Vacavant ¹⁰², V. Vacek ¹³², B. Vachon ¹⁰⁴, K.O.H. Vadla ¹²⁵, T. Vafeiadis ³⁶,
A. Vaitkus ⁹⁶, C. Valderanis ¹⁰⁹, E. Valdes Santurio ^{47a,47b}, M. Valente ^{156a}, S. Valentinetti ^{23b,23a},
A. Valero ¹⁶³, E. Valiente Moreno ¹⁶³, A. Vallier ^{102,ad}, J.A. Valls Ferrer ¹⁶³,
D.R. Van Arneeman ¹¹⁴, T.R. Van Daalen ¹³⁸, P. Van Gemmeren ⁶, M. Van Rijnbach ^{125,36},
S. Van Stroud ⁹⁶, I. Van Vulpen ¹¹⁴, M. Vanadia ^{76a,76b}, W. Vandelli ³⁶, M. Vandenbroucke ¹³⁵,
E.R. Vandewall ¹²¹, D. Vannicola ¹⁵¹, L. Vannoli ^{57b,57a}, R. Vari ^{75a}, E.W. Varnes ⁷,
C. Varni ^{17a}, T. Varol ¹⁴⁸, D. Varouchas ⁶⁶, L. Varriale ¹⁶³, K.E. Varvell ¹⁴⁷, M.E. Vasile ^{27b},
L. Vaslin ⁴⁰, G.A. Vasquez ¹⁶⁵, F. Vazeille ⁴⁰, T. Vazquez Schroeder ³⁶, J. Veatch ³¹,
V. Vecchio ¹⁰¹, M.J. Veen ¹⁰³, I. Velisek ¹²⁶, L.M. Veloce ¹⁵⁵, F. Veloso ^{130a,130c},
S. Veneziano ^{75a}, A. Ventura ^{70a,70b}, A. Verbytskyi ¹¹⁰, M. Verducci ^{74a,74b}, C. Vergis ²⁴,
M. Verissimo De Araujo ^{82b}, W. Verkerke ¹¹⁴, J.C. Vermeulen ¹¹⁴, C. Vernieri ¹⁴³,
P.J. Verschuuren ⁹⁵, M. Vessella ¹⁰³, M.C. Vetterli ^{142,ai}, A. Vgenopoulos ^{152,f},
N. Viaux Maira ^{137f}, T. Vickey ¹³⁹, O.E. Vickey Boeriu ¹³⁹, G.H.A. Viehhauser ¹²⁶, L. Vignani ^{63b},
M. Villa ^{23b,23a}, M. Villaplana Perez ¹⁶³, E.M. Villhauer ⁵², E. Vilucchi ⁵³, M.G. Vincter ³⁴,
G.S. Virdee ²⁰, A. Vishwakarma ⁵², C. Vittori ³⁶, I. Vivarelli ¹⁴⁶, V. Vladimirov ¹⁶⁷,
E. Voevodina ¹¹⁰, F. Vogel ¹⁰⁹, P. Vokac ¹³², J. Von Ahnen ⁴⁸, E. Von Toerne ²⁴,
B. Vormwald ³⁶, V. Vorobel ¹³³, K. Vorobev ³⁷, M. Vos ¹⁶³, K. Voss ¹⁴¹, J.H. Vossebeld ⁹²,
M. Vozak ¹¹⁴, L. Vozdecky ⁹⁴, N. Vranjes ¹⁵, M. Vranjes Milosavljevic ¹⁵, M. Vreeswijk ¹¹⁴,
R. Vuillermet ³⁶, O. Vujanovic ¹⁰⁰, I. Vukotic ³⁹, S. Wada ¹⁵⁷, C. Wagner ¹⁰³, J.M. Wagner ^{17a},
W. Wagner ¹⁷¹, S. Wahdan ¹⁷¹, H. Wahlberg ⁹⁰, R. Wakasa ¹⁵⁷, M. Wakida ¹¹¹, J. Walder ¹³⁴,
R. Walker ¹⁰⁹, W. Walkowiak ¹⁴¹, A. Wall ¹²⁸, A.Z. Wang ¹⁷⁰, C. Wang ¹⁰⁰, C. Wang ^{62c},
H. Wang ^{17a}, J. Wang ^{64a}, R.-J. Wang ¹⁰⁰, R. Wang ⁶¹, R. Wang ⁶, S.M. Wang ¹⁴⁸,
S. Wang ^{62b}, T. Wang ^{62a}, W.T. Wang ⁸⁰, X. Wang ^{14c}, X. Wang ¹⁶², X. Wang ^{62c},
Y. Wang ^{62d}, Y. Wang ^{14c}, Z. Wang ¹⁰⁶, Z. Wang ^{62d,51,62c}, Z. Wang ¹⁰⁶, A. Warburton ¹⁰⁴,
R.J. Ward ²⁰, N. Warrack ⁵⁹, A.T. Watson ²⁰, H. Watson ⁵⁹, M.F. Watson ²⁰, G. Watts ¹³⁸,
B.M. Waugh ⁹⁶, C. Weber ²⁹, H.A. Weber ¹⁸, M.S. Weber ¹⁹, S.M. Weber ^{63a}, C. Wei ^{62a},
Y. Wei ¹²⁶, A.R. Weidberg ¹²⁶, E.J. Weik ¹¹⁷, J. Weingarten ⁴⁹, M. Weirich ¹⁰⁰, C. Weiser ⁵⁴,
C.J. Wells ⁴⁸, T. Wenaus ²⁹, B. Wendland ⁴⁹, T. Wengler ³⁶, N.S. Wenke ¹¹⁰, N. Wermes ²⁴,
M. Wessels ^{63a}, K. Whalen ¹²³, A.M. Wharton ⁹¹, A.S. White ⁶¹, A. White ⁸, M.J. White ¹,
D. Whiteson ¹⁶⁰, L. Wickremasinghe ¹²⁴, W. Wiedenmann ¹⁷⁰, C. Wiel ⁵⁰, M. Wielers ¹³⁴,
C. Wiglesworth ⁴², L.A.M. Wiik-Fuchs ⁵⁴, D.J. Wilbern ¹²⁰, H.G. Wilkens ³⁶, D.M. Williams ⁴¹,
H.H. Williams ¹²⁸, S. Williams ³², S. Willocq ¹⁰³, B.J. Wilson ¹⁰¹, P.J. Windischhofer ³⁹,
F. Winklmeier ¹²³, B.T. Winter ⁵⁴, J.K. Winter ¹⁰¹, M. Wittgen ¹⁴³, M. Wobisch ⁹⁷, R. Wölker ¹²⁶,
J. Wollrath ¹⁶⁰, M.W. Wolter ⁸⁶, H. Wolters ^{130a,130c}, V.W.S. Wong ¹⁶⁴, A.F. Wongel ⁴⁸,
S.D. Worm ⁴⁸, B.K. Wosiek ⁸⁶, K.W. Woźniak ⁸⁶, K. Wraight ⁵⁹, J. Wu ^{14a,14e}, M. Wu ^{64a},
M. Wu ¹¹³, S.L. Wu ¹⁷⁰, X. Wu ⁵⁶, Y. Wu ^{62a}, Z. Wu ^{135,62a}, J. Wuerzinger ¹¹⁰,
T.R. Wyatt ¹⁰¹, B.M. Wynne ⁵², S. Xella ⁴², L. Xia ^{14c}, M. Xia ^{14b}, J. Xiang ^{64c}, X. Xiao ¹⁰⁶,

M. Xie ^{62a}, X. Xie ^{62a}, S. Xin ^{14a,14e}, J. Xiong ^{17a}, I. Xioidis ¹⁴⁶, D. Xu ^{14a}, H. Xu ^{62a}, H. Xu ^{62a}, L. Xu ^{62a}, R. Xu ¹²⁸, T. Xu ¹⁰⁶, Y. Xu ^{14b}, Z. Xu ^{62b}, Z. Xu ^{14a}, B. Yabsley ¹⁴⁷, S. Yacoob ^{33a}, N. Yamaguchi ⁸⁹, Y. Yamaguchi ¹⁵⁴, H. Yamauchi ¹⁵⁷, T. Yamazaki ^{17a}, Y. Yamazaki ⁸⁴, J. Yan ^{62c}, S. Yan ¹²⁶, Z. Yan ²⁵, H.J. Yang ^{62c,62d}, H.T. Yang ^{62a}, S. Yang ^{62a}, T. Yang ^{64c}, X. Yang ^{62a}, X. Yang ^{14a}, Y. Yang ⁴⁴, Y. Yang ^{62a}, Z. Yang ^{62a,106}, W-M. Yao ^{17a}, Y.C. Yap ⁴⁸, H. Ye ^{14c}, H. Ye ⁵⁵, J. Ye ⁴⁴, S. Ye ²⁹, X. Ye ^{62a}, Y. Yeh ⁹⁶, I. Yeletsikh ³⁸, B.K. Yeo ^{17a}, M.R. Yexley ⁹¹, P. Yin ⁴¹, K. Yorita ¹⁶⁸, S. Younas ^{27b}, C.J.S. Young ⁵⁴, C. Young ¹⁴³, Y. Yu ^{62a}, M. Yuan ¹⁰⁶, R. Yuan ^{62b,1}, L. Yue ⁹⁶, M. Zaazoua ^{35e}, B. Zabinski ⁸⁶, E. Zaid ⁵², T. Zakareishvili ^{149b}, N. Zakharchuk ³⁴, S. Zambito ⁵⁶, J.A. Zamora Saa ^{137d,137b}, J. Zang ¹⁵³, D. Zanzi ⁵⁴, O. Zaplatilek ¹³², C. Zeitnitz ¹⁷¹, H. Zeng ^{14a}, J.C. Zeng ¹⁶², D.T. Zenger Jr ²⁶, O. Zenin ³⁷, T. Ženiš ^{28a}, S. Zenz ⁹⁴, S. Zerradi ^{35a}, D. Zerwas ⁶⁶, M. Zhai ^{14a,14e}, B. Zhang ^{14c}, D.F. Zhang ¹³⁹, J. Zhang ^{62b}, J. Zhang ⁶, K. Zhang ^{14a,14e}, L. Zhang ^{14c}, P. Zhang ^{14a,14e}, R. Zhang ¹⁷⁰, S. Zhang ¹⁰⁶, T. Zhang ¹⁵³, X. Zhang ^{62c}, X. Zhang ^{62b}, Y. Zhang ^{62c,5}, Z. Zhang ^{17a}, Z. Zhang ⁶⁶, H. Zhao ¹³⁸, P. Zhao ⁵¹, T. Zhao ^{62b}, Y. Zhao ¹³⁶, Z. Zhao ^{62a}, A. Zhemchugov ³⁸, X. Zheng ^{62a}, Z. Zheng ¹⁴³, D. Zhong ¹⁶², B. Zhou ¹⁰⁶, C. Zhou ¹⁷⁰, H. Zhou ⁷, N. Zhou ^{62c}, Y. Zhou ⁷, C.G. Zhu ^{62b}, J. Zhu ¹⁰⁶, Y. Zhu ^{62c}, Y. Zhu ^{62a}, X. Zhuang ^{14a}, K. Zhukov ³⁷, V. Zhulanov ³⁷, N.I. Zimine ³⁸, J. Zinsser ^{63b}, M. Ziolkowski ¹⁴¹, L. Živković ¹⁵, A. Zoccoli ^{23b,23a}, K. Zoch ⁵⁶, T.G. Zorbas ¹³⁹, O. Zormpa ⁴⁶, W. Zou ⁴¹, L. Zwalinski ³⁶.

¹Department of Physics, University of Adelaide, Adelaide; Australia.

²Department of Physics, University of Alberta, Edmonton AB; Canada.

³(^a)Department of Physics, Ankara University, Ankara; (^b)Division of Physics, TOBB University of Economics and Technology, Ankara; Türkiye.

⁴LAPP, Université Savoie Mont Blanc, CNRS/IN2P3, Annecy; France.

⁵APC, Université Paris Cité, CNRS/IN2P3, Paris; France.

⁶High Energy Physics Division, Argonne National Laboratory, Argonne IL; United States of America.

⁷Department of Physics, University of Arizona, Tucson AZ; United States of America.

⁸Department of Physics, University of Texas at Arlington, Arlington TX; United States of America.

⁹Physics Department, National and Kapodistrian University of Athens, Athens; Greece.

¹⁰Physics Department, National Technical University of Athens, Zografou; Greece.

¹¹Department of Physics, University of Texas at Austin, Austin TX; United States of America.

¹²Institute of Physics, Azerbaijan Academy of Sciences, Baku; Azerbaijan.

¹³Institut de Física d'Altes Energies (IFAE), Barcelona Institute of Science and Technology, Barcelona; Spain.

¹⁴(^a)Institute of High Energy Physics, Chinese Academy of Sciences, Beijing; (^b)Physics Department, Tsinghua University, Beijing; (^c)Department of Physics, Nanjing University, Nanjing; (^d)School of Science, Shenzhen Campus of Sun Yat-sen University; (^e)University of Chinese Academy of Science (UCAS), Beijing; China.

¹⁵Institute of Physics, University of Belgrade, Belgrade; Serbia.

¹⁶Department for Physics and Technology, University of Bergen, Bergen; Norway.

¹⁷(^a)Physics Division, Lawrence Berkeley National Laboratory, Berkeley CA; (^b)University of California, Berkeley CA; United States of America.

¹⁸Institut für Physik, Humboldt Universität zu Berlin, Berlin; Germany.

¹⁹Albert Einstein Center for Fundamental Physics and Laboratory for High Energy Physics, University of Bern, Bern; Switzerland.

²⁰School of Physics and Astronomy, University of Birmingham, Birmingham; United Kingdom.

- ²¹(*a*) Department of Physics, Bogazici University, Istanbul; (*b*) Department of Physics Engineering, Gaziantep University, Gaziantep; (*c*) Department of Physics, Istanbul University, Istanbul; (*d*) Istinye University, Sariyer, Istanbul; Türkiye.
- ²²(*a*) Facultad de Ciencias y Centro de Investigaciones, Universidad Antonio Nariño, Bogotá; (*b*) Departamento de Física, Universidad Nacional de Colombia, Bogotá; Colombia.
- ²³(*a*) Dipartimento di Fisica e Astronomia A. Righi, Università di Bologna, Bologna; (*b*) INFN Sezione di Bologna; Italy.
- ²⁴Physikalisches Institut, Universität Bonn, Bonn; Germany.
- ²⁵Department of Physics, Boston University, Boston MA; United States of America.
- ²⁶Department of Physics, Brandeis University, Waltham MA; United States of America.
- ²⁷(*a*) Transilvania University of Brasov, Brasov; (*b*) Horia Hulubei National Institute of Physics and Nuclear Engineering, Bucharest; (*c*) Department of Physics, Alexandru Ioan Cuza University of Iasi, Iasi; (*d*) National Institute for Research and Development of Isotopic and Molecular Technologies, Physics Department, Cluj-Napoca; (*e*) University Politehnica Bucharest, Bucharest; (*f*) West University in Timisoara, Timisoara; (*g*) Faculty of Physics, University of Bucharest, Bucharest; Romania.
- ²⁸(*a*) Faculty of Mathematics, Physics and Informatics, Comenius University, Bratislava; (*b*) Department of Subnuclear Physics, Institute of Experimental Physics of the Slovak Academy of Sciences, Kosice; Slovak Republic.
- ²⁹Physics Department, Brookhaven National Laboratory, Upton NY; United States of America.
- ³⁰Universidad de Buenos Aires, Facultad de Ciencias Exactas y Naturales, Departamento de Física, y CONICET, Instituto de Física de Buenos Aires (IFIBA), Buenos Aires; Argentina.
- ³¹California State University, CA; United States of America.
- ³²Cavendish Laboratory, University of Cambridge, Cambridge; United Kingdom.
- ³³(*a*) Department of Physics, University of Cape Town, Cape Town; (*b*) iThemba Labs, Western Cape; (*c*) Department of Mechanical Engineering Science, University of Johannesburg, Johannesburg; (*d*) National Institute of Physics, University of the Philippines Diliman (Philippines); (*e*) University of South Africa, Department of Physics, Pretoria; (*f*) University of Zululand, KwaDlangezwa; (*g*) School of Physics, University of the Witwatersrand, Johannesburg; South Africa.
- ³⁴Department of Physics, Carleton University, Ottawa ON; Canada.
- ³⁵(*a*) Faculté des Sciences Ain Chock, Réseau Universitaire de Physique des Hautes Energies - Université Hassan II, Casablanca; (*b*) Faculté des Sciences, Université Ibn-Tofail, Kénitra; (*c*) Faculté des Sciences Semlalia, Université Cadi Ayyad, LPHEA-Marrakech; (*d*) LPMR, Faculté des Sciences, Université Mohamed Premier, Oujda; (*e*) Faculté des sciences, Université Mohammed V, Rabat; (*f*) Institute of Applied Physics, Mohammed VI Polytechnic University, Ben Guerir; Morocco.
- ³⁶CERN, Geneva; Switzerland.
- ³⁷Affiliated with an institute covered by a cooperation agreement with CERN.
- ³⁸Affiliated with an international laboratory covered by a cooperation agreement with CERN.
- ³⁹Enrico Fermi Institute, University of Chicago, Chicago IL; United States of America.
- ⁴⁰LPC, Université Clermont Auvergne, CNRS/IN2P3, Clermont-Ferrand; France.
- ⁴¹Nevis Laboratory, Columbia University, Irvington NY; United States of America.
- ⁴²Niels Bohr Institute, University of Copenhagen, Copenhagen; Denmark.
- ⁴³(*a*) Dipartimento di Fisica, Università della Calabria, Rende; (*b*) INFN Gruppo Collegato di Cosenza, Laboratori Nazionali di Frascati; Italy.
- ⁴⁴Physics Department, Southern Methodist University, Dallas TX; United States of America.
- ⁴⁵Physics Department, University of Texas at Dallas, Richardson TX; United States of America.
- ⁴⁶National Centre for Scientific Research "Demokritos", Agia Paraskevi; Greece.
- ⁴⁷(*a*) Department of Physics, Stockholm University; (*b*) Oskar Klein Centre, Stockholm; Sweden.

- ⁴⁸Deutsches Elektronen-Synchrotron DESY, Hamburg and Zeuthen; Germany.
- ⁴⁹Fakultät Physik , Technische Universität Dortmund, Dortmund; Germany.
- ⁵⁰Institut für Kern- und Teilchenphysik, Technische Universität Dresden, Dresden; Germany.
- ⁵¹Department of Physics, Duke University, Durham NC; United States of America.
- ⁵²SUPA - School of Physics and Astronomy, University of Edinburgh, Edinburgh; United Kingdom.
- ⁵³INFN e Laboratori Nazionali di Frascati, Frascati; Italy.
- ⁵⁴Physikalisches Institut, Albert-Ludwigs-Universität Freiburg, Freiburg; Germany.
- ⁵⁵II. Physikalisches Institut, Georg-August-Universität Göttingen, Göttingen; Germany.
- ⁵⁶Département de Physique Nucléaire et Corpusculaire, Université de Genève, Genève; Switzerland.
- ⁵⁷(^a) Dipartimento di Fisica, Università di Genova, Genova; (^b) INFN Sezione di Genova; Italy.
- ⁵⁸II. Physikalisches Institut, Justus-Liebig-Universität Giessen, Giessen; Germany.
- ⁵⁹SUPA - School of Physics and Astronomy, University of Glasgow, Glasgow; United Kingdom.
- ⁶⁰LPSC, Université Grenoble Alpes, CNRS/IN2P3, Grenoble INP, Grenoble; France.
- ⁶¹Laboratory for Particle Physics and Cosmology, Harvard University, Cambridge MA; United States of America.
- ⁶²(^a) Department of Modern Physics and State Key Laboratory of Particle Detection and Electronics, University of Science and Technology of China, Hefei; (^b) Institute of Frontier and Interdisciplinary Science and Key Laboratory of Particle Physics and Particle Irradiation (MOE), Shandong University, Qingdao; (^c) School of Physics and Astronomy, Shanghai Jiao Tong University, Key Laboratory for Particle Astrophysics and Cosmology (MOE), SKLPPC, Shanghai; (^d) Tsung-Dao Lee Institute, Shanghai; China.
- ⁶³(^a) Kirchhoff-Institut für Physik, Ruprecht-Karls-Universität Heidelberg, Heidelberg; (^b) Physikalisches Institut, Ruprecht-Karls-Universität Heidelberg, Heidelberg; Germany.
- ⁶⁴(^a) Department of Physics, Chinese University of Hong Kong, Shatin, N.T., Hong Kong; (^b) Department of Physics, University of Hong Kong, Hong Kong; (^c) Department of Physics and Institute for Advanced Study, Hong Kong University of Science and Technology, Clear Water Bay, Kowloon, Hong Kong; China.
- ⁶⁵Department of Physics, National Tsing Hua University, Hsinchu; Taiwan.
- ⁶⁶IJCLab, Université Paris-Saclay, CNRS/IN2P3, 91405, Orsay; France.
- ⁶⁷Centro Nacional de Microelectrónica (IMB-CNM-CSIC), Barcelona; Spain.
- ⁶⁸Department of Physics, Indiana University, Bloomington IN; United States of America.
- ⁶⁹(^a) INFN Gruppo Collegato di Udine, Sezione di Trieste, Udine; (^b) ICTP, Trieste; (^c) Dipartimento Politecnico di Ingegneria e Architettura, Università di Udine, Udine; Italy.
- ⁷⁰(^a) INFN Sezione di Lecce; (^b) Dipartimento di Matematica e Fisica, Università del Salento, Lecce; Italy.
- ⁷¹(^a) INFN Sezione di Milano; (^b) Dipartimento di Fisica, Università di Milano, Milano; Italy.
- ⁷²(^a) INFN Sezione di Napoli; (^b) Dipartimento di Fisica, Università di Napoli, Napoli; Italy.
- ⁷³(^a) INFN Sezione di Pavia; (^b) Dipartimento di Fisica, Università di Pavia, Pavia; Italy.
- ⁷⁴(^a) INFN Sezione di Pisa; (^b) Dipartimento di Fisica E. Fermi, Università di Pisa, Pisa; Italy.
- ⁷⁵(^a) INFN Sezione di Roma; (^b) Dipartimento di Fisica, Sapienza Università di Roma, Roma; Italy.
- ⁷⁶(^a) INFN Sezione di Roma Tor Vergata; (^b) Dipartimento di Fisica, Università di Roma Tor Vergata, Roma; Italy.
- ⁷⁷(^a) INFN Sezione di Roma Tre; (^b) Dipartimento di Matematica e Fisica, Università Roma Tre, Roma; Italy.
- ⁷⁸(^a) INFN-TIFPA; (^b) Università degli Studi di Trento, Trento; Italy.
- ⁷⁹Universität Innsbruck, Department of Astro and Particle Physics, Innsbruck; Austria.
- ⁸⁰University of Iowa, Iowa City IA; United States of America.
- ⁸¹Department of Physics and Astronomy, Iowa State University, Ames IA; United States of America.
- ⁸²(^a) Departamento de Engenharia Elétrica, Universidade Federal de Juiz de Fora (UFJF), Juiz de Fora; (^b) Universidade Federal do Rio De Janeiro COPPE/EE/IF, Rio de Janeiro; (^c) Instituto de Física,

- Universidade de São Paulo, São Paulo;^(d)Rio de Janeiro State University, Rio de Janeiro; Brazil.
- ⁸³KEK, High Energy Accelerator Research Organization, Tsukuba; Japan.
- ⁸⁴Graduate School of Science, Kobe University, Kobe; Japan.
- ⁸⁵^(a)AGH University of Krakow, Faculty of Physics and Applied Computer Science, Krakow;^(b)Marian Smoluchowski Institute of Physics, Jagiellonian University, Krakow; Poland.
- ⁸⁶Institute of Nuclear Physics Polish Academy of Sciences, Krakow; Poland.
- ⁸⁷Faculty of Science, Kyoto University, Kyoto; Japan.
- ⁸⁸Kyoto University of Education, Kyoto; Japan.
- ⁸⁹Research Center for Advanced Particle Physics and Department of Physics, Kyushu University, Fukuoka ; Japan.
- ⁹⁰Instituto de Física La Plata, Universidad Nacional de La Plata and CONICET, La Plata; Argentina.
- ⁹¹Physics Department, Lancaster University, Lancaster; United Kingdom.
- ⁹²Oliver Lodge Laboratory, University of Liverpool, Liverpool; United Kingdom.
- ⁹³Department of Experimental Particle Physics, Jožef Stefan Institute and Department of Physics, University of Ljubljana, Ljubljana; Slovenia.
- ⁹⁴School of Physics and Astronomy, Queen Mary University of London, London; United Kingdom.
- ⁹⁵Department of Physics, Royal Holloway University of London, Egham; United Kingdom.
- ⁹⁶Department of Physics and Astronomy, University College London, London; United Kingdom.
- ⁹⁷Louisiana Tech University, Ruston LA; United States of America.
- ⁹⁸Fysiska institutionen, Lunds universitet, Lund; Sweden.
- ⁹⁹Departamento de Física Teórica C-15 and CIAFF, Universidad Autónoma de Madrid, Madrid; Spain.
- ¹⁰⁰Institut für Physik, Universität Mainz, Mainz; Germany.
- ¹⁰¹School of Physics and Astronomy, University of Manchester, Manchester; United Kingdom.
- ¹⁰²CPPM, Aix-Marseille Université, CNRS/IN2P3, Marseille; France.
- ¹⁰³Department of Physics, University of Massachusetts, Amherst MA; United States of America.
- ¹⁰⁴Department of Physics, McGill University, Montreal QC; Canada.
- ¹⁰⁵School of Physics, University of Melbourne, Victoria; Australia.
- ¹⁰⁶Department of Physics, University of Michigan, Ann Arbor MI; United States of America.
- ¹⁰⁷Department of Physics and Astronomy, Michigan State University, East Lansing MI; United States of America.
- ¹⁰⁸Group of Particle Physics, University of Montreal, Montreal QC; Canada.
- ¹⁰⁹Fakultät für Physik, Ludwig-Maximilians-Universität München, München; Germany.
- ¹¹⁰Max-Planck-Institut für Physik (Werner-Heisenberg-Institut), München; Germany.
- ¹¹¹Graduate School of Science and Kobayashi-Maskawa Institute, Nagoya University, Nagoya; Japan.
- ¹¹²Department of Physics and Astronomy, University of New Mexico, Albuquerque NM; United States of America.
- ¹¹³Institute for Mathematics, Astrophysics and Particle Physics, Radboud University/Nikhef, Nijmegen; Netherlands.
- ¹¹⁴Nikhef National Institute for Subatomic Physics and University of Amsterdam, Amsterdam; Netherlands.
- ¹¹⁵Department of Physics, Northern Illinois University, DeKalb IL; United States of America.
- ¹¹⁶^(a)New York University Abu Dhabi, Abu Dhabi;^(b)University of Sharjah, Sharjah; United Arab Emirates.
- ¹¹⁷Department of Physics, New York University, New York NY; United States of America.
- ¹¹⁸Ochanomizu University, Otsuka, Bunkyo-ku, Tokyo; Japan.
- ¹¹⁹Ohio State University, Columbus OH; United States of America.
- ¹²⁰Homer L. Dodge Department of Physics and Astronomy, University of Oklahoma, Norman OK; United

States of America.

¹²¹Department of Physics, Oklahoma State University, Stillwater OK; United States of America.

¹²²Palacký University, Joint Laboratory of Optics, Olomouc; Czech Republic.

¹²³Institute for Fundamental Science, University of Oregon, Eugene, OR; United States of America.

¹²⁴Graduate School of Science, Osaka University, Osaka; Japan.

¹²⁵Department of Physics, University of Oslo, Oslo; Norway.

¹²⁶Department of Physics, Oxford University, Oxford; United Kingdom.

¹²⁷LPNHE, Sorbonne Université, Université Paris Cité, CNRS/IN2P3, Paris; France.

¹²⁸Department of Physics, University of Pennsylvania, Philadelphia PA; United States of America.

¹²⁹Department of Physics and Astronomy, University of Pittsburgh, Pittsburgh PA; United States of America.

¹³⁰(^a)Laboratório de Instrumentação e Física Experimental de Partículas - LIP, Lisboa; (^b)Departamento de Física, Faculdade de Ciências, Universidade de Lisboa, Lisboa; (^c)Departamento de Física, Universidade de Coimbra, Coimbra; (^d)Centro de Física Nuclear da Universidade de Lisboa, Lisboa; (^e)Departamento de Física, Universidade do Minho, Braga; (^f)Departamento de Física Teórica y del Cosmos, Universidad de Granada, Granada (Spain); (^g)Departamento de Física, Instituto Superior Técnico, Universidade de Lisboa, Lisboa; Portugal.

¹³¹Institute of Physics of the Czech Academy of Sciences, Prague; Czech Republic.

¹³²Czech Technical University in Prague, Prague; Czech Republic.

¹³³Charles University, Faculty of Mathematics and Physics, Prague; Czech Republic.

¹³⁴Particle Physics Department, Rutherford Appleton Laboratory, Didcot; United Kingdom.

¹³⁵IRFU, CEA, Université Paris-Saclay, Gif-sur-Yvette; France.

¹³⁶Santa Cruz Institute for Particle Physics, University of California Santa Cruz, Santa Cruz CA; United States of America.

¹³⁷(^a)Departamento de Física, Pontificia Universidad Católica de Chile, Santiago; (^b)Millennium Institute for Subatomic physics at high energy frontier (SAPHIR), Santiago; (^c)Instituto de Investigación Multidisciplinario en Ciencia y Tecnología, y Departamento de Física, Universidad de La Serena; (^d)Universidad Andres Bello, Department of Physics, Santiago; (^e)Instituto de Alta Investigación, Universidad de Tarapacá, Arica; (^f)Departamento de Física, Universidad Técnica Federico Santa María, Valparaíso; Chile.

¹³⁸Department of Physics, University of Washington, Seattle WA; United States of America.

¹³⁹Department of Physics and Astronomy, University of Sheffield, Sheffield; United Kingdom.

¹⁴⁰Department of Physics, Shinshu University, Nagano; Japan.

¹⁴¹Department Physik, Universität Siegen, Siegen; Germany.

¹⁴²Department of Physics, Simon Fraser University, Burnaby BC; Canada.

¹⁴³SLAC National Accelerator Laboratory, Stanford CA; United States of America.

¹⁴⁴Department of Physics, Royal Institute of Technology, Stockholm; Sweden.

¹⁴⁵Departments of Physics and Astronomy, Stony Brook University, Stony Brook NY; United States of America.

¹⁴⁶Department of Physics and Astronomy, University of Sussex, Brighton; United Kingdom.

¹⁴⁷School of Physics, University of Sydney, Sydney; Australia.

¹⁴⁸Institute of Physics, Academia Sinica, Taipei; Taiwan.

¹⁴⁹(^a)E. Andronikashvili Institute of Physics, Iv. Javakhishvili Tbilisi State University, Tbilisi; (^b)High Energy Physics Institute, Tbilisi State University, Tbilisi; (^c)University of Georgia, Tbilisi; Georgia.

¹⁵⁰Department of Physics, Technion, Israel Institute of Technology, Haifa; Israel.

¹⁵¹Raymond and Beverly Sackler School of Physics and Astronomy, Tel Aviv University, Tel Aviv; Israel.

¹⁵²Department of Physics, Aristotle University of Thessaloniki, Thessaloniki; Greece.

- ¹⁵³International Center for Elementary Particle Physics and Department of Physics, University of Tokyo, Tokyo; Japan.
- ¹⁵⁴Department of Physics, Tokyo Institute of Technology, Tokyo; Japan.
- ¹⁵⁵Department of Physics, University of Toronto, Toronto ON; Canada.
- ¹⁵⁶(^a) TRIUMF, Vancouver BC; (^b) Department of Physics and Astronomy, York University, Toronto ON; Canada.
- ¹⁵⁷Division of Physics and Tomonaga Center for the History of the Universe, Faculty of Pure and Applied Sciences, University of Tsukuba, Tsukuba; Japan.
- ¹⁵⁸Department of Physics and Astronomy, Tufts University, Medford MA; United States of America.
- ¹⁵⁹United Arab Emirates University, Al Ain; United Arab Emirates.
- ¹⁶⁰Department of Physics and Astronomy, University of California Irvine, Irvine CA; United States of America.
- ¹⁶¹Department of Physics and Astronomy, University of Uppsala, Uppsala; Sweden.
- ¹⁶²Department of Physics, University of Illinois, Urbana IL; United States of America.
- ¹⁶³Instituto de Física Corpuscular (IFIC), Centro Mixto Universidad de Valencia - CSIC, Valencia; Spain.
- ¹⁶⁴Department of Physics, University of British Columbia, Vancouver BC; Canada.
- ¹⁶⁵Department of Physics and Astronomy, University of Victoria, Victoria BC; Canada.
- ¹⁶⁶Fakultät für Physik und Astronomie, Julius-Maximilians-Universität Würzburg, Würzburg; Germany.
- ¹⁶⁷Department of Physics, University of Warwick, Coventry; United Kingdom.
- ¹⁶⁸Waseda University, Tokyo; Japan.
- ¹⁶⁹Department of Particle Physics and Astrophysics, Weizmann Institute of Science, Rehovot; Israel.
- ¹⁷⁰Department of Physics, University of Wisconsin, Madison WI; United States of America.
- ¹⁷¹Fakultät für Mathematik und Naturwissenschaften, Fachgruppe Physik, Bergische Universität Wuppertal, Wuppertal; Germany.
- ¹⁷²Department of Physics, Yale University, New Haven CT; United States of America.
- ^a Also Affiliated with an institute covered by a cooperation agreement with CERN.
- ^b Also at An-Najah National University, Nablus; Palestine.
- ^c Also at Borough of Manhattan Community College, City University of New York, New York NY; United States of America.
- ^d Also at Bruno Kessler Foundation, Trento; Italy.
- ^e Also at Center for High Energy Physics, Peking University; China.
- ^f Also at Center for Interdisciplinary Research and Innovation (CIRI-AUTH), Thessaloniki; Greece.
- ^g Also at Centro Studi e Ricerche Enrico Fermi; Italy.
- ^h Also at CERN, Geneva; Switzerland.
- ⁱ Also at Département de Physique Nucléaire et Corpusculaire, Université de Genève, Genève; Switzerland.
- ^j Also at Departament de Física de la Universitat Autònoma de Barcelona, Barcelona; Spain.
- ^k Also at Department of Financial and Management Engineering, University of the Aegean, Chios; Greece.
- ^l Also at Department of Physics and Astronomy, Michigan State University, East Lansing MI; United States of America.
- ^m Also at Department of Physics, Ben Gurion University of the Negev, Beer Sheva; Israel.
- ⁿ Also at Department of Physics, California State University, East Bay; United States of America.
- ^o Also at Department of Physics, California State University, Sacramento; United States of America.
- ^p Also at Department of Physics, King's College London, London; United Kingdom.
- ^q Also at Department of Physics, Stanford University, Stanford CA; United States of America.
- ^r Also at Department of Physics, University of Fribourg, Fribourg; Switzerland.
- ^s Also at Department of Physics, University of Thessaly; Greece.
- ^t Also at Department of Physics, Westmont College, Santa Barbara; United States of America.

- ^u Also at Hellenic Open University, Patras; Greece.
- ^v Also at Institutio Catalana de Recerca i Estudis Avancats, ICREA, Barcelona; Spain.
- ^w Also at Institut für Experimentalphysik, Universität Hamburg, Hamburg; Germany.
- ^x Also at Institute for Nuclear Research and Nuclear Energy (INRNE) of the Bulgarian Academy of Sciences, Sofia; Bulgaria.
- ^y Also at Institute of Applied Physics, Mohammed VI Polytechnic University, Ben Guerir; Morocco.
- ^z Also at Institute of Particle Physics (IPP); Canada.
- ^{aa} Also at Institute of Physics and Technology, Ulaanbaatar; Mongolia.
- ^{ab} Also at Institute of Physics, Azerbaijan Academy of Sciences, Baku; Azerbaijan.
- ^{ac} Also at Institute of Theoretical Physics, Iia State University, Tbilisi; Georgia.
- ^{ad} Also at L2IT, Université de Toulouse, CNRS/IN2P3, UPS, Toulouse; France.
- ^{ae} Also at Lawrence Livermore National Laboratory, Livermore; United States of America.
- ^{af} Also at National Institute of Physics, University of the Philippines Diliman (Philippines); Philippines.
- ^{ag} Also at Technical University of Munich, Munich; Germany.
- ^{ah} Also at The Collaborative Innovation Center of Quantum Matter (CICQM), Beijing; China.
- ^{ai} Also at TRIUMF, Vancouver BC; Canada.
- ^{aj} Also at Università di Napoli Parthenope, Napoli; Italy.
- ^{ak} Also at University of Colorado Boulder, Department of Physics, Colorado; United States of America.
- ^{al} Also at Washington College, Maryland; United States of America.
- ^{am} Also at Yeditepe University, Physics Department, Istanbul; Türkiye.
- * Deceased